UNIVERSITÉ DU LUXEMBOURG

PhD-FDEF-2025-024
The Faculty of Law, Economics and Finance

DISSERTATION

Defence held on 29 October 2025 in Luxembourg
to obtain the degree of

DOCTEUR DE L'UNIVERSITÉ DU LUXEMBOURG
EN SCIENCES ÉCONOMIQUES

by

Raian KUDASHEV

Born on 14 April 1998 in Surgut (Russian Federation)

CROSS-BORDER COMMUTING, TAX, CONGESTION AND JOB SEARCH IN THE GREATER REGION OF LUXEMBOURG: A PERSPECTIVE FROM QUANTITATIVE SPATIAL ECONOMICS.

Dissertation defence committee

Prof. Pierre M. PICARD, supervisor
Université du Luxembourg

Prof. Skerdilajda ZANAJ, chairperson
Université du Luxembourg

Prof. Dr. Gabriel M. AHLFELDT, member
Humboldt University of Berlin

Dr. Michał BURZYŃSKI, member
LISER

Prof. Jos van OMMEREN, member
Vrije Universiteit Amsterdam

To Alex.
You would be proud.

Affidavit / Statement of originality

I declare that this thesis:

- is the result of my own work. Any contribution from any other party, and any use of generative artificial intelligence technologies have been duly cited and acknowledged;
- is not substantially the same as any other that I have submitted; and
- is not being concurrently submitted for a degree, diploma or other qualification at the University of Luxembourg or any other University or similar institution except as specified in the text.

With my approval I furthermore confirm the following:

- I have adhered to the rules set out in the University of Luxembourg's Code of Conduct and the Doctoral Education Agreement (DEA)[1], in particular with regard to Research Integrity.
- I have documented all methods, data, and processes truthfully and fully.
- I have mentioned all the significant contributors to the work.
- I am aware that the work may be screened electronically for originality.

I acknowledge that if any issues are raised regarding good research practices based on the review of the thesis, the examination may be postponed pending the outcome of any investigation of such issues. If a degree was conferred, any such subsequently discovered issues may result in the cancellation of the degree.

Approved on 2025-08-02

[1] If applicable (DEA is compulsory since August 2020)

Acknowledgements

To be frank, I never imagined myself in academia while growing up. I thought it was something only *truly* talented people pursued. But I gave it a try nonetheless, and voilà – you hold in your hands a text to which I have dedicated the last four years of my life. I know I did my best, and I hope the pages ahead make that clear. I am both happy and tired, ready to close this chapter and move on to the next. That said, I am not certain that life works in chapters, and I realize perfectly well that closure is an illusion – most things in life are continuous, and drastic jumps are extremely rare (but more on that in Chapter 1). There is one thing that I know is *not* an illusion, though: I had a lot of fun. And I hope to carry this joy with me until the very end of my academic career, however long it may be.

I never imagined myself in academia, but now I do. More than that, I know there is no other career I would rather pursue. It has been quite a journey, and I cherish every bend and turn, every up and down along the way. This journey would have been impossible without all the people who, knowingly or unknowingly, contributed to making me the person I am today, and whose support brightened my days throughout my doctoral studies. This section – the most personal of them all – is for all of you.

First, I would like to express my deep gratitude to my supervisor, Prof. Picard, for his guidance, support, and patience. I am indebted to him for the countless meetings and discussions we had over the years, and for his time – the only resource we have that truly matters – that he so generously gave me. This journey would not have been possible without him. I learned a great deal from him, and I will carry that knowledge with me. Professor, thank you.

I am deeply grateful to Prof. Ahlfeldt for his valuable feedback, the inspiring course he taught in Berlin, his advice – both professional and personal – and for helping me find a community of like-minded young researchers. His support made my stay in Berlin one of the most rewarding periods of my life. I also thank him for serving as an external jury member for my defense. Your presence here means a great deal to me. I would like to thank Andrea, Immo, Felix, Kalle, Max, another Max, yet another Max, and Nina for their insightful comments, countless (occasionally vegan) kebabs, liters of Club-Mate, promising collaborations, and for sharing those wonderful days in Berlin with me. I hope I was able to help you as much as you helped me. We will meet again; I am certain of that.

I owe special thanks to Prof. Zanaj for agreeing to chair my defense, and for her excellent course in international public economics, which inspired the first chapter of this thesis. I am grateful to Prof. van Ommeren and Prof. Koster for the trust they have placed in me, and for the opportunity to continue my research in the Netherlands. I am committed to living up to this trust, and I look forward to our collaboration. I also thank Prof. van Ommeren for agreeing to serve as an external jury member for my defense.

I wish to acknowledge Dr. Burzyński and Dr. Verheyden for the opportunity to collaborate on an exciting project, as well as for their guidance and assistance. I am also grateful to Prof. Caruso, who, together with Dr. Burzyński, serves on my doctoral committee, for his comments, feedback, and the unique perspective of a geographer that helped me approach my work from a different angle and ask questions that no economist would ever consider. Finally, my appreciation goes to all those involved in the ACROSS Doctoral Training Unit, particularly Prof. Docquier and Prof. Beine. I also acknowledge the financial support from the National Research Fund of Luxembourg (FNR), which made my doctoral studies possible.

I would be completely lost on this journey without Noémie and Roswitha, whose wisdom knows no bounds. I am grateful to Anne-Sophie, Elisa, and Marina for their support and help. This thesis, including all its graphs and code, would not have been possible without Andreï Kostyrka and his exceptional courses in R and LaTeX. I would also like to thank Zhenya and Ksusha for their guidance and support during the early days of my PhD. Thank you for everything.

Somewhat unexpectedly, I would like to thank Emmanuel Macron[2] for his visit to Berlin on May 25, 2024, and the Berlin police for closing the city's central streets on that occasion. These events inspired a research question that will develop into a paper in the coming years. I am grateful to Prof. Akbar, Prof. Behrens, Prof. Fournier, Prof. Kulka, and Prof. Sleiman for their help in refining the idea.

To Adrij, Aleksa, Ale, Ari, Armin, Azamat, Cami, Ceci (the best office mate ever), Diane (the best flatmate ever), Etienne, Evie, Fede, Lena, Marco, Maria, Matte, Najada, Rana, Sakshi, Salvo, Silvia, Vanessa, and all my friends and colleagues in Luxembourg – thank you for everything: all those beers that we could fill a swimming pool with, long and deep conversations in bars, and brief small talk by the coffee machine; all the jokes we made (even the bad ones); all the conferences we attended; all the pitches we made; all the research ideas we shared; all the books and papers we discussed; all the trips we took; all the highway exits I missed; all the highway exits *you* missed; and all the hikes we had in the north of Luxembourg (which, frankly speaking, are not many). Thank you for all the laughter, all the smiles, and all the tears. Thank you for the inspiration you have given me and for being there. This journey would be meaningless without you. You were, and still are, my beacons of light in the open waters of life. *Danke, dankjewel, dhonnobad, faleminderit, gracias, grazie, grazzi, hvala, merci, multumesc, shukran, spasibo, tashakkur, teşekkürler.*

To my friends back home and those scattered around the globe – to Alyona, Borya, Dan, Danya, Kolya, Kolets, Maksim, Misha, Nastya, Nikita, Renat, Stas, Syama, Troy, Vanya, Vika, and Yura – I love you all, wherever you are now and wherever you will be. I wish you all could be here. Stay safe. *I do vstrechi v Moskve*.

Above all, my deepest gratitude goes to my family: my grandmothers, my parents, and my brother Iskander. In three generations, we made our way from Siberian GULAGs and remote villages in rural Bashkortostan to Luxembourg – from peasants to doctors within a single lifetime. It was never easy – it was in Russia, after all – yet you worked hard and never gave up. You endured. Those are very tough shoes to fill, but I believe I did a somewhat decent job trying. You did the impossible for me, and I hope that one day I can do the impossible for you. Thank you for everything, despite everything. *Bik zur rähmät. Min sezne yaratam.*

[2] Monsieur le Président, si vous lisez ceci (pour une raison qui n'est pas tout à fait claire), merci beaucoup !

Contents

List of Figures

List of Tables

Abstract

This thesis brings together a set of articles that examine economic activity in the Greater Region of Luxembourg, which comprises the Grand Duchy of Luxembourg, the German federal states of Saarland and Rhineland-Palatinate, the French departments of Moselle, Meuse, and Meurthe-et-Moselle, and the Belgian province of Luxembourg. The analysis focuses on fiscal competition, migration, housing, and cross-border commuting, using the framework of quantitative structural models in urban economics and economic geography.

In Chapter 1 (co-authored with Pierre M. Picard), we document large floorspace price discrepancies at Luxembourg's borders with Belgium, France, and Germany. Using data from the functional urban area of Luxembourg, we document significant floorspace price discontinuities at the borders of Luxembourg with Belgium, France, and Germany. Employing a quantitative spatial urban model and spatial regression discontinuity techniques, we show that differences in tax rates and tax importation account for 9% and 17% of the observed price jump, respectively. The remaining price discrepancy is explained by differences in productivity and amenities.

In Chapter 2 (co-authored with Pierre M. Picard), we study the effects of congestion relief in a spatial general equilibrium model of Luxembourg and its cross-border commuting zone. Using traffic speed data, we apply a difference-in-differences design on Luxembourg's highways to measure congestion severity and identify choke points. We then simulate counterfactual scenarios where highway speeds are set to free-flow levels and track the resulting changes in output, welfare, and fiscal revenues. Economic output rises in Luxembourg City and Esch, while other cities lose production but gain in resident welfare. For residents of Luxembourg City, we estimate a short-run welfare loss of €1,140 per person per year, which becomes a welfare gain of €3,490 in the long run after population reallocation. When accounting for migration from the outside economy, the welfare effect in Luxembourg City turns negative at €8,110 per person per year. The elimination of congestion induces a fiscal gain of €2.50 billion per year in the short run, €1.18 billion in the long run, and €7.04 billion when accounting for migration inflows.

In Chapter 3 (co-authored with Michał Burzyński and Bertrand Verheyden), we develop a spatial general equilibrium model of commuting that incorporates radiation-style sequential job search with endogenous wages and amenities. Calibrated to granular data for Luxembourg and its cross-border region, the model reproduces heterogeneous mobility responses across occupations and countries, and shows that shorter commutes can raise both wages and employment when larger opportunity sets intensify competition for labor.

Introduction

The Greater Region of Luxembourg is one of the most integrated yet heterogeneous cross-border labor markets in Europe. Historically, it developed as an industrial and mining basin spanning Luxembourg, Wallonia, Lorraine, Saarland, and Rhineland-Palatinate. The decline of heavy industry in the second half of the twentieth century shifted the region's economic center of gravity toward Luxembourg, which specialized in financial and service activities. With the establishment of the European Single Market and the Schengen Area, barriers to mobility across the borders of Luxembourg, France, Belgium, and Germany were largely removed, allowing daily cross-border commuting to expand to an exceptional scale. Today, nearly half of Luxembourg's workforce consists of commuters from neighboring countries, creating some of the densest and most persistent cross-border labor flows in the EU.

The collapse of the steel industry left deep scars in Wallonia and Lorraine, where deindustrialization led to persistent unemployment, population decline, and social dislocation. For these regions, access to the Luxembourgish labor market offers an economic lifeline, with daily commuting flows providing income and stability that would otherwise be difficult to sustain locally. At the same time, Luxembourg itself is not exempt from structural tensions. Despite its high wages and dynamic service economy, it has one of the highest shares of working poor in the European Union, largely due to housing costs. Housing shortages and affordability concerns are consistently ranked among the main issues facing residents. A further asymmetry arises from tax importation: labor income earned in Luxembourg is taxed at the place of work, and contributions from cross-border workers account for up to 20% of government revenue through income taxes and social security contributions. With little redistribution to the jurisdictions where these workers reside, the system effectively transfers resources from cross-border workers to residents of Luxembourg. Combined with severe congestion pressures, these imbalances reveal that the prosperity of the region is shared unevenly, and that integration through commuting generates both opportunities and frictions. My dissertation examines three specific frictions in detail.

The first friction is related to the role of **taxation** in shaping land and housing markets. Floorspace prices in Luxembourg City are markedly higher than those just across the border, with a discrepancy of roughly 60%. Taxation contributes to this pattern through two channels: directly, by affecting firms' cost structures, and indirectly, through the improved provision of public goods generated by tax importation. Using a quantitative spatial economic model, we decompose the discontinuity and find that taxation-related mechanisms account for up to 26% of the price gap – 9% from the direct tax effect, and 17% from tax importation. The role of tax importation is particularly contentious in political debates across the Greater Region. Luxembourgish politicians argue that while labor taxes and social security contributions are collected at the place of work, value-added tax is paid at the place of residence. They maintain

that any fiscal surplus generated by cross-border workers is offset by a shortfall in VAT taxes, as most of their consumption occurs outside Luxembourg. To evaluate this claim, we incorporate both labor-related and consumption taxes into the model. Counterfactual simulations show that although VAT provides significant revenue for neighboring countries, it does not offset the forgone labor tax revenue and social contributions. In fact, model predictions imply that closing Luxembourg's borders entirely would increase fiscal revenues in the surrounding countries, underscoring the scale of the fiscal extraction embedded in the current system.

The second friction is **congestion**. Despite high incomes and free public transport within Luxembourg, commuting flows from abroad generate severe rush-hour bottlenecks, particularly at border crossings and motorway exits. Congestion increases travel times and commuting costs for cross-border workers, while simultaneously limiting labor market access to the Luxembourgish core. These barriers redistribute welfare: residents of Luxembourg City, less exposed to highway congestion and more reliant on public transport, benefit from reduced labor market competition and lower housing rents, whereas commuters from France, Belgium, and Germany incur substantial time losses. In the second chapter of the thesis, we conduct an appraisal exercise of a counterfactual policy aimed at eliminating congestion. We assess the willingness to pay for such measures using the ex-post compensating wage variation. We find that this policy would yield significant utility gains almost everywhere, with the strongest gains observed in Thionville and Arlon, two major commuter towns located less than 30 km from Luxembourg City. The capital of Luxembourg is the only location in the economy where this policy would not immediately increase welfare but would actually decrease it in the short run; the reason for this is intensified labor market competition and upward housing pressure, primarily generated by the expanding demand for commercial real estate. However, such a counterfactual policy would generate substantial fiscal gains amounting to around €1.2 billion per year.

The third friction is related to the **job search process** itself. Standard models typically assume global optimization in commuting choices, yet empirical evidence shows that job searches are far from frictionless. In Luxembourg, opportunities in highly specialized sectors, such as finance, banking, and research, are abundant and relatively easy to access, while workers in manufacturing, services, or elementary occupations face greater search difficulties. These frictions shape the distribution of economic activity, but they are not well captured by conventional quantitative spatial models. To address this, we adapt a search-based framework inspired by radiation models of human mobility to an economic setting featuring endogenous wages and density-dependent congestion forces. Workers search outward from their residences and accept the first offer that yields a utility gain relative to staying at home – a mechanism rooted in reservation wage models and the "first-better" acceptance principle. Job search thus becomes a stochastic process that generates agglomeration without relying on knowledge spillovers. This formulation embeds realistic frictions into commuting choices and provides a structural explanation of how infrastructure and labor demand interact to produce spatial patterns of employment and residence. Calibrated to Luxembourg and its neighboring regions, the model shows that reductions in travel times expand opportunities unevenly across occupations, with significant consequences for the spatial allocation of labor.

Overall, this thesis advances the understanding of economic activity in the Greater Region. It emphasizes the importance of tax importation, cross-border commuting, congestion, and job search frictions for the welfare of residents, and it shows how these mechanisms interact with both the housing market and the public budget.

Chapter 1

Floorspace Price Discontinuities and Taxation in Cross-Border Commuting Areas

This chapter is based on joint work with Pierre M. Picard.

1.1 Introduction

The emergence of the European Union and the free movement of workers have led to cross-border commuting and, consequently, to cross-border housing markets. Prominent examples include the Swiss-French housing market around Geneva, the Swiss-French-German housing market around Basel, and the Danish-Swedish housing market around Copenhagen and Malmö. In particular, floorspace prices exhibit significant changes at these borders. Although several researchers recognize the existence of a "border effect" in cross-border housing markets within the EU (Sielker et al., 2022), to our knowledge, no attempts have been made to explain the underlying causes of these changes. Many observers attribute this land pattern to differing tax systems.

The objective of this chapter is to discuss the factors that explain floorspace price discontinuities at the borders of small jurisdictions with significant tax differences and cross-border labor mobility. We aim to unravel the importance of taxes on labor, goods, and land, along with local productivity, amenities, and public good provision in these price changes.

The chapter focuses on the metropolitan area of Luxembourg City, which is a compelling case study for several reasons. First, its functional urban area spans three neighboring countries: France, Germany, and Belgium, each with distinct taxation rules for labor, goods, and land. Second, this metropolitan area is highly monocentric, with Luxembourg City serving as the main economic hub, attracting commuters from within the country and across borders. Third, since all the countries involved are EU members, workers and firms face no mobility restrictions. Finally, the Luxembourg commuting area provides a prominent example of *tax importation*, the cross-border phenomenon whereby workers pay labor taxes in the country of employment rather than in their country of residence, thereby allocating tax revenue across national borders. Notably, Luxembourg does not have any fiscal arrangements with its neighboring countries to redistribute tax revenues. Labor income is taxed at the place of work, and almost no compensation is provided to the jurisdictions where cross-border workers reside.

In this context, the chapter empirically documents a sharp decrease in floorspace prices – by approximately 60% – on the non-Luxembourgish side of the border. It also documents that commercial development is significantly more concentrated on the Luxembourgish side. These facts are associated with lower tax rates in that country.

It is, however, difficult to assert and quantify a causal relationship between the spatial structure of real estate and taxation. One primary challenge is the limited variation in tax policies within the country and across its three neighboring nations, which restricts the empirical identification of causal effects. Another challenge is that taxes are confounded with many other factors, including local productivity, amenities, land development policies, and agents' choices regarding residential and business locations. This confounding problem is further exacerbated by endogeneity issues arising from production and amenity spillovers that span neighborhoods and jurisdictions. In particular, the econometric assumption of a "stable unit treatment value" is violated since the characteristics of one country can affect foreign locations through the relocation of population, firms, and employment. This interference between spatial units undermines the estimation of causal effects, which is particularly relevant in the context of cross-border labor and housing markets.[3] Consequently, it is necessary to explicitly account for spatial spillovers, which can be addressed using quantitative spatial models.

[3] As a consequence, a simple regression discontinuity design based on the available data is unlikely to reliably identify causal effects.

This chapter therefore develops and estimates a quantitative model that captures the stylized facts described above and assesses the magnitude of the effects of local taxes, productivity, amenities, and government interventions. The structural approach explicitly accounts for the general equilibrium nature of the economic environment and, therefore, for the endogeneity channels that cannot be properly addressed using reduced-form methods with the available data.

We combine this framework with a spatial regression discontinuity design methodology to measure the importance of each factor. More precisely, we conduct a counterfactual exercise where the considered factor is equalized across countries, and then we perform a spatial regression discontinuity analysis on the simulated data to estimate its effect on the price jump. As a result, we show that taxes explain only 9% of the jump observed at the Luxembourg border. Our findings indicate that 17% of the price jump is due to tax importation, another 64% is attributable to productivity differences, and 10% is attributable to natural amenity differences. More intuitively, the price of an 80 m^2 apartment in Luxembourg (in 2022) would be reduced by €28,320 if all taxes had been equalized and €57,040 if tax importation were eliminated.

Our research is of primary interest for several reasons. First, housing is one of the most important assets in modern economies. Many growing metropolitan areas are subject to intense policy debates concerning real estate prices and housing affordability, which often play a central role in election campaigns and results (e.g. Choi et al., 2025). In cross-border regions, these debates raise additional policy questions related to tax incentives and the mobility of labor and businesses, which are the central focus of this chapter. Second, our study of cross-border housing markets demonstrates that national borders—even within economically integrated areas—continue to generate significant discontinuities in housing markets. This insight is essential for evaluating how effectively labor and housing markets function across borders. This chapter offers tools to quantify these effects and to interpret their underlying causes. Third, our findings on the role of cross-country differences in taxation and development density illustrate how county public policy influences residential and business location decisions and shapes the housing market. Finally, our use of a quantitative spatial model combined with a regression discontinuity design illustrates how theoretical urban economic models can be empirically validated and refined. The observed price jump at the Luxembourg border functions as a revealed-preference instrument: its magnitude assigns a direct monetary value to the institutional, fiscal, labor market, and public good characteristics of the Luxembourg side relative to its neighboring regions.

This work relates to several branches of the urban economics literature. First, the chapter pertains to the small tax literature applied to urban structure. In relation to this chapter, Agrawal and Hoyt (2018) discusses the impact of tax differences on the structure of metropolitan areas that overlap different US jurisdictions. Compared to this literature, we examine a novel setting by focusing on Luxembourg as a prime example of tax competition for mobile workers. Second, we build upon existing frameworks by incorporating realistic geography and commuting frictions. Third, we analyze the general equilibrium effects associated with changes in tax rates on housing prices, population and employment reallocation, and productivity. Finally, we integrate several sources of government tax revenue and demonstrate that the effects of different taxes may offset each other.

Second, Luxembourg is a small jurisdiction that sets attractive tax rates. In their study of tax competition, Kanbur and Keen (1993) explain the tendency of smaller jurisdictions to resort to tax dumping. Numerous studies discuss tax competition for capital (Baldwin & Krugman, 2004; Janeba & Osterloh, 2013; Pieretti & Zanaj, 2011), residents (Baselgia & Martínez, 2023;

Schmidheiny & Slotwinski, 2015), and labor (Kleven et al., 2020). The present chapter expands on this literature by highlighting the spatial effects of taxes and tax importation on urban land prices, population, and employment.

Third, traditional urban economics literature often relies on stylized geographic models—such as linear or circular cities—where city structures are either exogenously imposed (e.g., Alonso, 1967) or endogenously determined by agglomeration and congestion forces (e.g., Fujita and Ogawa, 1982, Lucas and Rossi–Hansberg, 2002). In many of these models, land is fully specialized for either residential or commercial use, a simplification that lacks empirical realism. Moreover, under such assumptions—particularly with specialized land use and homogeneous residents—land market arbitrage eliminates land price discontinuities that might arise from differences in labor taxation. Specifically, when identical individuals reside along a strip straddling two jurisdictions, work in only one of them, and pay income taxes accordingly (as required by EU law), they place identical land bid rents on either side of the border. This symmetry prevents discontinuities in land prices. Therefore, to meaningfully explore the causal relationship between labor tax differentials and cross-border land price variation, it is relevant to study geographies with mixed land use, as is done in the recent wave of quantitative urban models.

For a decade, the literature has proposed studying quantitative urban models that are based on observed geographical settings and allow for mixed land uses (Ahlfeldt et al., 2015, Delventhal et al., 2022, Tsivanidis, 2019, etc.). This chapter is embedded in this literature and discusses the issues of geographical division into separate jurisdictions with distinct tax regimes. This approach requires highly granular data on prices, population, and employment. Therefore, the chapter relies heavily on various techniques for data disaggregation to obtain the low-level data needed to power these models. Some of the novel approaches are related to the work of Ahlfeldt (2011) and Ahlfeldt et al. (2021). Price data predictions utilize kriging methods, which account for spatial correlation structures (Wackernagel, 2003 and Cressie, 1988). We construct high-resolution population data by combining administrative and satellite data. Property price data are obtained through web scraping methods from the largest aggregator of property listings in Luxembourg and surrounding regions.

The chapter is organized as follows: Section 1.2 presents stylized facts about the residential and commercial floorspace markets, as well as tax discrepancies across the borders of the country of Luxembourg. Section 1.3 presents a quantitative urban economic model that includes tax collection and expenditure. Sections 1.4 and 1.5 discuss our data, parameter estimations, and model validation. Section 1.6 quantifies the effect of taxation on the model in the absence of geographic discrepancies. Section 1.7 uses counterfactual exercises to break down the factors explaining the price jump at the borders. Section 1.8 further discusses the effects of tax importation, cross-border workers, and potential home bias. Finally, Section 1.9 concludes the chapter. Methodological details and robustness exercises are relegated to the appendices.

1.2 Stylized facts

The focus of this chapter is on the commuting labor market of Luxembourg. This market is part of the Greater Region of Luxembourg, which includes the entire country of Luxembourg, the French region of Lorraine, the Belgian provinces of Luxembourg and Liège, and the German federal states of Saarland and Rhineland-Palatinate. It is the most significant cross-border commuting area in the European Union. Cross-border commuting occurs daily, primarily in the

direction of the city of Luxembourg, attracting up to 200,000 daily commuters, half of whom are from France. The functional urban area of Luxembourg extends beyond the borders of the Grand Duchy, with more than 70% of the total workforce commuting to Luxembourg from abroad and residing in border municipalities of adjacent countries.

In this section, we present three stylized facts about the commuting labor market around Luxembourg. First, we highlight a significant discrepancy in floorspace prices at country borders, with prices per square meter being lower outside Luxembourg. Second, we show that locations on the Luxembourgish side of the borders have more commercial development compared to neighboring areas within a 5 km band from the country borders. Finally, we demonstrate that taxes on goods, real property tax, and labor are significantly lower in Luxembourg than in any of its neighboring countries. Specifically, for labor tax, the marginal tax rate in Luxembourg is lower than in any neighboring country for any given level of gross monthly income.

1.2.1 Floorspace price jump at the border

We divide the geographical area into 1×1 km grid cells and derive the floorspace price indices using listings from `athome.lu`, the largest property price aggregator in Luxembourg. The price indices are adjusted for the hedonic characteristics of housing. Figure 1.1 plots the floorspace price indices as a function of the distance between the cells and their closest borders. These prices are, on average, 60% lower outside Luxembourg than in nearby municipalities within Luxembourg. While earlier literature has identified differences in real estate wealth between these countries (e.g., Mathä et al., 2018), our results highlight significant price discrepancies at the borders of these jurisdictions.

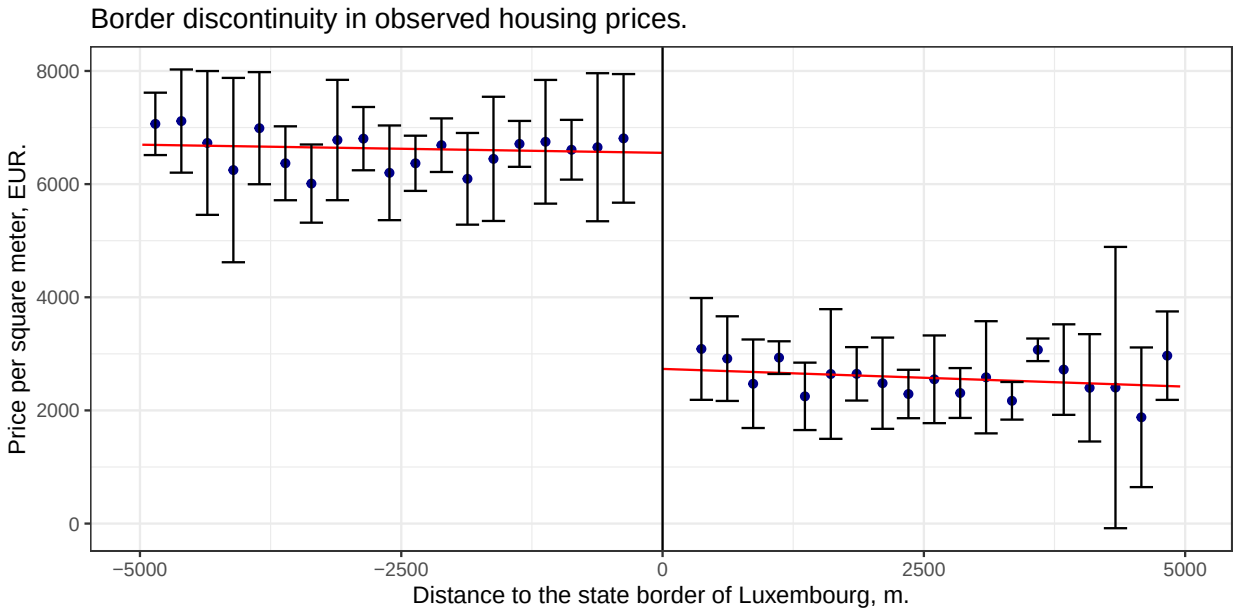

Note: The unit of observation is 1 × 1 kilometer cell. We use hedonics-adjusted cell-specific housing price indices obtained from the data. Negative values of the running variable correspond to cells in Luxembourg. The bars represent the 95% confidence interval. **Source:** `athome.lu` and own calculations.

Figure 1.1: Price jump magnitude in hedonics-adjusted observed housing prices.

To demonstrate the distribution of housing prices across the entire region, we extrapolate the obtained indices using the kriging method to generate the price field (see Appendix 1.B.5).

These price indices are mapped in Figure 1.2, which shows significant discrepancies at the borders of Luxembourg.

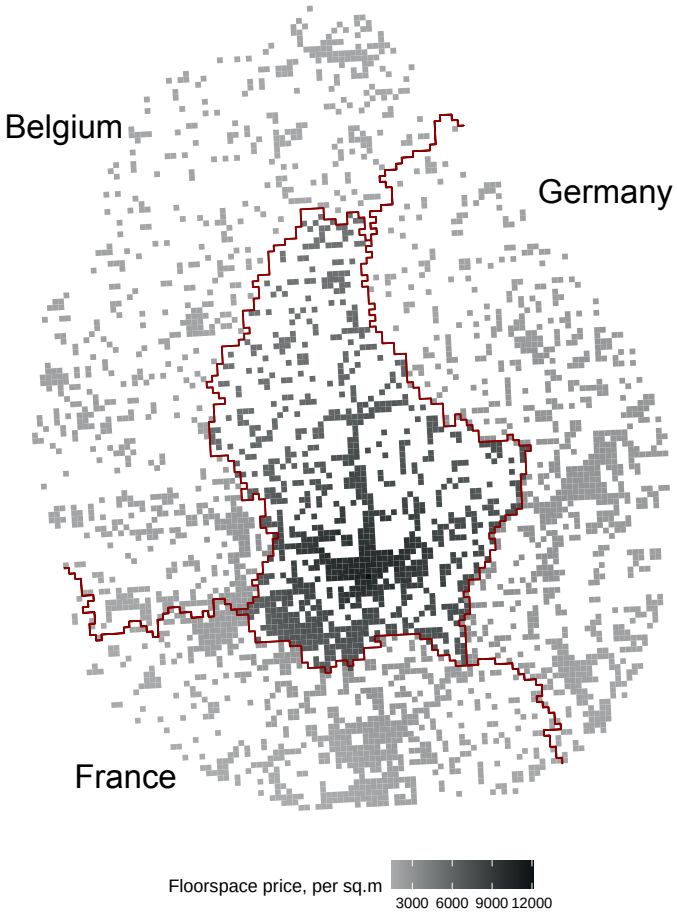

Note: The state borders are shown in red. **Source:** athome.lu and own calculations.

Figure 1.2: Average house prices adjusted for hedonic characteristics of listed properties (€/m^2)

1.2.2 Commercial and residential build-up

The second empirical observation concerns the spatial pattern of commercial build-up across the border of Luxembourg. To this end, we employ GHS-BUILT-S (2020) satellite imagery with high resolution to calculate the proportions of commercial and residential build-up for 100×100 m cells located inside and outside the borders of Luxembourg.[4]

Figure 1.3 depicts the average share of commercial build-up within a 5 km radius of the Luxembourg border. It provides evidence of a discontinuity in the proportion of commercial build-up at the border, with a significantly higher proportion of commercial build-up within

[4] GHS-BUILT-S differentiates residential and commercial areas using image processing and machine learning on high-resolution satellite imagery (Sentinel-2, Landsat) and building data from sources like Facebook, Microsoft, and OpenStreetMap. Built-up types are identified through reflectance, textural, and morphological features. Large structures (e.g., commercial buildings) are detected via textural and connected component analysis. Objects are classified using symbolic machine learning based on training data patterns. The method provides an accuracy level largely above 90% for Western Europe (see Table 4, Pesaresi and Panagiotis, 2023). The main advantage of using GHS-BUILT-S is that it circumvents the issues of administrative data partitioning and compatibility between countries.

Luxembourg's borders. Hence, firms still prefer to establish their production in Luxembourg despite the considerably higher floorspace prices.

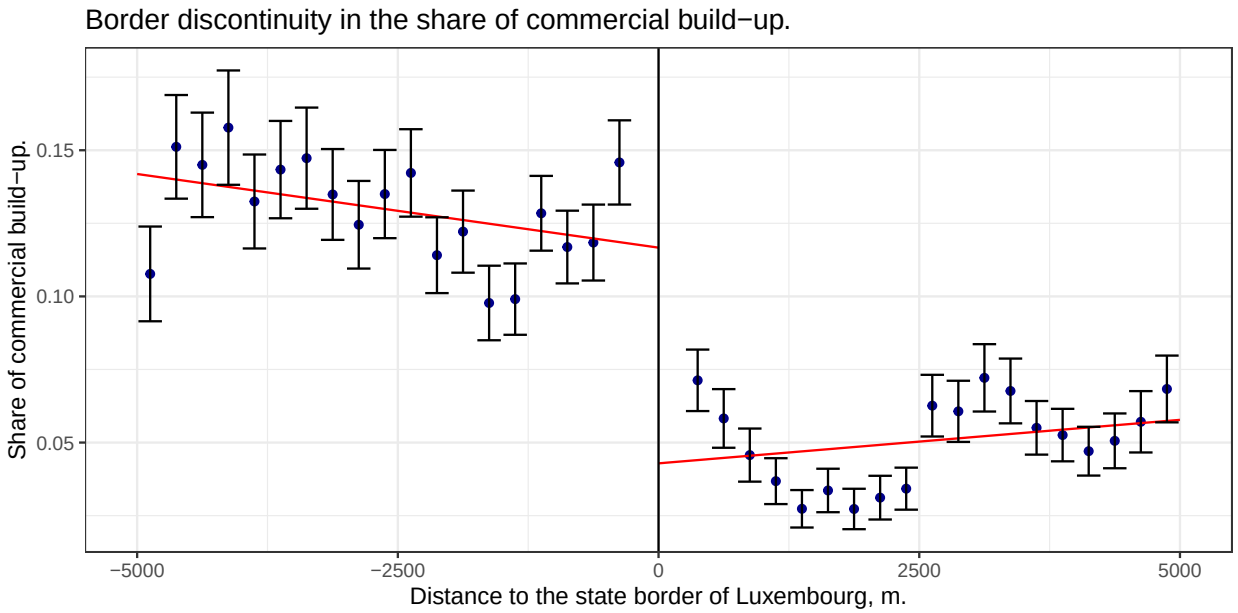

Note: Negative values of the running variable correspond to cells in Luxembourg. **Source:** GHS-BUILT-S (2020) satellite imagery by Copernicus Project.

Figure 1.3: Discontinuity in the share of commercial build-up at country borders.

1.2.3 Cross-border taxation

In the EU, countries are allowed to implement different taxation schemes, provided that they follow the EU tax directives on goods and OECD guidelines on labor taxation. For instance, the VAT Directive (2006/112/EC) ensures some level of commodity tax harmonization and implements the destination principle. By contrast, the EU does not have specific rules for taxing cross-border workers. Each Member State negotiates its own bilateral agreements with neighboring countries to handle the taxation of cross-border workers.

A cross-border commuter is defined as a person who is a resident of one state and commutes daily to work for an employer in another state. As EU treaties prohibit any discrimination against EU workers employed in any other EU country, cross-border workers in the Greater Region of Luxembourg are entitled to the same tax benefits for work-related and personal expenses as residents, provided their situations are comparable. Importantly, cross-border workers employed in Luxembourg pay their labor taxes in Luxembourg on the income earned there. Any additional income earned in the country of residence is taxed according to the regulations of that state. Double tax conventions currently limit cross-border workers working from home or from a third country to fewer than 25 workdays without triggering taxation in the country of residence.

The Luxembourgish cross-border workers are entitled to social security benefits from the Luxembourg state, such as pensions and health insurance. Pension remuneration only takes into account work experience obtained in Luxembourg. Medical expenses of cross-border workers in their country of residence are reimbursed by the National Health Fund of Luxembourg (CNS).

Each country has its unique combination of tax rates for corporate tax, labor tax, VAT, and

land tax. Table 1.1 presents the average rates in the countries studied. It is apparent that Luxembourg has the lowest tax rates in all categories. While the tax differences on goods are limited by EU tax harmonization, labor taxes differ significantly across countries. In particular, labor taxes are roughly 10 percentage points lower in Luxembourg. Ceteris paribus, this allows Luxembourgish firms to offer higher net wages and therefore attract cross-border workers.

Tax	Corporate	Labor	Goods (VAT)	Property
Luxembourg	0.260	0.382	0.17	0.0005
France	0.344	0.476	0.20	0.0125
Belgium	0.296	0.527	0.21	0.0055
Germany	0.298	0.495	0.19	0.0020

Note: The table shows effective tax rates. Labor tax is the tax wedge, i.e., the ratio between the taxes paid by an average single worker (a single person at 100% of average earnings, without children) and the total labor cost of the employer. Real property taxes are defined as property tax payments as a percent of the private capital stock. **Source:** OECD Tax Statistics (2017).

Table 1.1: Tax rates in the Greater Region.

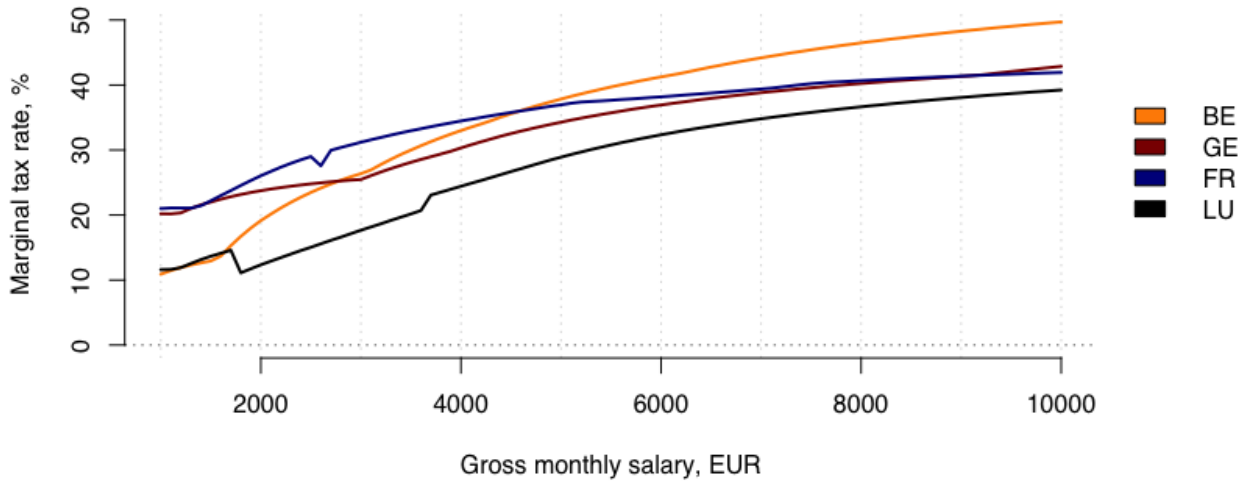

Note: Marginal tax rates are computed for a single worker without dependencies. **Source:** Eurostat Salary Calculator (2023) and own calculations.

Figure 1.4: Marginal tax rates.

The Luxembourg labor market is attractive for all income levels. In fact, although labor taxes are progressive in all countries, marginal labor tax rates are consistently lower there, as shown in Figure 1.4.

1.3 Model

In this section, we present a general equilibrium model adapted to the Luxembourg metropolitan area, which overlaps the countries of Belgium, France, Germany, and Luxembourg. The model is based on Ahlfeldt et al. (2015) and accounts for numerous cross-border workers and differing

taxation on labor, goods, and property across countries. Consumers pay value-added taxes (VAT), while both consumers and firms pay property taxes. In line with OECD and EU tax directives, firms pay labor taxes in the country of production, VAT is paid in the country of residence (destination principle), and property taxes are paid by firms and consumers in the country where houses and plants are located.

Furthermore, each country collects all local taxes and reinvests them in local public goods that enhance local amenities (e.g., schools, recreational areas, road infrastructure, security, etc.). The production of local amenities exhibits decreasing returns to scale and is allocated on a per capita basis within each spatial unit. This formulation of government intervention ensures analytical tractability in the model (e.g., Fajgelbaum et al., 2019) and aligns with the tax importation issues relevant to this metropolitan area (Kanbur and Keen, 1993).

The economy of the cross-national metropolitan area hosts H workers who live and work in several contiguous nations $n \in \mathcal{N}$. The geography consists of a set of locations $i, j \in \mathcal{I}$ that cover these nations in subsets $\mathcal{I}_n$ with $\mathcal{I} = \cup_n \mathcal{I}_n$ and $\mathcal{I}_n \cap \mathcal{I}_{n'} = \{\varnothing\}$. In this text, unless stated otherwise, location indices refer to the entire geography $\mathcal{I}$ while summations $\sum_i$ are also taken over the entire geography $\mathcal{I}$.

We begin by discussing the consumption and location choices of workers and firms.

1.3.1 Consumers

As in Ahlfeldt et al. (2015), each worker, denoted by the subscript $_o$, resides in location $i \in \mathcal{I}$ and works in another location $j \in \mathcal{I}$. She consumes c_{ijo} units of a single final good and l_{ijo} units of floorspace. She incurs a commuting disutility $d_{ij} = e^{\kappa \tau_{ij}} \in [1, \infty)$, where τ_{ij} is the commuting time (in minutes) from i to j, and $\kappa > 0$ expresses the logarithm of this disutility per time unit (minute). Furthermore, she benefits from an exogenous local residential amenity B_i and an endogenous local amenity G_i produced by the national government. She is endowed with a Cobb-Douglas utility function

$$U_{ijo} = \frac{z_{ijo} B_i G_i}{d_{ij}} \left(\frac{c_{ijo}}{\beta} \right)^{\beta} \left(\frac{l_{ijo}}{1-\beta} \right)^{1-\beta}, \tag{1.3.1}$$

where $\beta \in (0,1)$ denotes the share of goods in her expenditure. In this expression, z_{ijo} is an idiosyncratic preference shock over pairs of residential and workplace locations. As in Eaton and Kortum (2002), the latter is drawn from the Fréchet distribution with c.d.f. $F(z_{ijo}) = \exp\left(-z_{ijo}^{-\varepsilon}\right)$, where the shape parameter ε controls the dispersion of preference shocks. The greater ε is, the more homogeneous preferences are. This class of preference shocks generates an upward-sloping labor supply curve with Inada conditions in each location.

The worker's budget constraint is given by

$$w_j = t_i^c c_{ijo} + t_i^q Q_i l_{ijo},$$

where w_j denotes her net-of-tax wage earned at location j, Q_i the before-tax floorspace price, t_i^c and $t_i^q \in (1, \infty)$ the tax multipliers, respectively, on goods and floorspace. The VAT and floorspace tax rates are given by $t_i^c - 1$ and $t_i^q - 1$. Taxes are the same across locations within the same country but differ between countries. As mentioned above, goods and residential floorspace are consumed in the country of residence and are taxed there according to the

destination principle.[5] Such a tax treatment constitutes a major departure from Ahlfeldt et al. (2015). Assuming that goods are freely traded and transported at no cost across locations, the (before-tax) price of the good is equal everywhere and can be normalized to one w.l.o.g.

The timeline is as follows: first, the worker moves into the area before the realization of her preference shock. She then observes her preference shock realizations for all pairs of residential and workplace locations. Finally, she chooses her optimal locations to live and work, as well as her consumption levels, taking prices as given. We solve this sequence through backward induction.

After the realization of her preference shock, the worker chooses the consumption levels that maximize her utility, subject to her budget constraint. Her optimal demands for goods and floorspace are given by

$$c_{ijo} = \frac{\beta w_j}{t_i^c} \quad \text{and} \quad l_{ijo} = \frac{(1-\beta) w_j}{t_i^q Q_i}, \tag{1.3.2}$$

while she obtains an indirect utility given by

$$u_{ijo} = \frac{z_{ijo} B_i G_i w_j}{d_{ij} (t_i^c)^{\beta} (t_i^q Q_i)^{1-\beta}}, \tag{1.3.3}$$

which has the same Fréchet distribution as z_{ijo}.

The worker then chooses the pair of residence i and workplace j that maximizes this indirect utility. Using the properties of the maximum operator on variables with Fréchet distributions, one establishes the following expression for the probability of commuting between i and j:

$$\pi_{ij} = \frac{\Phi_{ij}}{\Phi}, \tag{1.3.4}$$

where

$$\Phi_{ij} = \left[\frac{B_i G_i w_j}{d_{ij} (t_i^c)^{\beta} (t_i^q Q_i)^{1-\beta}} \right]^{\varepsilon},$$

and $\Phi = \sum_i \sum_j \Phi_{ij}$. Summing probabilities across workplaces for a given residence, we obtain the probability of residing in i,

$$\pi_{Ri} = \sum_j \Phi_{ij} / \Phi. \tag{1.3.5}$$

Similarly, the probability of working in j is given by

$$\pi_{Mj} = \sum_i \Phi_{ij} / \Phi. \tag{1.3.6}$$

Residential and employment populations are then given by $H_{Ri} = \pi_{Ri} H$ and $H_{Mj} = \pi_{Mj} H$. Conditional on residing in i, the probability of commuting to j is given by $\pi_{ij|i} = \pi_{ij} / \pi_{Ri} = \Phi_{ij} / \left(\sum_{j'} \Phi_{ij'} \right)$, which yields

$$\pi_{ij|i} = \frac{(w_j / d_{ij})^{\varepsilon}}{\sum_{j'} (w_{j'} / d_{ij'})^{\varepsilon}}. \tag{1.3.7}$$

[5] This is the case for most commodities and services purchased by residents.For simplicity, we assume away the possibility of cross-border shopping.

Finally, before preference shocks are realized and locations and consumption are chosen, workers obtain an expected utility $\mathbb{E}[u] = \Gamma_0 \Phi^{\frac{1}{\varepsilon}}$, where the expectation is taken over the distribution of preference shocks. $\Gamma_0 = \Gamma(1 - 1/\varepsilon)$ and $\Gamma(\cdot)$ denote the Gamma function. Under free mobility, workers enter the geographical area if their expected utility exceeds their reservation utility in the wider economy, $\bar{U}$. In an open city equilibrium, it must be that

$$\mathbb{E}[u] = \bar{U}. \tag{1.3.8}$$

1.3.2 Firms

Firms operate under constant returns to scale and perfect competition, selling final goods at a unit price in the global market. In each location j, they produce Y_j units of the final good using H_{Mj} units of labor and S_{Mj} units of floorspace, according to a Cobb–Douglas production function

$$Y_j = A_j H_{Mj}^{\alpha} S_{Mj}^{1-\alpha}, \tag{1.3.9}$$

where A_j is a location-specific productivity and $\alpha \in (0, 1)$ denotes the share of labor in total cost. Production cost is given by $t_j^w w_j H_{Mj} + t_j^q q_j S_{Mj}$, where w_j is the net-of-tax wage, q_j is the floorspace price, $t_j^w > 1$ is the labor tax multiplier, and $t_j^q > 1$ is the floorspace tax multiplier. The labor tax rate is given by $t_j^w - 1$.

Firms maximize their profits. Their optimal input is given by $H_{Mj} = \alpha Y_j / (w_j t_j^w)$ and $S_{Mj} = (1-\alpha) Y_j / (q_j t_j^q)$. Under free entry, they make zero profits, which occurs if the following zero-profit condition holds:

$$A_j = \left[\frac{t_j^w w_j}{\alpha} \right]^{\alpha} \left[\frac{t_j^q q_j}{1-\alpha} \right]^{1-\alpha}. \tag{1.3.10}$$

Intuitively, excessively high wages or floorspace prices reduce the number of firms in a location, which pushes wages and floorspace prices downward. Similarly, higher local productivity pushes wages and floorspace prices upward. This establishes a negative relationship between local wages and floorspace prices à la Roback (1982).

1.3.3 Construction sector

Floorspace S_j is supplied by a competitive construction sector that uses capital K_j and land L_j as inputs, producing floorspace with a technology given by $S_i = K_i^{\mu} L_i^{1-\mu}$, where μ is a parameter. The capital price is determined by the international capital market, while the land price is endogenous. As in Ahlfeldt et al. (2015), the floorspace supply by this sector is given by

$$S_i = \phi_i L_i^{1-\mu}, \tag{1.3.11}$$

where $\phi_i \equiv K_i^{\mu}$ refers to *density of development*, which acts as a location-specific floorspace supply shifter.

1.3.4 Government

Each government collects national taxes and reinvests them in the form of local public investments that produce G_i units of local amenities in national locations. To reflect the reality of the countries under study, we assume that the government treats its residents equally and invests the same amount g_i per resident (e.g. schools, infrastructure, etc.). Local amenities are assumed to be given by the following production function

$$G_i = (g_i)^{\zeta}, \tag{1.3.12}$$

where $\zeta \in (0,1)$ captures decreasing returns to scale. Note that the expected consumption of goods and the expected consumption of floorspace in a location i are equal to $\mathbb{E}[c|i] = (\beta/t_i^c)\mathbb{E}[w|i]$ and $\mathbb{E}[l|i] = ((1-\beta)/t_i^w)\mathbb{E}[w|i]$, where $\mathbb{E}[w|i]$ is the expected wage conditional on residing in location i. As a result, the government budget constraint of country n takes the following form:

$$\begin{aligned}\sum_{i\in\mathcal{I}_n} g_i H_{Ri} &= \sum_{i\in\mathcal{I}_n}\left[\frac{t_i^c-1}{t_i^c}\beta + \frac{t_i^q-1}{t_i^q}(1-\beta)\right]\mathbb{E}[w|i]H_{Ri} \\ &\quad + \sum_{j\in\mathcal{I}_n}\Big[(t_j^w-1)w_j H_{Mj} + (t_j^q-1)q_j S_{Mj}\Big].\end{aligned}$$

Here, the left-hand side expresses government spending, and the right-hand side expresses taxes on national residents and firms. Since taxes and per capita investments are equal within this country, we can index them by the same country index n, so that

$$\begin{aligned}g_n &= \frac{t_n^c-1}{t_n^c}\beta\frac{\sum_{i\in\mathcal{I}_n}\mathbb{E}[w|i]H_{Ri}}{\sum_{i\in\mathcal{I}_n}H_{Ri}} + \frac{t_n^q-1}{t_n^q}(1-\beta)\frac{\sum_{i\in\mathcal{I}_n}\mathbb{E}[w|i]H_{Ri}}{\sum_{i\in\mathcal{I}_n}H_{Ri}} \\ &\quad + (t_n^w-1)\frac{\sum_{j\in\mathcal{I}_n} w_j H_{Mj}}{\sum_{i\in\mathcal{I}_n}H_{Ri}} + (t_n^q-1)\frac{\sum_{j\in\mathcal{I}_n} q_j S_{Mj}}{\sum_{i\in\mathcal{I}_n}H_{Ri}}.\end{aligned} \tag{1.3.13}$$

At given prices and spatial distributions of firms and residents, higher taxes increase tax revenues and local government investments. Observe that the third term shows the effect of the labor tax component, which leads to labor tax importation. Ceteris paribus, a rise in location j's employment increases per capita government investment by

$$\frac{\partial g_n}{\partial H_{Mj}} = \frac{(t_n^w-1)w_j}{\sum_{i\in\mathcal{I}_n}H_{Ri}}. \tag{1.3.14}$$

A smaller residential population, therefore, increases the tax benefits of attracting more firms to the country. This factor is particularly important for Luxembourg, where many workers commute from neighboring countries.

1.3.5 Urban externalities

In every location j, local productivity A_j depends on production fundamentals a_j and production externalities Υ_j. Production fundamentals capture factors that make a location more productive,

independent of the surrounding density of economic activity. Production externalities relate the productivity in a location to the employment density of its neighboring locations. The structure of productivity is as follows:

$$A_j = a_j \Upsilon_j^{\lambda}, \quad \text{and} \quad \Upsilon_j = \sum_i e^{-\delta \tau_{ij}} \left(\frac{H_{Mi}}{L_i} \right). \tag{1.3.15}$$

In this definition, externalities increase with employment densities H_{Mi}/L_i in surrounding locations i and decline with travel time to those locations, following a spatial decay parameter δ. The parameter λ controls the importance of externalities in overall productivity.

Similarly, the local amenity B_j depends on residential fundamentals b_i and residential externalities Ω_i:

$$B_j = b_j \Omega_i^{\eta}, \quad \text{and} \quad \Omega_i = \sum_j e^{-\rho \tau_{ij}} \left(\frac{H_{Rj}}{L_j} \right), \tag{1.3.16}$$

where H_{Rj}/L_j is the residential density, ρ the spatial decay, and η controls the importance of residential externalities in overall amenity. As in Ahlfeldt et al. (2015), there exists a potential for multiple equilibria in the model if externalities are strong enough relative to the exogenous differences in characteristics across locations.

1.3.6 Market clearing and equilibrium

In equilibrium, markets clear in every location. As mentioned above, product and capital prices are fixed by external (international) markets. The prices of labor and floorspace result from the balances in local supply and demand. We discuss the clearing conditions for the labor and floorspace markets.

On one hand, the labor market in location j balances the demand for workers by firms H_{Mj} with the number of commuters who offer their workforce there. This gives the labor market clearing condition: $H_{Mj} = \sum_i \pi_{ij|i} H_{Ri}$. Using the value of $\pi_{ij|i}$, this implies

$$H_{Mj} = \sum_i \frac{(w_j / d_{ij})^{\varepsilon}}{\sum_{j'} (w_{j'} / d_{ij'})^{\varepsilon}} H_{Ri}. \tag{1.3.17}$$

On the other hand, the floorspace market clears in every location if the floorspace supplied by the construction sector, S_i, expressed in (1.3.11), matches the demand from residents and firms. In equilibrium, floorspace is allocated to the highest bidder among firms and residents. To reflect the presence or absence of these two demand segments, we introduce the share of commercial floorspace over total floorspace, $\theta_j \in [0, 1]$. The market clearing condition in the commercial segment can then be expressed as

$$\theta_j S_j = A_j^{\frac{1}{\alpha}} \left[\frac{1-\alpha}{t_j^q q_j} \right]^{\frac{1}{\alpha}} H_{Mj}, \tag{1.3.18}$$

while the one in the residential segment is

$$(1-\theta_i)S_i = (1-\beta)\frac{E[w_j|i]H_{Ri}}{t_i^q Q_i}. \tag{1.3.19}$$

Finally, in equilibrium, floorspace must be fully commercial if firms pay more than residents, and fully residential if they cannot. Floorspace must mix commercial and residential activities when firms and residents offer the same price. Let P_i be the equilibrium floorspace price. Then,

$$\begin{cases} P_i = q_i \text{ and } \theta_i = 0 & \text{if } q_i > Q_i, \\ P_i = q_i \text{ and } \theta_i \in [0,1] & \text{if } q_i = Q_i, \\ P_i = Q_i \text{ and } \theta_i = 1 & \text{if } q_i < Q_i. \end{cases} \tag{1.3.20}$$

To sum up, economic geography is defined by a collection of preference and cost parameters $\{\alpha, \beta, \mu, \varepsilon, \kappa\}$, urban externality parameters $\{\delta, \lambda, \eta, \rho\}$, vectors of national tax multipliers $\{t^c, t^q, t^w\}$, vectors of location characteristics $\{a, b, \varphi, L, \xi\}$, a commuting time matrix τ, and a reservation utility $\bar{U}$. Equilibrium is defined by the population H and the vectors of prices $\{Q, q, w\}$, shares $\{\pi_M, \pi_R, g, \theta\}$, and local productivities and amenities $\{A, B, G\}$ that respectively solve the conditions for free mobility (1.3.8), commercial and residential floorspace market clearing (1.3.18), labor market clearing (1.3.17), residential and workplace choices (1.3.5) and (1.3.6), government budget balance (1.3.13), floorspace market arbitrage (1.3.20) and production of urban externalities and local public goods (1.3.15), (1.3.16) and (1.3.12). (See details in Appendix 1.A)

1.4 Data

In this section, we describe the datasets used for parameter estimation and model calibration. We explain our data sources and constructions for commuting times, population and employment densities, floorspace prices, and wages.

Our analysis focuses on the functional area around Luxembourg, which we define as the entire country of Luxembourg and a 50 km deep band within the adjacent areas of France, Belgium, and Germany. Furthermore, we apply the data on a grid of 1×1 km cells covering this geographic area, resulting in a grid with 11,800 cells, as shown in Figure 1.2. To concentrate on urban clusters and minimize computational intensity, we exclude cells with residential and employment densities below 100 individuals per km^2, resulting in 3,182 urbanized cells (non-blank cells in Figure 1.2).

1.4.1 Travel flows and times

To assess travel flows and time, we use the 2017 Luxembourgish "LuxMobil" survey (Ministry of Mobility and Public Works) and the 2017 “Population Census – Mobility Flow Database” (INSEE) for the French departments bordering Luxembourg (Meuse, Moselle, Meurthe-et-Moselle). The data include domestic and cross-border commutes between Luxembourg and France. We restrict the sample to work commutes to and from municipalities located within the functional area defined above. The merged data yield 447 municipalities, from which we construct our travel flow matrix. Pairs of municipalities with no observed commutes are assigned a zero flow. Due to the granularity and anisotropic nature of commute travel, the travel flow matrix includes about 6% non-zero values.

To encompass the entire geographical area, we calculate travel times using the existing road

network with OpenStreetMap and the Open Source Routing Machine, or OSRM (Giraud, 2022). With this algorithm, we calculate the free-flow minimal travel times by car. A focus on car flows is justified by the LuxMobil survey, which reveals that more than 85% of commutes are made by car. Travel within 1 km is predominantly made on foot. Free-flow travel times do not account for congestion. We use this approach to calculate the travel times between the centroids of the municipalities from the "LuxMobil" survey and French census data, as well as between the centers of the grid cells of the commuting matrix. The travel time within a cell or municipality is calculated as the average travel time between a set of 50 randomly selected points along existing roads. Table 1.2 reports summary statistics for the number of commuters and commuting times between all municipalities and those with non-zero flows.

	Mean	SD	Min	Max	Observations
Number of commuters	1.6	34.8	0.0	12,249	199,764
Travel time (min)	53.6	23.9	1.9	139.0	199,764
Number of commuters (non-zero flow)	27.5	144	1	12,249	11,277
Travel time (min, non-zero flow)	28	14.8	2.7	101.8	11,277

Note: The data reports numbers of commuters and travel time for pairs of municipalities within and outside Luxembourg that are located within 50 km from the state border of Luxembourg. The numbers of commuters are extracted from the "LuxMobil" survey and the French Population Census in 2017. Travel times are calculated with OSRM between the centroids of municipalities. Travel time within the same municipality is given by the minimum between the average travel time by car and on foot between 50 randomly drawn points within each municipality.

Table 1.2: Summary statistics for commuting data within 50 km from the border of Luxembourg.

1.4.2 Residential and employment populations

We take the residential population for every 1 × 1 km grid cell from the Global Human Settlement Layer Population Grid (GHS-POP-2023) issued by the European Commission's Joint Research Centre. Population counts are derived from official census and administrative records at the municipal level for 2020, harmonized and disaggregated using satellite-derived built-up area information.

We construct our employment data by mapping administrative employment records to every 1 ×1 km grid cell according to the municipality's footprint and the cell's total build-up information reported in the GHS-BUILT-S dataset issued by the aforementioned Centre. Administrative employment records capture the number of workers at their place of work in the municipalities of Luxembourg, Germany, France, and Belgium, including cross-border employment. A dasymetric mapping strategy is used to accurately allocate employment to grid cells (see details in Appendix 1.B).

	Mean	SD	Min	Max	Observations
Population (individuals/cell)	512	828	5	13,364	3,182
Employment (individuals/cell)	512	2,015	0	40,108	3,182
Prices (€ /m^2)	3,715.5	2,440.4	1,440.4	12,083.4	3,182

Note: Population and employment report the numbers of residents and workers per cell. Floorspace price gives the price index (€ /m^2) attributed to each cell after hedonic price adjustment.

Table 1.3: Summary statistics on cell data.

Restricting the dataset to the Luxembourg functional area results in 11,800 cells. To facilitate

numerical computations, we also exclude all cells with population or employment density less than 100 individuals per km^2. This results in 3,182 active cells as depicted in Figure 1.2, which capture 91.5% of the total population and 97.5% of total employment. We finally equalize population and employment in the economy by scaling the employment in each cell by the ratio of total population to total employment. The summary statistics of the residential population and employment in the cells are presented in the first two rows of Table 1.3.

1.4.3 Floorspace prices

We build floorspace price indices using information on property prices obtained from the largest property listings aggregator, `athome.lu`. This source covers the Grand Duchy of Luxembourg and adjacent regions in France, Belgium, and Germany, while offering property listings for sale and rental properties with geocoded information and hedonic characteristics (from which we retain ten features, including surface area). Data was collected from the website between March and September 2022. Because this data includes twice as many price observations as rental ones, we construct the index for floorspace prices. Housing prices and rents, however, exhibit very similar characteristics (Appendix 1.B.4 and 1.B.5). Outliers in the highest 5% and lowest 5% of prices are removed in each country.

A floorspace price index is computed for each cell using a hedonic price regression model or geostatistical interpolation. More precisely, for the cells with property listings, we run hedonic regressions of the logarithm of prices across the geographical area, including surface area and other hedonic controls, along with a fixed effect for each cell. The fixed effect yields the price index of the cell (Appendix 1.B.4). For cells without property listings, we interpolate the price index between all available cells with more than 5 listings using a universal kriging procedure (Appendix 1.B.5). The summary statistics of price indices are described in the third row of Table 1.3, which are consistent with those in Figure 1.2

1.4.4 Wages

Finally, to estimate the Fréchet parameter ε, we use the net hourly wage data at the municipal level. For Luxembourg, this data is approximated by adjusting the official average gross yearly wages in 2020 from the Luxembourg statistical office (STATEC), using the 2017 tax brackets (single worker, Tax Class 1) and dividing by the average annual hours worked (OECD data). For France, INSEE provides nominal hourly wage data by French municipal communes (with populations over 2,000) for a single worker with no dependents.

1.5 Estimations

For this chapter, we estimate four parameters specific to the functional area of Luxembourg using the data above. These parameters include the commuting elasticity κ, the Fréchet scale parameter ε, the productivity spillover parameter λ, and the residential spillover parameter η. Other parameters will be sourced from the literature.

1.5.1 Semi-elasticity of commuting

The parameter bundle, $\varepsilon\kappa$, denoted here as ν, is estimated using data on work travel by car in Luxembourg and surrounding countries, provided by the "LuxMobil" survey and the French

census. We use the equation for the unconditional commuting probability (1.3.4) and write it as

$$\log \pi_{ij} = -\nu\tau_{ij} + \xi_i + \zeta_j + \epsilon_{ij}. \tag{1.5.1}$$

Here, ξ_i represents origin-specific fixed effects, such as amenities and floorspace prices, while ζ_j captures destination-specific fixed effects. The origin-specific and destination-specific variables are absorbed by the fixed effects.

Dependent variable:	Commuting flows, log		
	LuxMobil	INSEE	Both
OSRM Travel Time, min	-0.110***	-0.129***	-0.116***
	(0.006)	(0.005)	(0.004)
Origin FE	Yes	Yes	Yes
Destination FE	Yes	Yes	Yes
Origin	LU	FR	LU+FR
Destination	LU	FR	LU+FR
R^2	0.810	0.842	0.840
Observations	13,689	52,649	116,827

Note: Departure communes are within 50 km from the state border of Luxembourg. Standard errors in parentheses. * p < 0.1, ** p < 0.05, *** p < 0.01.

Table 1.4: Commuting elasticity estimation.

To estimate this regression model, we associate the work trips made by car, provided by the "LuxMobil" survey and the French census, with the travel times computed above. To balance municipality sizes in Luxembourg and France, we consider French municipalities with more than 2,000 residents. Results are presented in Table 2.C.1. We use the Poisson Pseudo-Maximum-Likelihood (PPML) regression model to account for the count nature and the zeros in commuting flows.

Columns 1 to 3 present PPML estimates for the baseline regression based on different subsamples. Column 1 utilizes "LuxMobil" survey data only. Column 2 uses data from the INSEE commuting survey only. Column 3 uses a combined commuting survey. Estimates are robust to the choice of datasets and the countries of travel origins and destinations (see Appendix 1.C.1). In the subsequent analysis, we use the results in Column 3 with the estimate $\nu = 0.116$.

1.5.2 Residence and workplace preferences

We choose the Fréchet parameter ε that produces wage dispersion closest to the observed one (Ahlfeldt et al., 2015). More formally, we minimize the absolute difference between the variances of the logarithm of the observed wages and the wages simulated by the model, $|\text{var}(\log w_m^{data}) - \text{var}(\log w_m^{sim}(\varepsilon))|$. The net wages w_m^{data} are observed at the municipal level, and the simulated wages $w_m^{sim}(\varepsilon)$ are computed for each cell based on labor market conditions (1.3.17) and then aggregated for each municipality. We find the minimizer $\varepsilon = 4.2$, which yields the value of κ equal to 0.027 (see details in Appendix 1.C.2).

1.5.3 Local characteristics

We recover local productivities A_j, amenities B_i, and development densities ϕ_i by inverting the model using our data on floorspace prices, population, and employment densities, as well as the parameter values estimated previously and those sourced from the literature (see Table 1.6 below). To this end, we invert the model using our data on floorspace prices, population, and employment densities, including the values of the previously estimated parameters. Specifically, the conditions of the labor market (1.3.17) yield wages based on the observed residential populations and travel times. Zero-profit conditions (1.3.10) yield local productivities from these wages and observed floorspace prices. This enables us to establish the government budget and local public good production in (1.3.14). Finally, local amenities are recovered from the identities of residential density (1.3.5). The density of development is obtained from (1.3.11). (See details in Appendix 1.D)

1.5.4 Urban externalities

We finally estimate the importance of externalities in local productivity and amenities. The local productivity and amenities for each location i are defined in (1.3.15) and (1.3.16). We estimate the parameters λ and η, and borrow the decay parameters ρ and δ from Ahlfeldt et al. (2015). Both equations are estimated using the available data on residential and employment densities.

However, we need to consider the endogeneity issue whereby local productivities and amenities are determined by the employment and population densities of surrounding residential and employment areas, which are, in turn, influenced by those productivities and amenities. To address this issue, we instrument production and amenity externalities Υ_i and Ω_i with the spatial distribution of commercial and residential floor area in 1975. More specifically, we compute those externalities from the employment and population imputed from the residential and non-residential built-up area GHS-BUILT-S dataset for 1975 (see details in Appendix 1.C.3). The exclusion restriction is based on the sharp deindustrialization that followed the steel market collapse of 1974-1975. In 1975, manufacturing accounted for more than 45% of total employment in Luxembourg. By 2021, its share had decreased to below 10%.

Table 1.5 presents our regression results. Following Combes et al. (2010) and Combes and Gobillon (2015), the regression models include geographic controls to account for first-nature determinants that may affect current productivity and amenity simultaneously with past population and employment patterns. These geographic controls are also interacted with country indicator variables to allow for country-specific heterogeneity.

The first-stage regression results displayed in Panel A report a strong correlation between current and instrumented externalities, confirming the relevance of the instruments. The second-stage regression results presented in Panel B report significant agglomeration effects and small corrections for endogeneity, which are consistent with the literature, as in Combes and Gobillon (2015). Our estimate for the agglomeration elasticity, 0.07, lies at the upper end of the estimates in the literature (between 0.04 and 0.06), which can be attributed to the current specialization of Luxembourg in banking and services. [6] Finally, our estimate of the elasticity of residential amenity with respect to residential density, 0.028, is significant. This low value is explained by our geography, with a medium-sized city of 150,000 people surrounded

[6] Graham and Gibbons (2019) find agglomeration elasticities about 0.08 for UK business services. Hörcher and Graham (2024) find agglomeration elasticities up to 0.15 for London.

by relatively sparsely populated areas. For the subsequent simulation, we choose the value of 0.03 for the elasticity of amenity with respect to the density spillover.

Dependent variable:	$\log \Upsilon$	$\log \Omega$	log A		log B	
			OLS	IV	OLS	IV
Panel A: First Stage						
$\log \hat{\Upsilon}$	0.949***					
	(0.008)					
$\log \hat{\Omega}$		1.039***				
		(0.004)				
Geographic Controls	Yes	Yes				
Observations	2,658	3,182				
R^2	0.911	0.967				
F-Statistics	1,593.69	5,460.05				
Panel B: Second Stage						
$\log \Upsilon$			0.084***	0.070***		
			(0.005)	(0.006)		
$\log \Omega$					0.032***	0.028***
					(0.003)	(0.003)
Geographic Controls			Yes	Yes	Yes	Yes
R^2			0.431	0.429	0.194	0.193
Wu-Hausman				44.18***		54.74***
Observations			2,658	2,658	3,182	3,182

Note: Geographic controls include log of distance to forests and water, mean elevation, and terrain ruggedness (absolute difference in elevation per cell). All geographic controls are interacted with country fixed effects. Country fixed effects are not included as a separate control. Standard errors in parentheses. * $p < 0.1$, ** $p < 0.05$, *** $p < 0.01$

Table 1.5: Instrumental variable regression results.

1.5.5 Summary

Parameter	Description	Value	Source
ε	Residence–workplace heterogeneity	4.2	Own estimation
λ	Productivity externalities	0.07	Own estimation
η	Amenity externalities	0.03	Own estimation
κ	Commuting disutility	0.028	Own estimation
α	Firms' labor expenditure share	0.7	Valentinyi and Herrendorf (2008)
$1-\beta$	Consumers' housing expenditure share	0.33	Combes et al. (2019)
μ	Housing capital expenditure share	0.65	Combes et al. (2021)
δ	Productivity spatial decay	0.36	Ahlfeldt et al. (2015)
ρ	Amenity spatial decay	0.76	Ahlfeldt et al. (2015)
ζ	Public good production	0.25	Fajgelbaum et al. (2019)

Table 1.6: Parameters.

Table 1.6 summarizes the values and sources of the parameters used in our analysis. The first four rows report the parameters estimated from the data. The remaining rows present

the parameters sourced from the literature. These latter parameters are utilized in the model inversion described above.

1.5.6 Overidentification checks

In this section, we validate the model inversion using additional empirical data. First, we demonstrate that the observed density of development aligns with the model predictions. Second, after controlling for geographic terrain features and the observed number of buildings, we show that neither production nor residential fundamentals exhibit a discontinuity at the border.

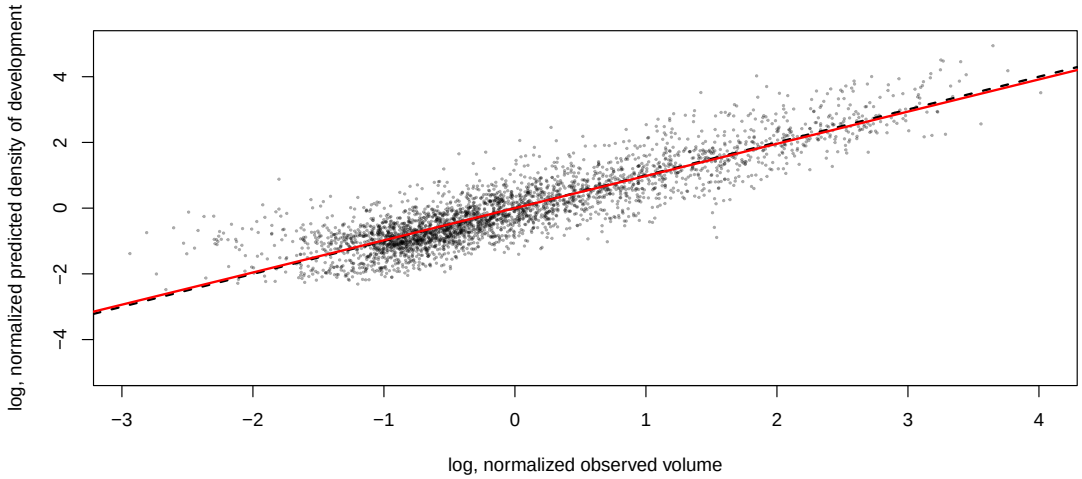

Note: The black dashed line represents the diagonal, while the solid red line indicates the OLS best-fit line. We consider cells with residential and employment density higher than 100 people per km^2. Each axis is normalized by the geometric mean of its respective values. **Source:** GHS-BUILT-V (2020) satellite imagery, Copernicus Project.

Figure 1.5: Predicted density of development against observed build-up volume.

First, we check whether the density of development predicted by the model is greater in locations with more observed build-up volume. Satellite data allow us to observe the build-up volume in each grid cell. Figure 1.5 shows the predicted development density plotted against the observed build-up volume. The figure confirms a strong correlation between these two variables ($R^2 = 0.787$) and a slope coefficient close to one. A similar conclusion holds for the correlation with building height and space (see Appendix 1.D.3).

Then, we show that, controlling for observable first-nature land characteristics and the number of observed buildings, neither production nor residential fundamentals exhibit a discontinuity at the border. To verify this, we focus on a 5 km wide band across the state border of Luxembourg and run a regression discontinuity specification with location in the country of Luxembourg as the treatment indicator and proximity to the state border of Luxembourg as a running variable. Fundamental productivities a_j and amenities b_i are adjusted for the effects of geographical controls to eliminate first-nature advantages, as well as the number of observed buildings. Table 1.7 indicates that cells with similar geographical characteristics and a similar number of buildings inside and outside Luxembourg have very similar fundamental productivities and amenities. The same holds true for the density of development ϕ, which exhibits no jump at the border of Luxembourg.

Dependent variable:	Calibrated values			Residualized values		
	$\log a$	$\log b$	$\log \phi$	$\log a$	$\log b$	$\log \phi$
Luxembourg	0.321***	0.072*	-0.042	0.058	0.008	0.075*
	(0.064)	(0.038)	(0.197)	(0.085)	(0.073)	(0.045)
Distance to border, km	0.014	-0.009	-0.055	0.008	0.009	-0.016**
	(0.012)	(0.007)	(0.037)	(0.014)	(0.014)	(0.007)
Residualized values	No	No	No	Yes	Yes	Yes
Observations	516	567	567	516	567	567
R^2	0.249	0.007	0.019	0.014	0.004	0.010

Note: The table shows regression discontinuity estimates for residualized residential and production fundamentals, and density of development. We restrict cells located within 5 km from the state border of Luxembourg, and reporting non-zero fundamental productivities or amenities. Luxembourg is a dummy variable that is equal to 1 if the cell lies within the country of Luxembourg. To balance cell characteristics across the cutoff, the fourth, fifth, and sixth columns use residualized values of production fundamentals, residential fundamentals, and density of development. Residualized values are defined as residuals of the OLS regression of the latter on geographic controls and the number of observed buildings for the whole sample of locations. The list of geographical controls is identical to those used in Table 1.D.3. Robust standard errors in parentheses. * $p < 0.1$, ** $p < 0.05$, *** $p < 0.01$.

Table 1.7: Effect of Luxembourg on production and residential fundamentals, and density of development.

In Appendix 1.D.3, we further check that Luxembourg's administrative border does not affect workers' expected income, commuting market access, productivity, or the residential spillover predicted by the model, while it does affect floorspace prices and commercial build-up shares. This suggests that the model replicates the commercial build-up jump and its magnitude. Finally, we also show that fundamental productivities and residential amenities correlate with observable first-nature features.

1.6 Effects of taxation

As stated in the stylized facts, discrepancies in country taxes are essential factors influencing economic activity in the Luxembourg metropolitan area. In this section, we discuss the general equilibrium effects of taxes in a stylized geography. This geography allows us to disentangle the impact of taxes on economic variables from the effects of location characteristics.

Toward this aim, we consider a circular and featureless geographical area with a 75 km radius, covered by 1×1 km grid cells and including two jurisdictions. The first jurisdiction occupies the area within 25 km of the central point, while the second jurisdiction is larger and covers the remaining area. The central jurisdiction, therefore, has a smaller land area. The geography is featureless in the sense that the residential fundamentals, production fundamentals, and density of development are set equal to one in each cell. The travel distances between cells are determined by Euclidean distances. The only differences between locations are the VAT, land, and labor tax regimes. The area mimics Luxembourg's actual commuting market to account for similar commuting times and urban externalities. Model parameters are set to those reported in Table 1.6, which will allow for comparison with the following sections.

We present four different scenarios. In the baseline scenario, both countries set identical tax rates, equal to the average observed in Belgium, France, Germany, and Luxembourg. In each of the alternative scenarios, the central jurisdiction reduces its taxes – on goods, floorspace, or labor, respectively – to the levels observed in Luxembourg, while the other jurisdiction

maintains the baseline tax level. We consider an open city where workers arrive from or exit to the external economy. Numerical simulation results are presented in Figures 1.6 to 1.8.[7]

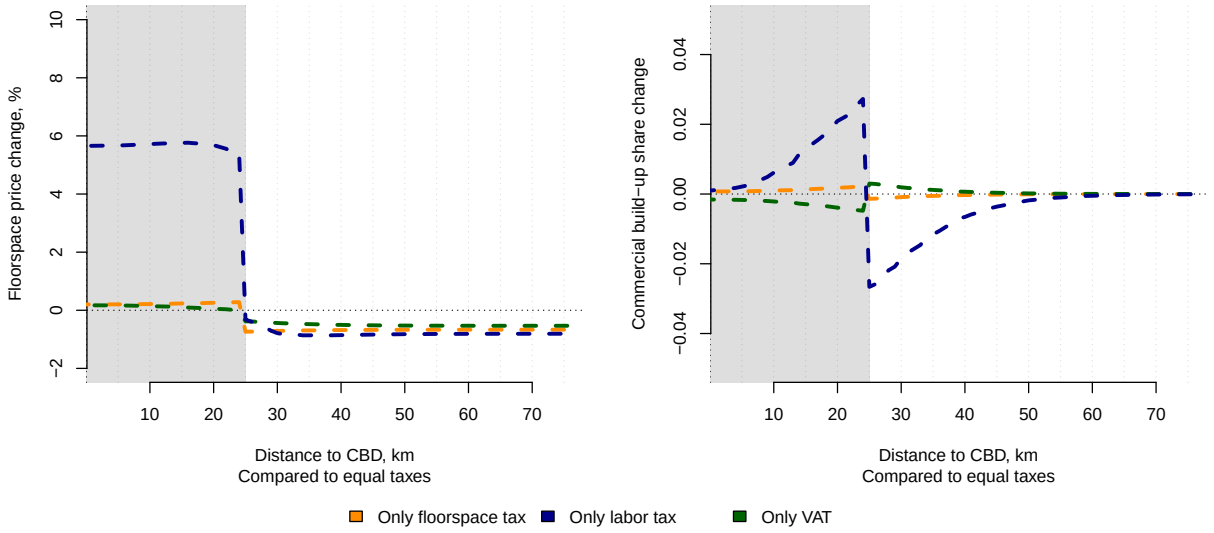

Figure 1.6: Changes in floorspace prices and in share of commercial build-up.

Figure 1.6 shows that the labor tax discrepancy causes a 7% increase in floorspace prices and a drop of about four percentage points in the share of commercial build-up at the jurisdiction border, which is consistent with our stylized facts. The labor tax difference generates the main spatial disparities. Nevertheless, while relative changes in floorspace prices are stable within each jurisdiction, commercial build-up declines at the center and steadily rises as one moves toward the border. At this point, it dramatically falls and then recovers to the baseline level.

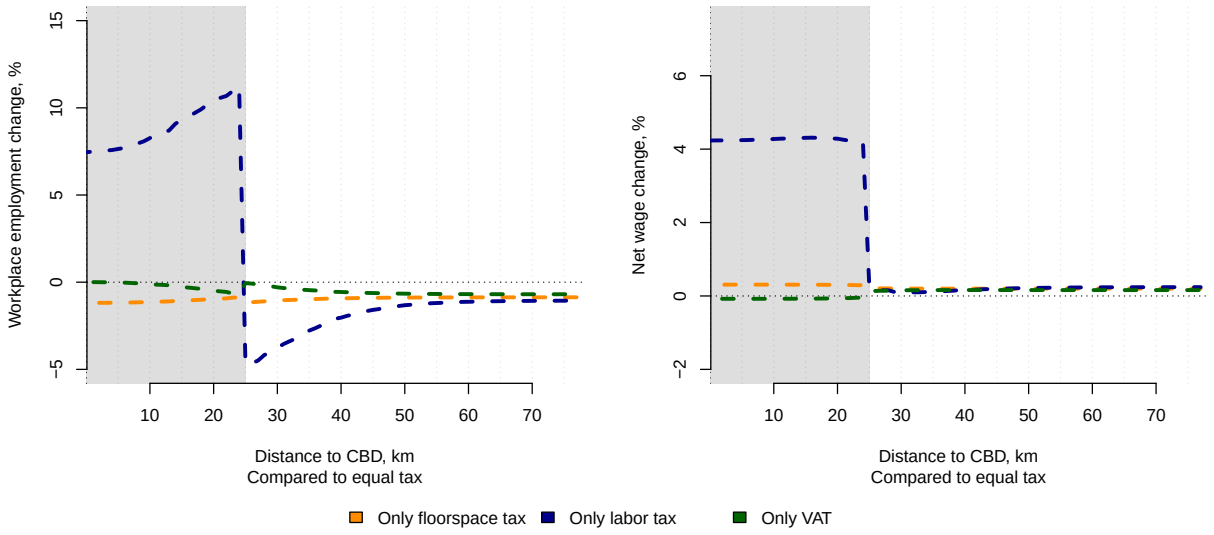

Figure 1.7: Changes in workplace employment and net local wages.

[7] Because of computing time and memory constraints, we restrict the number of grid cells by keeping one cell out of every four cells.

Figure 1.7 shows that a lower labor tax in the central jurisdiction raises net wages and attracts more employment there, while it decreases employment without significantly affecting wages in the outer, larger jurisdiction. Employment rapidly falls by 15% across the border. This is because workers in the border neighborhoods are attracted by large wage differences and incur small travel times to jobs there. The employment difference is largely attributed to the 4% discrepancy in net wages. However, note that only half of the 9 percentage point labor tax difference is passed on to workers' wages due to imperfect spatial mobility. Again, the effects of VAT and real property taxes on workplace employment are negligible compared to the effect of the change in labor tax.

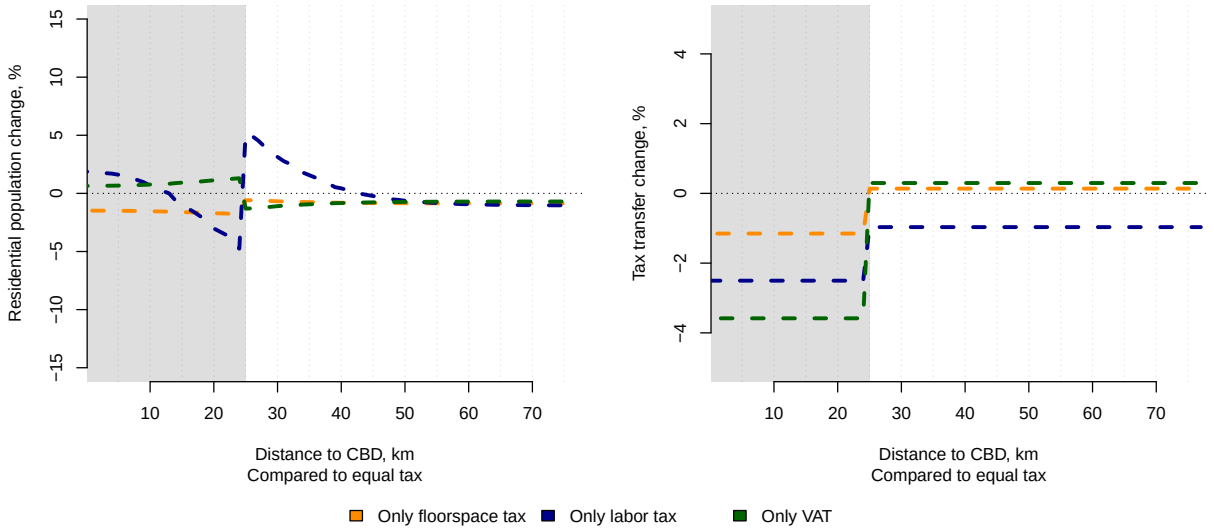

Figure 1.8: Changes in residential employment and public capital investment in local amenities compared to the baseline scenario of no differences in taxation.

The left panel of Figure 1.8 shows that the difference in labor tax encourages the residential population to live close to the border of the external jurisdiction, where floorspace prices are lower and well-paid jobs are still accessible. In contrast, residents avoid proximity to the border of the central jurisdiction, where they must compete for floorspace with more firms at higher prices.

Changes in public capital investment in local amenities are depicted in the right panel of Figure 1.8. From this numerical exercise, the 9 percentage point decrease in labor tax in the central jurisdiction results in a reduction of per-resident tax revenues and local public amenities by only 2.5% in this area and by 1% in the outer jurisdiction. This supports the idea of a tax importation mechanism, whereby the outer jurisdiction loses a share of workers and labor tax contributions. The mechanism is, nevertheless, too weak to generate an increase in per-resident tax revenues in the central jurisdiction. The differences in VAT and floorspace taxes also significantly reduce the central jurisdiction's tax revenues and local public capital investment.

To sum up, the main effect on the spatial economic structure of geography lies in the discrepancies in labor tax regimes. These discrepancies generate significant differences in floorspace prices, commercial development, employment, net wages, residential population density, and local public investment across the border, especially near the border. Second, while employment and commercial activity increase on the interior side of the border and decrease on the exterior

side, the population follows the opposite pattern. These features reflect the key stylized facts outlined in Section 1.2.

1.7 Main results

In this section, we discuss the main results of the chapter. The objective is to disentangle taxation-related effects from the effects of productivity and amenities specific to the country of Luxembourg.

Towards this aim, we decompose the observed floorspace price jump and assess the relative impact of its components. First, we perform a series of nested counterfactual exercises in which we sequentially remove border discontinuities in tax rates, the tax importation mechanism, and discontinuities in fundamental productivities and amenities. By altering only one parameter at a time in each counterfactual, we attribute changes in the price jump to each specific factor. We eliminate tax importation by assuming that all tax revenues collected in the metropolitan area of Luxembourg are gathered by a supranational central administration, which reinvests its revenue on a per capita basis in local public goods across the entire area. Tax rates are maintained at their actual levels.

Dependent variable:	Floorspace price (€/m^2)				
	(1)	(2)	(3)	(4)	(5)
Luxembourg	3,219.266***	2,357.100***	1,988.742***	29.076	-154.898
	(163.329)	(170.512)	(163.650)	(136.544)	(132.991)
Distance to border, km	126.211***	121.205***	112.964***	67.449***	65.425***
	(30.529)	(31.871)	(30.589)	(25.522)	(24.858)
No tax importation	No	Yes	Yes	Yes	Yes
Equal taxes	No	No	Yes	Yes	Yes
No jump in a	No	No	No	Yes	Yes
No jump in b	No	No	No	No	Yes
Observations	568	568	568	568	568
R^2	0.791	0.673	0.623	0.053	0.020

Note: Luxembourg is a dummy variable that is equal to 1 if the cell lies in the country of Luxembourg. Column 1 shows the observed price jump at the border. Column 2 shows the price jump after eliminating the tax importation mechanism. Column 3 shows the price jump after equalizing all taxes across all countries. We equalize taxes to the average across 4 countries. Column 4 additionally eliminates cross-border productivity differences. Finally, Column 5 additionally eliminates residential fundamentals discontinuities. Robust standard errors in parentheses. To adjust fundamental amenity and productivity differences, we use shifters reported in the first two columns of Table 1.7. * p < 0.1, ** p < 0.05, *** p < 0.01.

Table 1.8: Nested counterfactual floorspace price discontinuities.

In Table 1.8, we present the results of our nested counterfactual exercises, showing how different factors contribute to the observed floorspace price jump. Column 1 reports the actual observed floorspace price jump across the border. The subsequent regression estimates reflect the simulated price jump under various counterfactual scenarios. Column 2 shows the floorspace price jump when we eliminate the tax importation mechanism. Column 3 shows the floorspace price jump when we equalize all taxes to their average values across the commuting area. Columns 4 and 5 further eliminate cross-border discontinuities in productivity and residential amenity fundamentals.

The first row of Table 1.8 shows that the effect of the Luxembourg location dummy vanishes as we eliminate tax importation, differences in taxes, fundamental productivities, and fundamental residential amenities. When all local tax and geographical features are eliminated (last column), the spatial economy converges to a monocentric city similar to the actual one (see Appendix 1.E).

The diminishing R^2 suggests the explanatory power of each factor. From the first row, it can be established that the tax importation mechanism explains 27% of the observed price jump. Differences in tax rates account for an additional 11%, while differences in production fundamentals contribute a further 62%. Residential fundamental amenities do not contribute to this. The fact that the Luxembourg coefficient in Column 5 is not significantly different from zero confirms that only the aforementioned factors contribute to the price jump.

The preceding analysis considers a specific sequence for eliminating differences among the four identified factors, although fifteen other sequences are possible. At the same time, interactions and nonlinearities may influence the effect associated with eliminating each factor. To assess the impact of each factor across all possible sequences, we compute the effect of the Luxembourg jurisdiction on floorspace prices across all sixteen possible sequences and then estimate a linear regression model with the coefficient of the Luxembourg dummy variable as the dependent variable and these factors as independent variables. The results are reported in Table 1.9. The high R^2 value and low RMSE indicate that the relationship is well approximated by a linear specification. The coefficients in the table indicate the average value of eliminating each factor's difference. According to the table, on average, tax importation explains 17% of the price jump. Tax differences explain 9% of the floorspace price jump. Spatial differences in fundamental productivities and residential amenities explain 64% and 10% of the effect.[8]

Dependent variable:	Impact on floorspace price, €/m^2
Equal taxes	-354.7
No tax importation	-638.8
No jump in a	-2,413.7
No jump in b	-372.3
Observations	16
R^2	0.990
RMSE	256.6

Note: We report the estimation of the meta regression of the Luxembourg dummy coefficient in Table 1.8 on the dummies for equal taxes, no tax importation, and no jumps in a, and b. We report two measures of non-linearity of the effects: R^2 and residual mean square error (RMSE).

Table 1.9: Meta-regression.

From a policy perspective, tax rates and the tax redistribution policy can be adjusted by policymakers. The results above suggest that the average price for an 80 m^2 apartment in Luxembourg could be reduced by €51,040 if the tax revenue were redistributed to all residents of the Greater Region by a centralized supranational authority. Similarly, a resident of Luxembourg would pay €28,320 less if tax rates were equalized to the average across the four countries.

[8] The share of the effect attributed to each factor is computed as its coefficient estimate divided by the sum of all coefficient estimates in Table 1.9.

1.8 Discussion

In this section, we conclude our investigation by discussing the effects of cross-border work and home bias.

1.8.1 Cross-border commuting

Under the EU's fundamental right to free movement of workers, individuals are entitled to seek and accept employment in a country where they do not reside. In the cross-border region examined in this chapter, workers are expected to optimize their choice of residence based on local amenities, income prospects, and the degree of spatial mobility. By arbitraging between locations across the border, workers are expected to smooth the spatial structure of floorspace prices. We assess how cross-border mobility mitigates spatial differences in floorspace prices.

Dependent variable:	Floorspace price (€/m^2)				
	(1)	(2)	(3)	(4)	(5)
Luxembourg	3,219.266***	3,003.058***	2,682.147***	228.064	80.387
	(200.343)	(186.757)	(180.385)	(155.188)	(154.866)
Distance to border, km	126.211***	95.098***	91.330***	55.722**	53.269*
	(32.786)	(31.188)	(30.021)	(27.188)	(27.304)
No cross-border	No	Yes	Yes	Yes	Yes
Equal taxes	No	No	Yes	Yes	Yes
No jump in a	No	No	No	Yes	Yes
No jump in b	No	No	No	No	Yes
Observations	568	568	568	568	568
R^2	0.791	0.766	0.744	0.096	0.050

Note: Luxembourg is a dummy variable that is equal to 1 if the cell lies in the country of Luxembourg. Column 1 shows the observed price jump at the border. Column 2 shows the price jump after eliminating cross-border commuting. Column 3 additionally shows the price jump after equalizing all taxes across all countries. We equalize taxes to the average across 4 countries. Column 5 additionally eliminates cross-border productivity differences. Finally, Column 6 additionally eliminates residential fundamentals discontinuities. Robust standard errors in parentheses. To adjust fundamental amenity and productivity differences, we use shifters reported in the first two columns of Table 1.7. * $p < 0.1$, ** $p < 0.05$, *** $p < 0.01$.

Table 1.10: Counterfactuals with no cross-border commuting.

Towards this aim, we construct a counterfactual scenario with no cross-border commuting by assigning infinite travel time to cross-border commutes. Travel times within countries remain unchanged. Workers and firms can freely relocate across countries. The impact of Luxembourg's jurisdiction on the floorspace price around the border is reported in Table 1.10 [9]. In the scenario with closed borders, the tax importation effect is mechanically eliminated, as each worker works in the country of her residence. We therefore do not include the elimination of tax importation in the series of nested counterfactuals. Column 2 shows a decrease in the floorspace price per m^2 by €216.2 in Luxembourg in the absence of the free movement of workers (first row). This effect is driven by a larger decrease in floorspace prices on the Luxembourgish side due to the loss of tax importation, compared to the decline in floorspace prices in neighboring countries due to the loss of access for cross-border workers to the Luxembourgish labor market.

The effect of the distance to the CBD of the city of Luxembourg weakens (second row) since commuting directions differ on each side of the border. The equalization of local taxes, productivity,

[9] See Supplementary Appendix 1.G.6 for description of the evolution of endogenous outcomes.

and residential amenities mainly explains the floorspace price discrepancy. When differences in local factors across countries are controlled for, Luxembourg exhibits no floorspace price premium (Column 5).

1.8.2 Home bias

In cross-border regions, individuals may have preferences for local goods and legal systems. For example, access to and compensation for ancillary rights, such as child education, pensions, or healthcare, may differ across borders and be subject to restrictions or uncertainty. As a result, individuals may exhibit a home bias in their residential or employment choices.

In this subsection, we examine the impact of home bias on floorspace price differences. To this end, we assume that individuals incur an additional disutility shock when working in a country different from their country of residence. That is, we postulate $d_{ij} = e^{\kappa\tau_{ij}+T_{ij}}$, where T_{ij} measures the utility discount when i and j lie in different jurisdictions. Intuitively, such home bias generates an effect that is similar to, but weaker than, the closing-border scenario described above. The objective is to assess the actual magnitude of this disutility shock. To measure this, we extend the approach discussed in Section 1.5.1 to account for a potential discount associated with crossing a border (see Appendix 1.F). We then run the same sequence of counterfactual scenarios as in Table 1.8 with the measured home bias.

Dependent variable:	Floorspace price (€/m^2)					
	(1)	(2)	(3)	(4)	(5)	(6)
Luxembourg	3,219.266***	2,935.385***	2,452.877***	2,027.139***	-21.042	-179.938
	(200.343)	(185.553)	(180.858)	(178.983)	(166.848)	(164.445)
Distance to border, km	126.211***	118.089***	114.216***	107.497***	67.495**	64.655**
	(32.786)	(30.373)	(29.377)	(28.867)	(28.170)	(28.023)
Home bias	No	Yes	Yes	Yes	Yes	Yes
No tax importation	No	No	Yes	Yes	Yes	Yes
Equal taxes	No	No	No	Yes	Yes	Yes
No jump in a	No	No	No	No	Yes	Yes
No jump in b	No	No	No	No	No	Yes
Observations	568	568	568	568	568	568
R^2	0.791	0.785	0.745	0.690	0.044	0.018

Note: Luxembourg is a dummy variable that is equal to 1 if the cell lies in the country of Luxembourg. Column 1 shows the observed price jump at the border. Column 2 shows the price jump after introducing home bias. Column 4 additionally shows the price jump after equalizing all taxes across all countries. We equalize taxes to the average across 4 countries. Column 5 additionally eliminates cross-border productivity differences. Finally, Column 6 additionally eliminates residential fundamentals discontinuities. Robust standard errors in parentheses. To adjust fundamental amenity and productivity differences, we use shifters reported in the first two columns of Table 1.7. * $p < 0.1$, ** $p < 0.05$, *** $p < 0.01$.

Table 1.11: Counterfactuals with home bias.

Results are shown in Table 1.11. Column 2 indicates that the presence of a home bias decreases the floorspace price jump at the border by 9%. This is because home-biased residents of neighboring countries perceive their access to the Luxembourg labor market as less favorable, which lowers their expected incomes and, consequently, reduces floorspace prices in those areas. Nevertheless, the elimination of tax importation reduces the floorspace price difference by 15%, and the equalization of taxes reduces it further by 13%, which is similar to the effect found in the absence of home bias. Differences in fundamental productivity explain 63% of the floorspace price decline at the border. As in Section 1.8.1, home bias mitigates the arbitrage intensity of floorspace prices across the border.

1.9 Conclusion

In this chapter, we highlight the existence of a jump in floorspace prices and the share of commercial buildings at the borders of Luxembourg and its neighboring countries. We discuss the drivers behind this observation by combining a quantitative urban economic model with spatial regression discontinuity techniques to decompose the relative contributions of taxes, productivity, and amenities. Our analysis underscores the critical role of geography and commuting frictions in shaping labor competition. It considers the full range of taxes on labor, land, and goods to account for possible offsetting effects. It also incorporates the labor tax importation mechanism, through which the labor taxes of cross-border workers are spent on local public goods for the residents of Luxembourg.

Our theoretical discussion suggests that international differences in labor taxation contribute more to explaining the border gap in floorspace prices and the share of commercial buildings than differences in property or goods taxation. However, our quantitative model indicates that tax differences are not the predominant drivers of these disparities. Indeed, we estimate that tax differences account for up to 9% of the observed price jump, with the remaining gap largely driven by tax importation (17% of the price jump) and local productivity differences (64% of the price jump). Equalizing tax regimes across borders would reduce the price of an 80 m^2 apartment by €28,320. Eliminating tax importation by creating a supranational authority that redistributes the total tax revenue of the economy to all its residents would lead to a larger reduction of €51,040. This finding sheds light on the relative importance of international taxes and tax importation in shaping the spatial structure of economic activities and values. While restrictions on cross-border mobility and/or home bias preferences can magnify the observed price differentials, they do not substantially increase the relative importance of tax effects.

This chapter focuses on the key economic mechanisms underlying cross-border housing and labor markets, which can be disentangled using our data. However, it leaves aside several important questions that are reserved for future research. Notably, the chapter abstracts from an important discussion of fiscal compensation. As shown in the chapter, tax importation is associated with the under-provision of public goods in countries bordering Luxembourg, which raises the question of whether cross-border workers or the affected territories should be compensated for these losses. The extent of compensation, its allocation across jurisdictions, and the design of an optimal compensation scheme are subjects of ongoing political debate in the region. These issues are of considerable interest, but they lie beyond the scope of this chapter. Furthermore, the roles of transport infrastructure development and congestion merit further investigation, particularly within a fiscal federalism framework where neighboring jurisdictions differ in their resource endowments, political institutions, and policy incentives.

Appendix

1.A Theoretical model

Here, we provide a detailed definition of spatial general equilibrium.

Given parameters $\{\alpha, \beta, \mu, \varepsilon, \kappa, \lambda, \delta, \eta, \rho\}$, location characteristics $\{\varphi, L, \xi, \tau\}$, productivity and amenities $\{a, b\}$, reservation utility $\bar{U}$, and tax multipliers $\{t^c, t^q, t^w\}$, the spatial general equilibrium is given by the scalar H and the vectors $\{\pi_M, \pi_R, Q, q, w, \theta, g\}$ that solve the following system of equations:

$$\bar{U} = \Gamma_0 \left[\sum_{i\in\mathcal{I}} \sum_{j\in\mathcal{I}} (d_{ij}(t_i^q Q_i)^{1-\beta}(t_i^c)^{\beta})^{-\varepsilon} (B_i G_i w_j)^{\varepsilon} \right]^{\frac{1}{\varepsilon}},$$

$$\begin{aligned}
\pi_{Ri} &= \frac{\sum_{s\in\mathcal{I}} (d_{is}(t_i^q Q_i)^{1-\beta}(t_i^c)^{\beta})^{-\varepsilon} (B_i G_i w_s)^{\varepsilon}}{\sum_{r\in\mathcal{I}} \sum_{s\in\mathcal{I}} (d_{rs}(t_r^q Q_r)^{1-\beta}(t_r^c)^{\beta})^{-\varepsilon} (B_r G_r w_s)^{\varepsilon}}, \quad \forall i \in \mathcal{I}. \\
\pi_{Mj} &= \frac{\sum_{r\in\mathcal{I}} (d_{rj}(t_r^q Q_r)^{1-\beta}(t_r^c)^{\beta})^{-\varepsilon} (B_r G_r w_j)^{\varepsilon}}{\sum_{r\in\mathcal{I}} \sum_{s\in\mathcal{I}} \left(d_{rs}(t_r^q Q_r)^{1-\beta}(t_r^c)^{\beta}\right)^{-\varepsilon} (B_r G_r w_s)^{\varepsilon}}, \quad \forall j \in \mathcal{I}.
\end{aligned}$$

$$q_j = \frac{(1-\alpha) A_j^{\frac{1}{1-\alpha}}}{t_j^q} \left(\frac{\alpha}{w_j t_j^w} \right), \quad \forall j \in \mathcal{I}.$$

$$\begin{aligned}
&\begin{cases}
P_i = q_i \text{ and } \theta_i = 0 & \text{if } q_i > Q_i, \\
P_i = q_i \text{ and } \theta_i \in [0,1] & \text{if } q_i = Q_i, \\
P_i = Q_i \text{ and } \theta_i = 1 & \text{if } q_i < Q_i.
\end{cases} \\
\theta_j \phi_j L_j^{1-\mu} &= A_j^{\frac{1}{\alpha}} \left(\frac{1-\alpha}{q_j t_j^q} \right)^{\frac{1}{\alpha}} H \pi_{Mj}, \quad \forall j \in \mathcal{I}. \\
(1-\theta_i)\phi_i L_i^{1-\mu} &= (1-\beta) \left(\sum_{s\in\mathcal{I}} \frac{(w_s/d_{is})^{\varepsilon}}{\sum_r^S (w_r/d_{ir})^{\varepsilon}} w_s \right) \frac{H \pi_{Ri}}{t_i^q Q_i}, \quad \forall i \in \mathcal{I}.
\end{aligned}$$

$$\begin{aligned}
g_i &= \frac{t_n^c - 1}{t_n^c} \beta \frac{\sum_{i\in\mathcal{I}_n} \mathbb{E}[w|i] H_{Ri}}{\sum_{i\in\mathcal{I}_n} H_{Ri}} + \frac{t_n^q - 1}{t_n^q} (1-\beta) \frac{\sum_{i\in\mathcal{I}_n} \mathbb{E}[w|i] H_{Ri}}{\sum_{i\in\mathcal{I}_n} H_{Ri}} \\
&\quad + (t_n^w - 1) \frac{\sum_{j\in\mathcal{I}_n} w_j H_{Mj}}{\sum_{i\in\mathcal{I}_n} H_{Ri}} + (t_n^q - 1) \frac{\sum_{j\in\mathcal{I}_n} q_j S_{Mj}}{\sum_{i\in\mathcal{I}_n} H_{Ri}}, \quad \forall i \in \mathcal{I}_n. \\
G_i &= g_i^{\zeta}, \quad \forall i \in \mathcal{I}_n.
\end{aligned}$$

1.B Data

1.B.1 Commuting times

We impute travel time within each cell or municipality using the average travel time between 50 randomly selected points along the existing road network of the spatial unit. Travel time is defined as the minimum of the travel times by car and on foot. Car travel times are obtained from OSRM. Since OSRM assumes that pedestrians follow the same road network as vehicles, we instead proxy pedestrian travel time by dividing the Euclidean distance between the selected points by an assumed pedestrian speed of 5 km/h, to better reflect pedestrian flexibility.

1.B.2 Population data

Population measurement is extracted from the GHS-POP-2023 dataset, produced by the European Commission's Joint Research Centre as part of the Global Human Settlement Layer (GHSL) initiative. It provides 1×1 gridded residential population estimates for 2020. The GHS-POP-2023 dataset sources its population data from official census counts and administrative records provided by national statistical offices. These official figures are harmonized and disaggregated into grid cells using satellite-derived built-up area information. Population counts from these official sources are disaggregated into grid cells using a dasymetric mapping strategy that employs built-up area information from the GHS-BUILT product derived from satellite imagery.

1.B.3 Employment data

We construct our employment data by mapping municipal-level records to our grid of 1×1 km cells as a function of municipalities' footprint and commercial volumes.

The data on employment (at the place of work) is obtained at the municipal level from national statistical agencies. Employment in Luxembourg is obtained from the IGSS (Inspection générale de la sécurité sociale) employment data from 2020, recording the number of workers per municipality based on the place of work, including both residents and cross-border workers. Employment in Germany is obtained from the Regionaldatenbank Deutschland supplies data from the Registry of Employees subject to Social Security Contributions at the place of work at the municipal level for 2020. Employment in France is sourced from the INSEE Municipal Data Registry, covering the employed population at the place of work. Workers are assigned to their municipality of residence when their activities cross municipalities (e.g., truck drivers, taxi drivers, VRP representatives, itinerant traders, or fishermen). We consider three French departments adjacent to Luxembourg, with census information available for 2021. Employment in Belgian municipalities bordering Luxembourg are provided by the Walloon Statistical Agency (IWEPS) for 2020, using methods consistent with those applied in France.

We further use the built-up volume information from the GHS-BUILT-V dataset, produced by the European Commission's Joint Research Centre. Built-up volumes are identified from Landsat satellite imagery using automated classification techniques. We use the volume allocated to dominant non-residential and residential at a 1×1 km spatial resolution. The dataset has global geographical coverage and is available for 2020.

We allocate employment across the grid cells as follows. We allocate the observed municipal employment according to the share of the municipal building volume attributed to municipal land. That is, the employment in cell j is given by $H_{Mj} = \sum_m H^m_{Mj}$ where H^m_{Mj} is the employment

of municipality m allocated in cell j, which is given by $H^m_{Mj} = H^m_M L^m_j V_j / (\sum_k L^m_k V_k)$ where H^m_M is the observed administrative employment in municipality m, L^m_j is the observed area of municipality m in cell j and V_j is the volume of build-up observed in cell j. Finally, because our simulations require attributing a single country to each cell, we assign each cell j to the country with the largest area in the cell. Consistently, we erase the land surface of the other country. That is, we set $L^{m'}_j = 0$ if $L^m_j > L^{m'}_j$ where m and m' are municipalities of two different countries.

Our employment data turns out to be more accurate than existing high-resolution employment databases, in particular the daytime population densities reported in the ENACT 2011 Population Grids of the European Commission. See discussion in supplementary section 1.G.1.

1.B.4 Floorspace prices

Rental and sale property listing data is obtained from March to September 2022 from the at-home.lu website, which jointly covers Luxembourg, Germany, France, and Belgium. Listings with valid geographical coordinates and housing characteristics (longitude, latitude, prices/rents, hedonics) are selected, resulting in 11,319 property listings and 5,366 rental listings. We remove the top 5% and bottom 5% of listings based on prices and rents, respectively for Luxembourg and countries outside Luxembourg. This yields 4,819 rentals (4,362 in Luxembourg) and 10,183 property purchase listings (6,740 in Luxembourg).

We assign each cell to a single country. A cell is assigned a country if and only if more than half of its area lies within the country's border. The rest of the area and the listing located in it are discarded. This leaves 4,790 rentals (4,352 in Luxembourg) and 10,137 property purchase listings (6,716 in Luxembourg).

Finally, the data is filtered by property type to include houses, apartments, offices, studios, bedrooms, detached and semi-detached houses, and duplexes. This step results in a final dataset of 8,916 property purchase listings (6,016 in Luxembourg) and 4,149 rental listings (3,807 in Luxembourg) used for computing cell fixed effects. Since the sale property listings are twice as numerous and spread over more cells, they are naturally preferred for estimating the floorspace price index.

The cell i's price index is computed as the fixed effect η_i in the hedonic price regression model $\log Q_{ni} = \mathbb{H}_n'\beta + \eta_i + \epsilon_{ni}$, where Q_{ni} denotes the price per m^2 for housing unit n in grid cell i, $\mathbb{H}_n$ is a vector of hedonic characteristics, and ϵ_{ni} is the error term.

The regression results for prices per square meter are presented in Table 1.B.1. The first column includes only house characteristics, while the second column adds the cells' fixed effects. The latter controls for neighborhood amenities and productivity, transport infrastructure, access to employment, etc. The high explanatory power is noticeable in the second column. Fixed effects are balanced between countries. In our specification, we get 973 price indices, of which 496 are in Luxembourg.

Dependent variable:	Price per m^2	
	No cell fixed effects	With cell fixed effects
log, Surface	-0.049***	-0.239***
	(0.015)	(0.007)
Number of Rooms	-0.110***	-0.016***
	(0.004)	(0.002)
Number of Bedrooms	0.001	-0.001
	(0.002)	(0.001)
Number of Bathrooms	0.007*	-0.002
	(0.004)	(0.002)
Furnished	0.009	-0.008
	(0.012)	(0.006)
Age, decade	0.008***	0.004***
	(0.001)	(0.000)
Age^2, decade 10^{-3}	-0.004***	-0.002***
	(0.001)	(0.000)
Balcony surface	0.009***	0.002***
	(0.001)	(0.001)
Age not defined	0.015	-0.035***
	(0.012)	(0.005)
Type FE	Yes	Yes
Type FE × Number of Rooms	Yes	Yes
Thermal Insulation FE	Yes	Yes
Cell FE	No	Yes
R^2	0.488	0.926
Observations	8916	8916

Note: "Type of FE" refers to the types of properties: apartments, bedrooms, detached houses, duplexes, houses, offices, semi-detached houses, studios. Thermal insulation refers to the grade of the house's thermal certificate. Standard errors in parentheses. * $p < 0.1$, ** $p < 0.05$, *** $p < 0.01$.

Table 1.B.1: Hedonic regressions for purchase prices.

1.B.5 Universal kriging

Universal kriging is a geostatistical method for predicting values at unsampled locations by combining a deterministic trend with spatially correlated errors (Matheron, 1963). The trend is modeled as a linear function of known covariates (e.g., a constant, spatial coordinates, or other predictors). The spatial dependence is captured through a variogram, which describes how the variance of the differences between observations increases with distance between them.

In our context, the universal kriging approach assumes that the price index is given by $\eta_i = \mathbb{H}_i'.\beta + \epsilon_i$, $i = 1, ..., N$ where $\mathbb{G}_i$ are characteristics of cell, ϵ_i is an error with $E[\epsilon_i] = 0$ and variance $E[\left(\epsilon_i - \epsilon_j\right)^2] = 2\gamma(d_{ij})$ where d_{ij} is the distance between two cells i and j. The main assumption is that the function $\gamma(d)$ is a function of distance d given by the variogram fitted with the dataset. The unbiased predictor of the price index of an outside cell n with characteristics $\mathbb{G}_n$ is then given by $\widehat{\eta}_n \equiv \sum_{i=1}^N \omega_i \eta_i$ where the weights ω_i and coefficients β are chosen to minimize the variance of the prediction error $E\left[(\eta_n - \widehat{\eta}_n)^2\right]$. Unbiasedness requires $\sum_{i=1}^N \omega_i = 1$ and $\sum_{i=1}^N \omega_i \mathbb{G}_i = 1$. The minimization is repeated for every cell prediction.

In this chapter, the vector of cell's characteristics $\mathbb{G}_i$ includes the logarithms of local population

$\log(1+H_{Ri})$, local employment $\log(1+H_{Mi})$, travel time to central business district for Luxembourg cells $\log(1+d_i^{CBD}) \times LUX_i$. The variogram $\gamma(d)$ is estimated from the data by averaging squared differences between nearby points, and then fitted with an exponential function.

To enhance precision, we restrict data to the cells with more than five listing observations. This is because the price indices estimated for cells with very few listing observations are expected to include significant error components. Figure 1.B.1 shows the mean absolute errors (MAEs) of the prediction of the price index as a function of the minimum number of listings per cell. The bars reflect standard errors. The reader can see that MAEs drop significantly until we keep the cells with more than five listings. Figure 1.B.1 also shows the MAEs of the prediction using the OLS regression, $\eta_i = \mathbb{G}_i'\beta + \epsilon_i$. One can see that kriging predictions are systematically more precise than OLS predictions, because they capture the spatial correlation between neighboring price indices.

The supplementary material 1.G.3 further quantifies the advantage of the kriging approach and compares the results with price and rental listings.

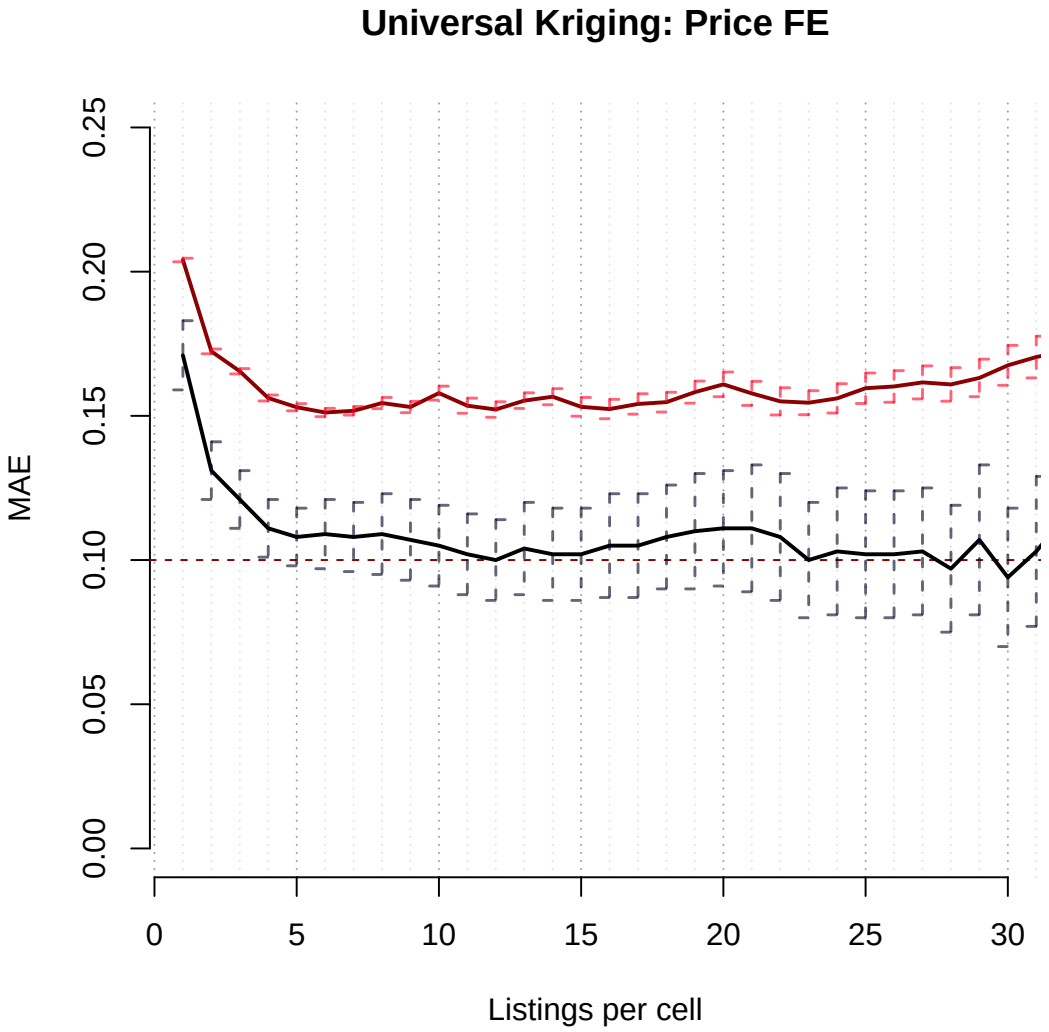

Note: The table reports the mean absolute error (MAE) for cell-specific price fixed-effect prediction using universal kriging (black) and compares it to OLS prediction (red). The out-of-sample prediction quality is assessed with a 5-fold cross-validation. "Listings per cell" denotes the minimum number of listings in the cells of the sample that is used for prediction. Standard errors of MAE are shown by brackets.

Figure 1.B.1: Precision of kriging and OLS predictions.

1.C Estimations

1.C.1 Robustness checks on semi-elasticity of commuting

The semi-elasticity commuting parameter κ is estimated from the regression equation (2.C.1), where we use the travel flow data from the LuxMobil survey and the INSEE census data. Table 1.C.1 allows for comparison of the estimations with various combinations of databases and pairs of origin and destination countries. Column 1 reproduces column 1 of Table 2.C.1 with only travels in the country Luxembourg reported by the LuxMobil survey. Column 2 shows almost the same coefficient using LuxMobil travels from the country of Luxembourg to the whole Luxembourg functional area. Column 3 reports a slightly lower coefficient within the whole functional area using LuxMobil travels. This is potentially explained by a selection bias in LuxMobil survey that mainly focuses on individuals working in the country of Luxembourg. Column 4 reports a slightly higher coefficient for travels of INSEE census data within the French municipalities, which have a slightly different communication infrastructure. Column 5 gives a similar coefficient for travel from France to Luxembourg and France. Column 6 reproduces column 3 of Table 2.C.1 with travels within Luxembourg and France using both datasets. Overall, estimates are similar in all settings.

Dependent variable:	Commuting flows, log					
	(1)	(2)	(3)	(4)	(5)	(6)
OSRM Travel Time, min	-0.110***	-0.109***	-0.100***	-0.122***	-0.111***	-0.116***
	(0.006)	(0.006)	(0.004)	(0.005)	(0.003)	(0.004)
Survey	LuxMobil	LuxMobil	LuxMobil	INSEE	INSEE	Both
Country of Origin	LU	LU	All	FR	FR	LU + FR
Country of Destination	LU	All	All	FR	LU + FR	LU + FR
Origin FE	Yes	Yes	Yes	Yes	Yes	Yes
Destination FE	Yes	Yes	Yes	Yes	Yes	Yes
Observations	13689	16263	25308	86114	191367	214468
R^2	0.810	0.815	0.821	0.835	0.831	0.850

Table 1.C.1: Commuting flows elasticity with respect to the travel time.

1.C.2 Fréchet scale parameter

We choose the Fréchet parameter ε that produces the wage dispersion closest to the observed one (Ahlfeldt et al., 2015). Toward this aim, we minimize the absolute difference between the variances of the logarithm of the observed wages and the wages simulated by the model, $|\text{var}(\log w_m^{data}) - \text{var}(\log w_m^{sim}(\varepsilon))|$ where $|.|$ is the absolute value operator. In this expression, variances are taken over the municipalities m. w_m^{data} denotes the net wage reported at the municipal level, while $w_m^{sim}(\varepsilon)$ is the employment-weighted average of simulated wages across the cells in the municipality. That is, denoting the set of cells in the municipality by $j \in \mathbb{J}_m$, we set $w_m^{sim}(\varepsilon) = \sum_{j \in \mathbb{J}_m} w_j^{sim}(\varepsilon)(H_{Mj} / \sum_{j' \in \mathbb{J}_m} H_{Mj'})$ where $w_j^{sim}(\varepsilon)$ denotes the simulated wage in cell j while H_{Mj} is given by the observed employment in the cell j. The vector of simulated wages $w_j^{sim}(\varepsilon)$ is obtained by numerically solving the labor market conditions (1.3.17) for w_j at each value of ε, using the observed residential populations H_{Ri}, observed travel time τ_{ij} and the above-estimated semi-elasticity of commuting ν. Figure 1.C.1 shows the plot of this difference between observed and simulated wage variances. It has a minimizer at $\varepsilon = 4.2$.

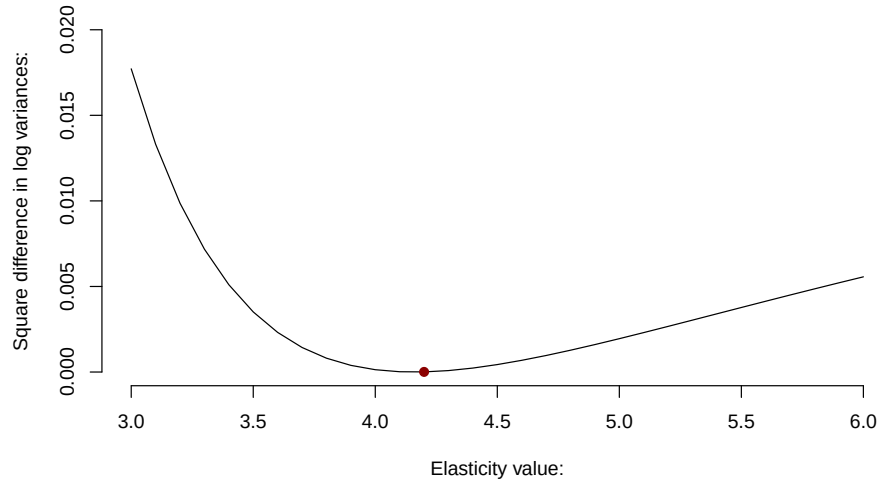

Note: The wages are the hourly net wages in Luxembourgish municipalities and French municipalities in the departments bordering Luxembourg.

Figure 1.C.1: Difference between variances of observed and simulated (log) wages as a function of ε.

1.C.3 Urban externalities

Instruments for the productivity and amenity regressions are derived from the spatial distribution of commercial and residential floor area in 1975.

First, we estimate employment-to-buildup conversion coefficients $(\hat{\alpha}_M, \hat{\beta}_M)$ and $(\hat{\alpha}_R, \hat{\beta}_R)$, by regressing 2020 the logarithm of employment and log-population on the logarithm of 2020 commercial and residential buildup areas. Results are reported in Table 1.C.2.

Dependent variable:	Employment (log, 2020)	Population (log,2020)
Residential build-up (log, 2020) (β_R)	1.107***	
	(0.008)	
Commercial build-up (log, 2020) (β_M)		1.175***
		(0.009)
Intercept (α_M, α_R)	0.375***	-1.358***
	(0.030)	(0.052)
Observations	3182	3182
R^2	0.855	0.854

Table 1.C.2: Population and employment and build-up areas.

Second, we apply those coefficients to commercial build-up data for 1975, using the variables $SNRES_s^{1975}$ and $SRES_s^{1975}$ in the GHS-BUILT-S database. This yields the 1975 predicted employment: $\hat{H}_{Mj} = e^{\hat{\alpha}_M} \left(SNRES_j^{1975}\right)^{\hat{\beta}_M}$ and $\hat{H}_{Ri} = e^{\hat{\alpha}_R} \left(SRES_i^{1975}\right)^{\hat{\beta}_R}$.

Finally, we impute the instrumental variables for urban externalities for 1975 using the following expressions: $\hat{\Upsilon}_j = \sum_{i \in \mathcal{I}} e^{-\delta \tau_{ij}} \hat{H}_{Mi} / L_i$ and $\hat{\Omega}_i = \sum_{j \in \mathcal{I}} e^{-\rho \tau_{ij}} \hat{H}_{Rj} / L_j$.

To visualize instrumental variables, Figure 1.C.2 shows the changes in residential and productivity spillover estimates between 1975 and 2010. Productivity spillovers experience declines in areas of former industrial production in France (Thionville, Metz), Saarland, and south of Luxembourg (Esch, Differdange, Dudelange).

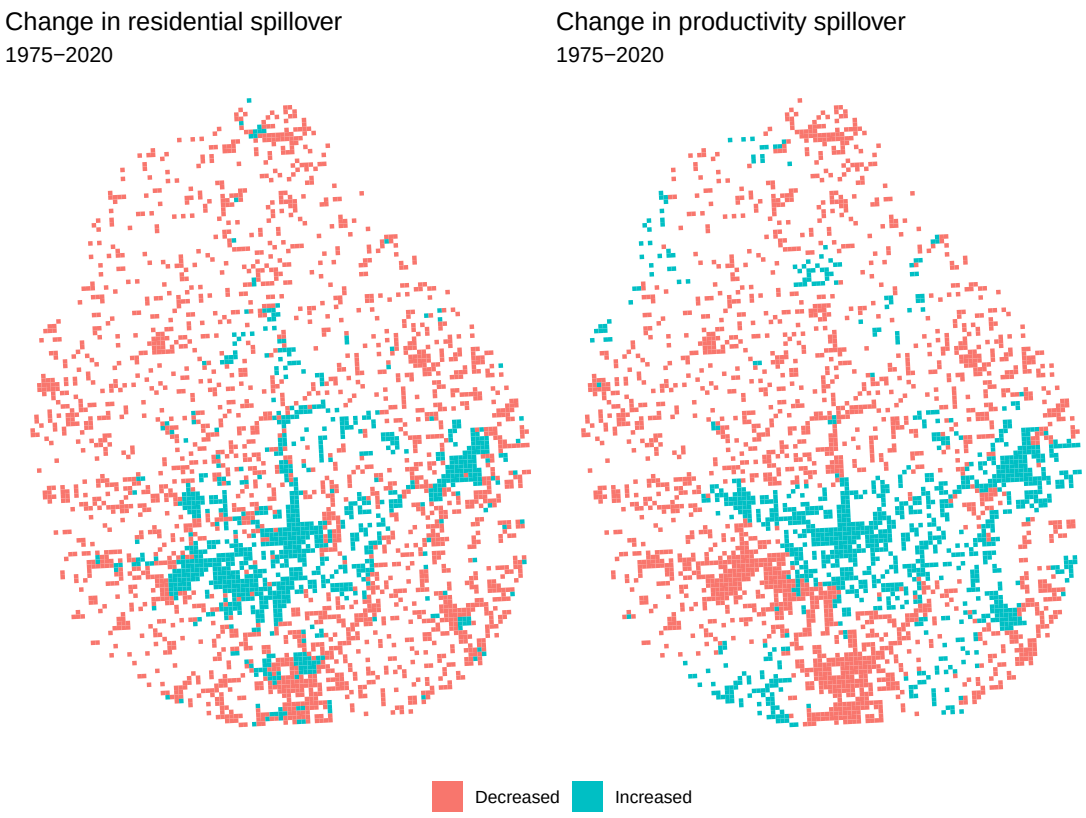

Figure 1.C.2: Changes between residential and productivity spillover estimates between 1975 and 2010.

Table 1.5 reports the first- and second-stage regression results for the constructed spillover instrument. Following Combes et al., 2010 and Combes and Gobillon, 2015, geographic controls are incorporated to account for first-nature determinants that may affect both present-day productivity and past population and employment patterns. Since these variables plausibly influence both historical and current employment distributions, the exclusion restriction is assumed to hold only conditional on geographic controls. These geographic control variables are interacted with country indicator variables to allow for country-specific slope heterogeneity. Nevertheless, no separate country fixed effects are introduced, thus cross-country differences are represented exclusively through the observed covariates and their interactions.

A robustness check with alternative instruments is available in the Supplementary Appendix 1.G.4.

1.D Model inversion, calibration and validation

In this appendix, we detail the procedure used to invert the model, the resulting benchmark model, and an additional validity check.

1.D.1 Model inversion

The inversion of the model recovers the vectors of the characteristics of the unobserved location A, B, a, b, and φ using the values of the parameters $\alpha, \beta, \mu, \varepsilon, \kappa, \lambda, \delta, \eta$, and ρ as well as our data vectors on the residential population, H_R, employment at work, H_M, commuting time, τ, floorspace rents, Q, and tax multipliers, t^c, t^q, and t^w. (Vectors and matrices are denoted by deleting references to i and j.) We apply the following steps:

1. Given $\{\varepsilon, \kappa\}$ and the observed data $\{H_M, H_R, \tau\}$, we determine the equilibrium wage vector w from the labor market clearing condition (1.3.17).
2. Given $\{\varepsilon, \kappa, \alpha, \beta, \mu\}$, the observed data $\{\mathbb{Q}, H_M, H_R, \tau, t^c, t^q, t^w\}$ and the wage vector w, we determine the public investment in local amenities g from the government budget constraint 1.3.14.
3. Given $\{\varepsilon, \kappa, \alpha, \beta, \mu\}$, the observed data $\{\mathbb{Q}, H_M, H_R, \tau\}$, wages w and public investment in local amenities g, we determine the residential amenities, B, from residential choice probabilities (1.3.5) and local productivity, A, from zero-profit condition (1.3.10).
4. Given $\{\lambda, \eta, \rho, \nu\}$, the observed data $\{H_M, H_R, \tau\}$, local productivities A and amenities B, we determine the fundamental residential amenities, b, from (1.3.16) and fundamental productivities, a, from (1.3.15).
5. Given $\{\varepsilon, \kappa, \alpha, \beta, \mu\}$, the observed data $\{\mathbb{Q}, H_M, H_R, \tau\}$, wages w and productivity A, we determine the density of development φ and a share of commercial buildup θ from land market clearing condition 1.3.11, commercial (1.3.18) and residential (1.3.19) floorspace demand and floorspace market clearing condition 1.3.20.

1.D.2 Local fundamental characteristics

Figure 1.D.1 presents the results of the model inversion. The top left panel displays the spatial distribution of the density of development, which is higher in urban areas with high residential and workplace employment. The figure shows the existence of a fall at the Luxembourgish jurisdiction border. The top right panel shows the distribution of the share of commercial build-up. Regions with a greater share of commercial build-up align with large urban areas. The middle panels show the spatial distribution of local productivity, A, and residential amenities, B. The middle left panel indicates the presence of a high-productivity cluster located in and around the city of Luxembourg. Surrounding towns, such as Arlon, Echt, Metz, and Trier, exhibit much smaller productivity hikes. The middle right panel shows the spatial distribution of the local amenities. Residential amenities are more pronounced in the city of Luxembourg and Trier than in other urban areas. Finally, the bottom panels show the spatial distribution of fundamental productivities, a, and fundamental residential amenities, b. Production fundamentals peak in the city of Luxembourg, while residential fundamentals are more dispersed and show no significant peaks.

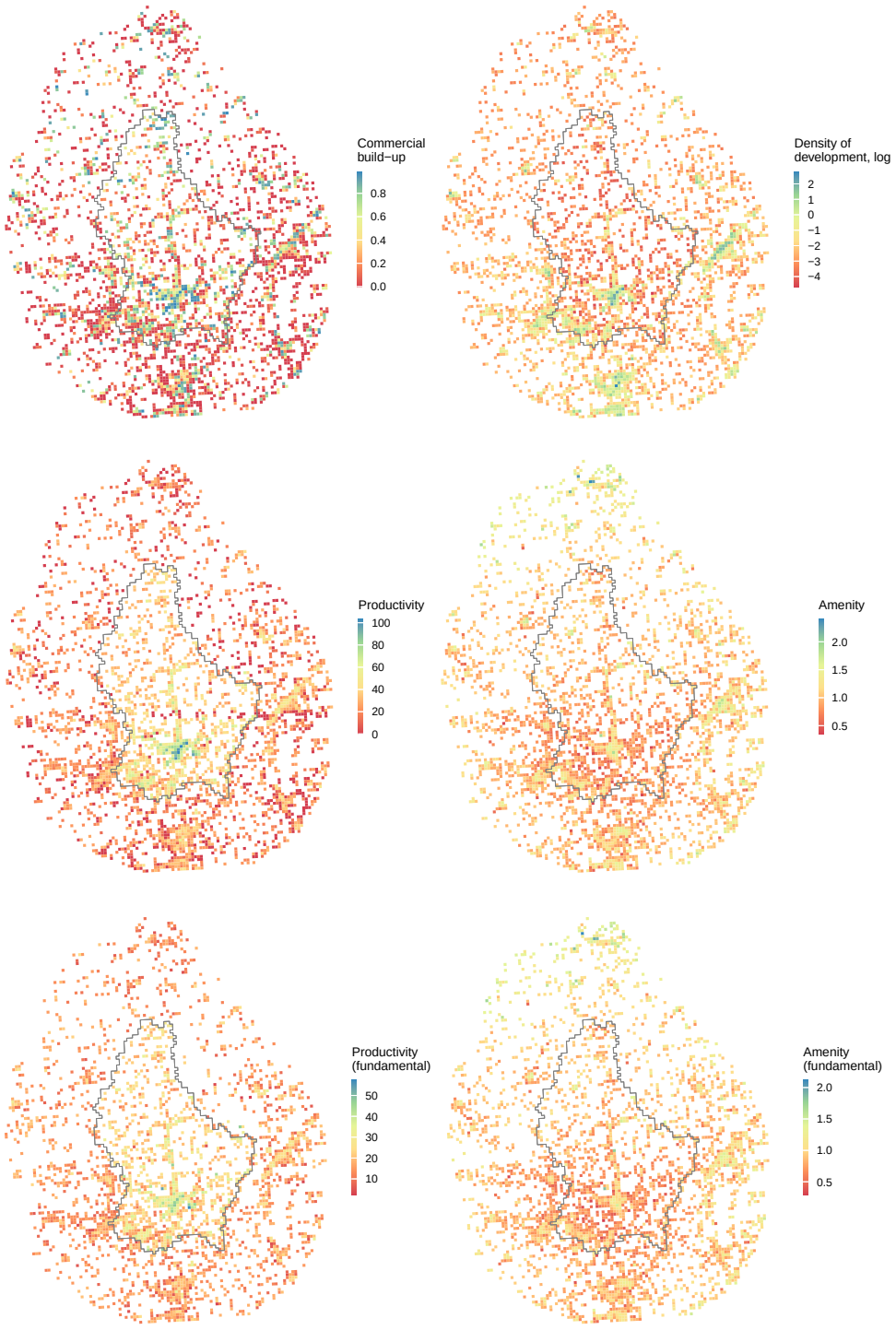

Note: Only cells with workplace employment or residential employment density above 100 people per km^2 are shown.

Figure 1.D.1: Calibration results for density of development (top left), commercial land use (top right), local productivity (middle left), local amenities (middle right), production fundamentals (bottom left), and residential amenity fundamentals (bottom right).

1.D.3 Over-identification

Table 1.D.1 shows the result of the OLS regression of the density of development predicted by the model on the average height, volume, and space of buildings observed from satellite data.

Dependent variable:	$\log \phi$		
	(1)	(2)	(3)
log, average building height	2.217***		
	(0.047)		
log, build-up volume		0.979***	
		(0.011)	
log, build-up area			1.314***
			(0.020)
Observations	3182	3182	3182
R^2	0.574	0.787	0.716

Note: Robust standard errors in parentheses.
* p < 0.1, ** p < 0.05, *** p < 0.01

Table 1.D.1: OLS regression of predicted density of development and observed average building height, volume, and space. Heteroskedasticity-robust standard errors are reported in parentheses.

To further check the validity of the model, Table 1.D.2 shows the effect of Luxembourg's administrative border on six endogenous variables predicted by the model: workers' expected income, commuting market access, productivity and residential spillover, floorspace rents, and commercial build-up share. We only use cells with both residential and commercial floorspace. The first four columns suggest no significant effect on expected worker income, commuting market access, and residential spillovers. The last two columns show significant discontinuities in floorspace price and commercial build-up share, which are consistent with those observed in the stylized facts. This suggests that the model replicates the commercial build-up jump and its magnitude.

Dependent variable:	Expected income	Commuting access	Productivity spillover	Residential spillover	Floorspace prices	Commercial build-up
Luxembourg	-0.020	0.047	5.418	173.631	3221.181***	0.127**
	(0.047)	(0.141)	(81.385)	(547.599)	(209.798)	(0.055)
Distance to border, km	0.013	0.052*	30.499*	316.709***	122.284***	0.004
	(0.010)	(0.029)	(16.544)	(120.930)	(34.652)	(0.010)
Observations	517	517	517	517	517	517
R^2	0.008	0.032	0.025	0.062	0.782	0.053

Note: We consider cells located within 5 km from the state border of Luxembourg and we consider only cells with mixed floorspace use. Luxembourg is a dummy variable that is equal to 1 if the cell lies in the country of Luxembourg. Robust standard errors in parentheses.
* p < 0.1, ** p < 0.05, *** p < 0.01

Table 1.D.2: Parametric regression discontinuity estimates for total workers' income, commuting market access, productivity, and residential spillover, floorspace prices, and share of commercial build-up.

We propose a final validity check for production and residential amenity fundamentals by examining their correlation with observable first-nature characteristics. Both production and residential fundamentals reflect environmental characteristics, such as proximity to water sources, forests, pastures, vineyards, and former industrial sites. Following Ahlfeldt et al., 2015, we regress these fundamentals on distances to extraction sites, water, forests, roads, vineyards, pastures, and green urban areas, as well as on noise levels. The regression results are shown in

Table 1.D.3. Fundamental amenities increase with lower noise levels and with proximity to water bodies, and decrease with proximity to extraction sites, roads, pastures, and vineyards. The opposite is true for production fundamentals—their value increases as one gets closer to roads and green urban areas. The fact that production fundamentals decrease with proximity to water bodies can be partly explained by the nature of modern production, where proximity to water bodies no longer offers a productivity advantage. We use all available calibrated fundamentals to run this regression.

Dependent variable:	a	b
Distance to extraction sites (log)	-0.320*	0.018***
	(0.190)	(0.004)
Distance to water (log)	0.792***	-0.009**
	(0.172)	(0.004)
Distance to forests (log)	0.278***	0.006***
	(0.072)	(0.002)
Distance to roads (log)	-0.913***	0.033***
	(0.160)	(0.005)
Distance to vineyards (log)	-0.539***	0.014***
	(0.139)	(0.003)
Distance to pastures (log)	0.463***	0.004***
	(0.056)	(0.001)
Distance to green urban areas (log)	-2.320***	0.004
	(0.254)	(0.005)
Noise level	-10.152	-2.207***
	(9.854)	(0.202)
Observations	3178	3178
R^2	0.122	0.067

Note: Columns 1 and 2 report regression results for the fundamental productivity and amenity. The quietness index takes values from 0 to 100, where 0 denotes the location with the least noise. We use CORINE Land Cover data from the Copernicus Project to measure the distance to different amenities. Robust standard errors are in parentheses.
* $p < 0.1$, ** $p < 0.05$, *** $p < 0.01$

Table 1.D.3: Regression of calibrated production fundamentals, a, and residential fundamentals, b, on observed geographical characteristics.

1.E Featureless geography

The last column of Table 1.8 shows the (insignificant) effect of the Luxembourgish area in the absence of tax differences and geographical features. In this case, residential and commercial choices are driven solely by commuting distances. In the presence of spatial externalities, it is important to assess whether the featureless equilibrium deviates significantly from the benchmark model, which mainly maps to a monocentric city surrounded by a subset of secondary cities.

Figure 1.E.1 shows the main economic variables in the featureless geography. It can be seen that wages, floorspace prices, employment, and population follow the characteristics of a monocentric city centered around the city of Luxembourg, with sub-centers in the areas of Arlon, Esch, and Metz. The wages are lower in the center, reflecting the average preference for the center discussed in Thisse et al., 2024. Floorspace rents fall with distance from the urban center. This gives reassurance about the applicability of the model in the absence of first-nature characteristics.

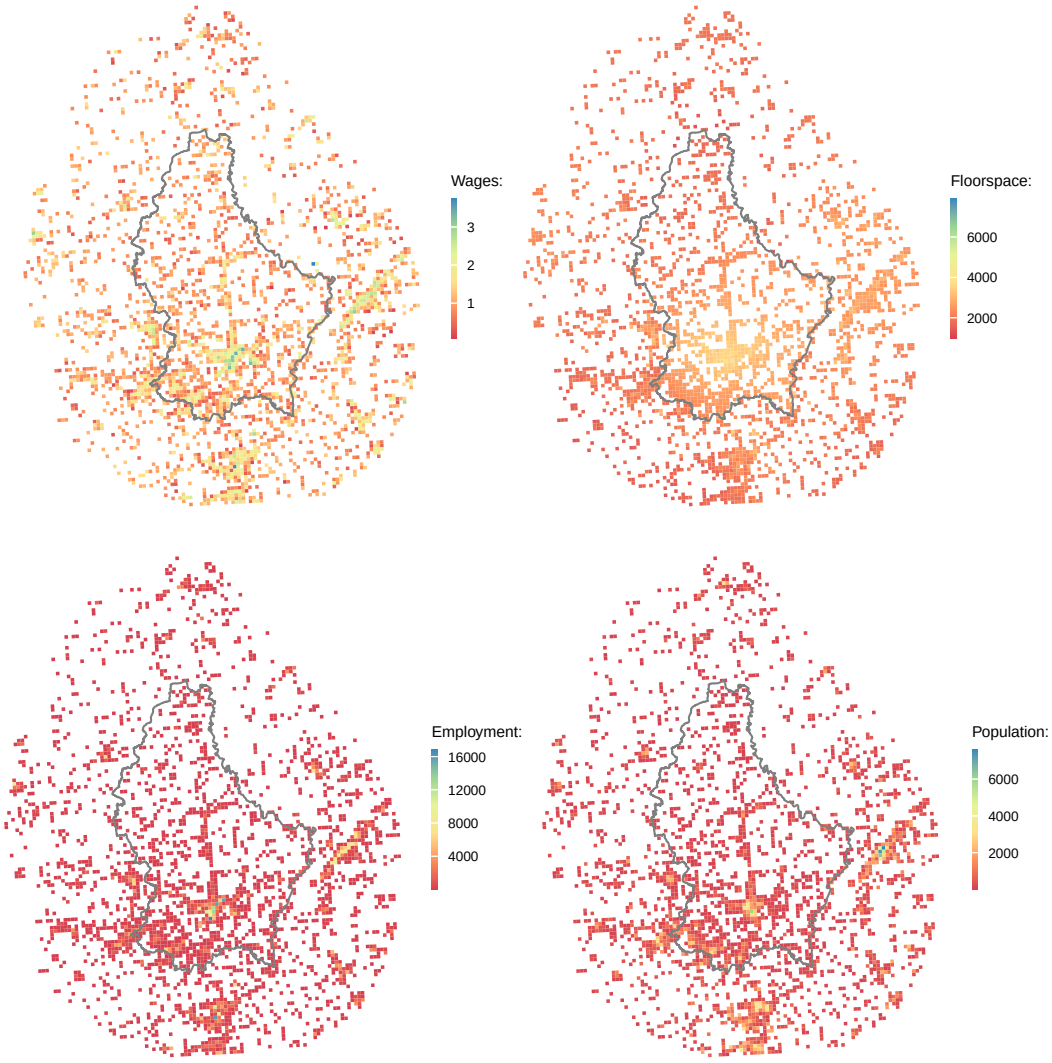

Note: Only cells with workplace employment or residential employment density above 50 people per km^2 are shown.

Figure 1.E.1: Spatial distribution of economic variables in the featureless geography.

1.F Home bias

We estimate the following specification:

$$\log \pi_{ij} = -\nu \tau_{ij} - \nu' \tau'_{ij} + \xi_i + \zeta_j + \epsilon_{ij}, \tag{1.F.1}$$

where τ_{ij} denotes the commuting time between residence location i and job-place location j; τ'_{ij} is a cross-border dummy equal to 1 if the residence and job-place are located in different countries, and 0 otherwise; ξ_i captures residence-specific fixed effects (such as amenities and floorspace prices); ζ_j captures job-place-specific fixed effects (e.g., productivity); and ϵ_{ij} is an error term. Estimation results are reported in Table 1.F.1. We pick the value for home bias discount from Column 2 as the baseline for the subsequent simulations.

Dependent variable	Commuting flows, log	
	(1)	(2)
OSRM Travel Time, min	-0.116***	-0.110***
	(0.004)	(0.004)
Crossing Border		-1.513***
		(0.222)
Origin FE	Yes	Yes
Destination FE	Yes	Yes
Observations	116827	116827
R^2	0.840	0.845

Note: Data from "LuxMobil" survey and INSEE Commuting Survey. Departure communes are within 50 km of the state border of Luxembourg. Robust standard errors are in parentheses. * p < 0.1, ** p < 0.05, *** p < 0.01.

Table 1.F.1: Estimation of home bias and commuting elasticity.

1.G Supplementary materials

1.G.1 Comparison between constructed employment data and ENACT data

Our employment data turns out to be more accurate than existing high-resolution databases, in particular the daytime population densities reported in the ENACT 2011 Population Grids of the European Commission. This grid cell information combines satellite imagery and administrative data from Eurostat for the entire EU at a 1×1 km resolution (Schiavina et al. (2020)). The daytime population is derived from workplace population data obtained from employment statistics and travel surveys, with spatial allocation informed by CORINE land use data. However, ENACT 2011 disaggregates population information from NUTS3 regions according to build-up volumes. This is an issue for the country of Luxembourg, which constitutes a single NUTS-3 region. This discrepancy is shown in Figure 1.G.1, which plots the administrative municipal employment data as a function of the ENACT 2021 values aggregated at the municipal level. By contrast, our approach reports employment levels and provides better precision because it disaggregates information from the municipal level. Figure 1.G.2 plots our employment data and the ENACT employment data and shows the strong correlation between the two datasets.

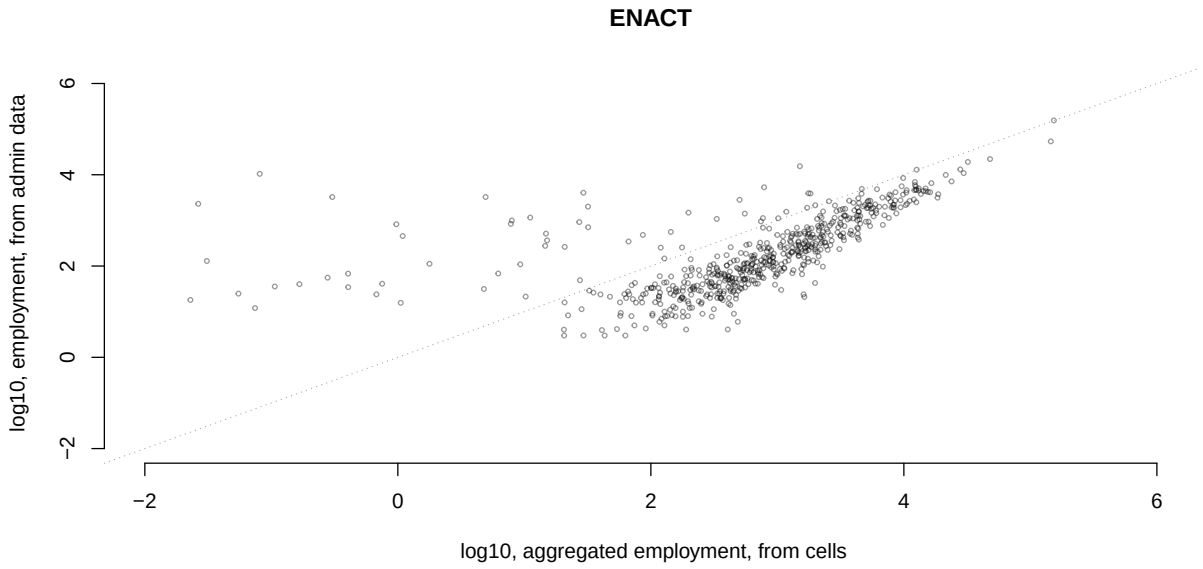

Figure 1.G.1: Comparison between administrative employment records and aggregated ENACT daytime data, by municipality.

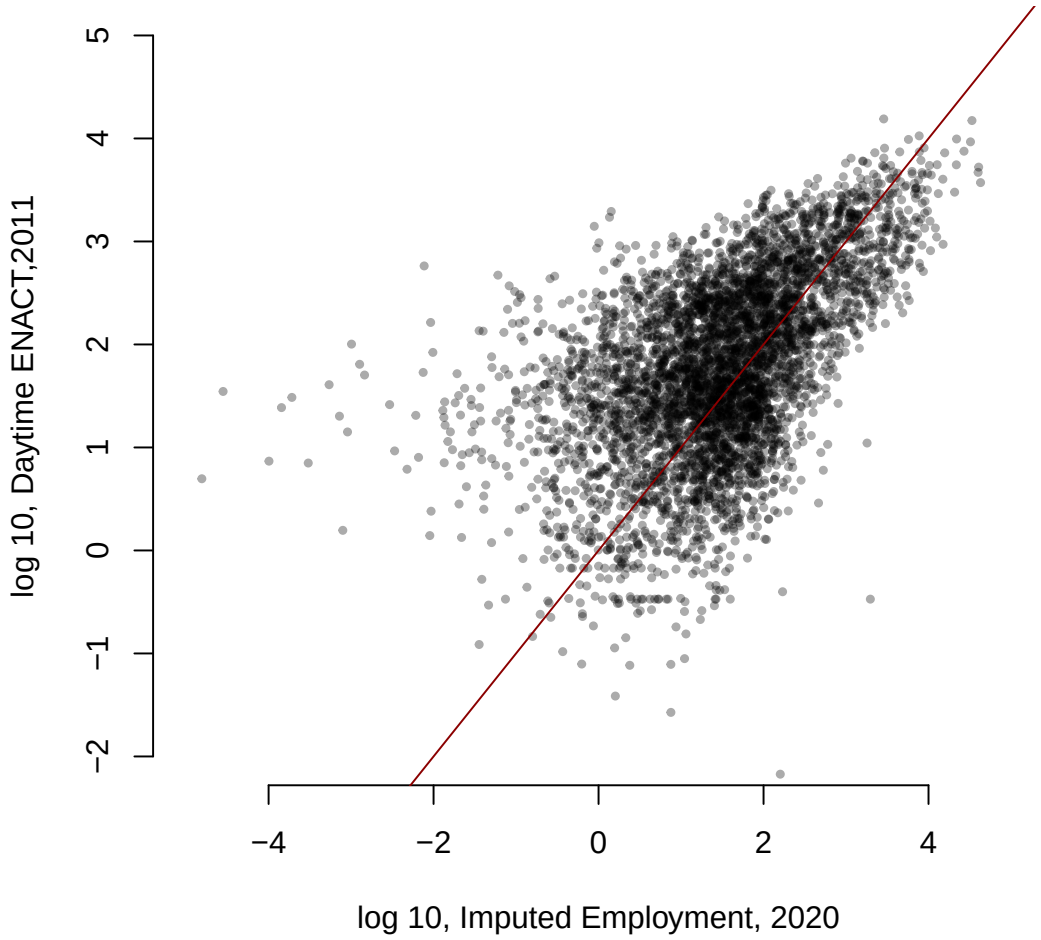

Figure 1.G.2: Comparison between our 2020 imputed values for employment and daytime ENACT population data.

1.G.2 Robustness on hedonic price regression

Table 1.G.1 gives information about the number of cells that include more than 1, 2, 3, 5 and 10 observations of price and rent listings. Restricting to a minimum number of 5 listings reduces the number of cells by about half.

FE Type	Country	All	≥ 2	≥ 3	≥ 5	≥ 10
Price FEs	Luxembourg	496	297	296	216	116
	Not Luxembourg	478	367	223	150	77
Rent FEs	Luxembourg	295	193	142	104	69
	Not Luxembourg	149	60	27	15	6

Note: The table depicts the number of cells with 0 or more, 2 or more, 3 or more, 5 or more and 10 or more listings per cell for both rental and purchase prices.

Table 1.G.1: Count of cells according to the number of listings per cell for rents and purchase prices.

Table 2.D.1 compares the hedonic price regressions for rental prices (columns 1 and 5) and purchase prices (columns 2 and 6) without and with cell fixed effects. It also displays the results with the merger of rental and price listings with dummy control for a purchase in Luxembourg (columns 3 and 7) and dummy control for a purchase (versus rental) (columns 4 and 8).

	Without cell fixed effects				With cell fixed effects			
	Separate		Pooled		Separate		Pooled	
Dependent variable:	Rent, log	Price, log	Rent, log	Rent, log	Rent, log	Price, log	Rent, log	Rent, log
log, Surface	-0.112***	-0.049***	-0.130***	-0.093***	-0.156***	-0.239***	-0.165***	-0.165***
	(0.005)	(0.015)	(0.004)	(0.006)	(0.004)	(0.007)	(0.003)	(0.003)
Number of Rooms	-0.079***	-0.110***	-0.045***	-0.108***	-0.004	-0.016***	-0.018***	-0.018***
	(0.006)	(0.004)	(0.002)	(0.003)	(0.006)	(0.002)	(0.002)	(0.002)
Number of Bedrooms	0.003	0.001	-0.002*	0.003*	0.000	-0.001	-0.001*	-0.001*
	(0.003)	(0.002)	(0.001)	(0.002)	(0.002)	(0.001)	(0.001)	(0.001)
Number of Bathooms	0.008	0.007*	0.003	0.010***	0.004	-0.002	-0.001	-0.001
	(0.005)	(0.004)	(0.002)	(0.003)	(0.004)	(0.002)	(0.002)	(0.002)
Furnished	0.085***	0.009	0.024***	0.021**	0.039***	-0.008	0.006	0.002
	(0.013)	(0.012)	(0.007)	(0.009)	(0.010)	(0.006)	(0.005)	(0.005)
Age, decade	0.016***	0.008***	0.004***	0.007***	0.007**	0.004***	0.004***	0.004***
	(0.005)	(0.001)	(0.001)	(0.001)	(0.004)	(0.000)	(0.000)	(0.000)
Age^2, decade 10^{-3}	0.092***	-0.004***	-0.002***	-0.004***	0.059**	-0.002***	-0.002***	-0.002***
	(0.034)	(0.001)	(0.000)	(0.001)	(0.027)	(0.000)	(0.000)	(0.000)
Balcony surface	0.003	0.009***	0.005***	0.009***	-0.003	0.002***	0.002***	0.002***
	(0.003)	(0.001)	(0.001)	(0.001)	(0.003)	(0.001)	(0.001)	(0.001)
Year not defined	-0.028	0.015	-0.011	0.020**	-0.019	-0.035***	-0.026***	-0.022***
	(0.019)	(0.012)	(0.007)	(0.010)	(0.016)	(0.005)	(0.006)	(0.006)
Purchase: Lux			6.035***				5.919***	
			(0.010)				(0.009)	
Purchase: Not Lux			4.862***				5.516***	
			(0.012)				(0.017)	
Purchase				5.685***				5.837***
				(0.014)				(0.008)
Type FE	Yes	Yes	Yes	Yes	Yes	Yes	Yes	Yes
Type FE × Rooms	Yes	Yes	Yes	Yes	Yes	Yes	Yes	Yes
Insulation FE	Yes	Yes	Yes	Yes	Yes	Yes	Yes	Yes
Buy FE	No	No	No	Yes	No	No	No	Yes
Buy FE × Lux	No	No	Yes	No	No	No	Yes	No
Cell FE	No	No	No	No	Yes	Yes	Yes	Yes
R^2	0.590	0.488	0.983	0.965	0.820	0.926	0.992	0.992
Observations	4,149	8,916	13,065	13,065	4,149	8,916	13,065	13,065

Note: Types of properties used: Apartments (reference), bedrooms, detached houses, duplexes, houses, offices, semi-detached houses, studios. Robust standard errors in parentheses. * p < 0.1, ** p < 0.05, *** p < 0.01.

Table 1.G.2: Hedonic regression outcomes for purchase prices and rents.

1.G.3 Robustness on kriging regression and rental values

In the universal kriging approach, the deterministic trend of the cell's price index is given by $\eta_i = \mathbb{G}_i'.\beta + \epsilon_i$, or

$$\eta_i = \beta_1 \log(1 + d_i^{CBD}) \times LUX_i + \beta_2 \log(1 + POP_i) + \beta_3 \log(1 + EMP_i) + \epsilon_i \tag{1.G.1}$$

where d_i^{CBD} denotes the distance to the central business district, LUX_i is an indicator for being in Luxembourg, and POP_i and EMP_i represent local population and employment figures, respectively.

This expression can also be used in an OLS regression model, the results of which are shown in Table 1.G.3. This table includes specifications with rent listings, price listings, and pooled transaction listings. Price listings are more numerous and, therefore, have stronger explanatory power. The combination of rental and price listing further increases the explanatory power.

The table includes specifications with all cells or only those with more than five listings. The explanatory power is higher with the latter, as it removes error components of price/rent indices.

Dependent variable:	FE^{Rent}	FE^{Rent}	FE^{Price}	FE^{Price}	FE^{Rent}	FE^{Rent}	FE^{Rent}	FE^{Rent}
log, d(CBD)	-0.420***	-0.276**	-0.339***	-0.298***	-0.362***	-0.321***	-0.377***	-0.321***
	(0.072)	(0.124)	(0.043)	(0.052)	(0.041)	(0.047)	(0.043)	(0.048)
Luxembourg	0.091	0.489	0.880***	0.998***	0.400**	0.462***	0.641***	0.764***
	(0.262)	(0.438)	(0.165)	(0.203)	(0.156)	(0.178)	(0.161)	(0.180)
log, Population	-0.016	-0.004	-0.013	-0.011	-0.013	-0.008	-0.016	-0.010
	(0.021)	(0.021)	(0.014)	(0.021)	(0.013)	(0.016)	(0.012)	(0.016)
log, Employment	-0.001	-0.010	0.004	-0.008	0.002	-0.007	0.006	-0.004
	(0.018)	(0.027)	(0.013)	(0.020)	(0.012)	(0.015)	(0.012)	(0.016)
log, d(CBD) × Lux	0.127*	0.048	0.048	0.012	0.064	0.044	0.088*	0.056
	(0.073)	(0.127)	(0.046)	(0.060)	(0.044)	(0.052)	(0.045)	(0.053)
Observations	444	119	973	366	1073	419	1073	419
Sample	All	5+	All	5+	All	5+	All	5+
Pooled transactions	No	No	No	No	Yes	Yes	Yes	Yes
R^2	0.745	0.812	0.844	0.912	0.724	0.846	0.819	0.911
Transaction FE	No	No	No	No	No	No	Yes	Yes
Transaction-country FE	No	No	No	No	Yes	Yes	No	No

Table 1.G.3: OLS predictions for values of hedonics-adjusted cell fixed effects.

Table 1.G.3 compares the prediction errors of kriging and OLS methods for various minimum numbers of listings in the cells used to make a prediction. The figure shows that the OLS predictions yield higher mean absolute errors. This is because they do not consider spatial correlation. The top panels show that kriging regression errors are smaller for price listings than for rent listings, which justifies our choice of using the dataset with prices. The top-left panels show that price prediction errors diminish with the number of listings per cell and become stable for cells with more than five listings. The bottom panels show the prediction errors with pooled listings. Although they increase the number of cells with many listings, pooled listings do not bring significantly more accuracy.

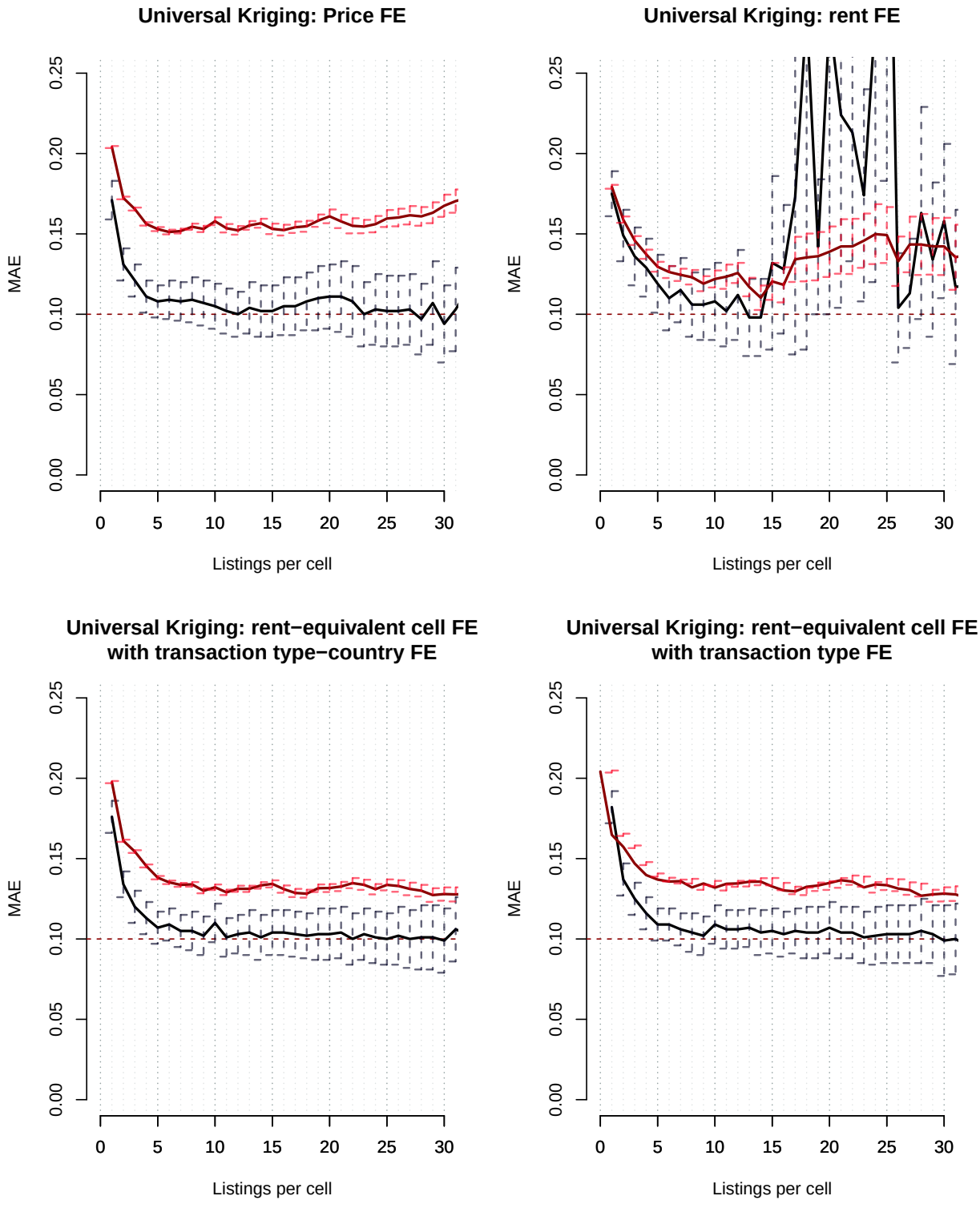

Note: We report predictions based on purchase prices (top left), rents (top right), rent equivalent housing prices with transaction type and country fixed effects (bottom left), rent equivalent with transaction type fixed effects (bottom right). Standard errors of MAE are reported.

Figure 1.G.3: Mean absolute errors for universal kriging (black) and OLS (red) predictions.

Table 1.G.4 reports the same information and yields the same conclusion for cells with all listings and with more than five listings.

Model	Variable	Listings per cell	N	MAE	RMSE	R^2
OLS	FE^{Rent}	All	444	0.179	0.228	0.740
		More than 5	119	0.130	0.165	0.787
	FE^{Price}	All	973	0.204	0.273	0.843
		More than 5	366	0.153	0.194	0.910
Kriging	FE^{Rent}	All	444	0.175	0.226	0.741
		More than 5	119	0.121	0.155	0.811
	FE^{Price}	All	973	0.172	0.244	0.874
		More than 5	366	0.108	0.147	0.948

Note: Both universal kriging and OLS use the deterministic specification (Equation 1.G.1). Values in the "Listings per cell" column denote the minimum listing threshold for cell fixed effects used for prediction. Out-of-sample prediction quality is assessed using 5-fold cross-validation. For universal kriging, optimal semivariogram models may vary.

Table 1.G.4: Out-of-sample prediction quality metrics for different model specifications for the natural logarithm of prices and rents.

1.G.4 Urban externalities

As a robustness check, Table 1.G.5 reproduces the empirical analysis of urban externalities with an instrument based on the proximity to ancient Roman cities and vicus settlements in ancient times for population, and another instrument based on distance to locations of Gaul Gold hoards and Roman coins for current employment. Table 1.G.5 presents the main results of our IV estimations with previous and current instruments. Columns (1) and (4) use the above 1975 build-up instrument, columns (2) and (5) the ancient times instruments, and columns (3) and (6) include both instruments. Results include the F-statistics from the first-stage regression, which confirm the relevance of our instruments. Wu-Haussman test statistics signal the presence of endogeneity in most situations. The small Sargan statistics in columns (3) and (6) suggest that the overidentifying restrictions are not violated for production and amenity externalities. Production externalities (columns 1 to 3) are mildly affected by the instruments. For amenity externalities (columns 4 to 6), the instrument of ancient city proximity seems too weak to conclude about a significant externality effect of residential amenity.

Dependent variable:	$\log A$			$\log B$		
	(1)	(2)	(3)	(4)	(5)	(6)
$\log \Upsilon$	0.070***	0.098***	0.070***			
	(0.006)	(0.034)	(0.006)			
$\log \Omega$				0.028***	-0.003	0.027***
				(0.003)	(0.020)	(0.003)
Geographic Controls	Yes	Yes	Yes	Yes	Yes	Yes
Instrument: 1975 build-up	Yes	No	Yes	Yes	No	Yes
Roman	No	Yes	Yes	No	Yes	Yes
First stage F-Statistics	16792.89***	61.32***	8395.37***	73161.07***	82.20***	38011.62***
Sargan Statistics			0.671			2.292
Sargan p-value			0.413			0.130
Wu-Hausman	44.18***	0.175	44.01***	54.74***	3.118*	61.691***
Observations	2658	2658	2658	3182	3182	3182
R^2	0.429	0.429	0.429	0.193	0.163	0.193

Table 1.G.5: Instrumental variable regressions with old and new instruments.

1.G.5 Tax importation

We eliminate importation taxes by assuming that all tax revenues collected in the metropolitan area of Luxembourg are collected by a supranational central administration, which reinvests its revenue on a per capita basis in local public goods across the entire geography. Tax rates are maintained at their baseline levels. Changes in endogenous variables of the model are reported in Table 1.G.6.

Country	Belgium	France	Germany	Luxembourg
Change in population, %	24.57	28.61	14.01	-24.31
Change in employment, %	7.81	6.75	7.58	3.19
Change in per capita tax transfer, %	52.31	64.00	28.71	-36.03
Change in total tax revenue, %	89.72	110.93	46.74	-51.58
Change in expected income, %	1.12	1.55	-0.15	0.61
Change in floorspace prices, %	13.64	16.92	7.97	-7.77
Change in wages at workplace, %	-3.55	-3.20	-2.17	-0.13
Total population change: 4.89 %				

Note: We report changes in total population and employment by country, changes in population-weighted averages for tax transfer, changes in total tax revenue, expected income, and average floorspace price, and changes in employment-weighted average for wages at workplace.

Table 1.G.6: Changes in endogenous variables of the model in a counterfactual with no tax importation.

1.G.6 Cross border commuting

In Table 1.G.7, we report changes in the endogenous outcomes of the model after the prohibition of cross-border commuting. The reported values correspond to the difference between the baseline and the counterfactual analyzed in Column 2 of Table 1.10. We observe a decrease in the total population of the economy by 13.68%, which roughly corresponds to the number of cross-border workers currently commuting to Luxembourg. We observe a decrease in expected income for Belgium, France, and Germany, as well as a decrease in floorspace prices for all four countries. Per capita tax transfers decrease in Luxembourg and increase elsewhere, which is indicative of the mechanical elimination of the tax importation effect in the counterfactual with closed borders.

Country	Belgium	France	Germany	Luxembourg
Change in population, %	-23.17	-24.43	-15.67	-1.73
Change in employment, %	16.58	39.37	13.92	-38.89
Change in per capita tax transfer, %	30.01	43.41	23.24	-25.55
Change in total tax revenue, %	-0.12	8.38	3.92	-26.83
Change in expected income, %	-18.26	-21.77	-9.92	11.70
Change in floorspace prices, %	-11.07	-14.81	-8.49	-15.35
Change in wages at workplace, %	-1.57	-3.19	-0.99	10.46
Total population change: -13.68 %				

Note: We report changes in total population and employment by country, changes in population-weighted averages for tax transfer, changes in total tax revenue, expected income, and average floorspace price, and changes in employment-weighted average for wages at workplace.

Table 1.G.7: Changes in endogenous variables of the model in a counterfactual with no cross-border commuting.

1.G.7 Multiple equilibria

In Section 1.6, we examine the effect of taxation in a seamless geography where firms and residents are located on a disk matching the dimensions of our empirical area. In such a setting, fundamental local productivities, amenities, and development densities are equalized across space. The aim is to compare the observed and predicted impacts of taxes on floorspace prices and the share of commercial buildings, using the parameter estimates from our empirical analysis. We find and discuss a spatial equilibrium in which employment is more concentrated at the center of the disk—that is, a configuration with monocentric properties. This naturally raises the question of equilibrium multiplicity.

We here adopt a heuristic approach to test for the existence of equilibria other than the benchmark discussed in the seamless geography on the 75 km-ray disk with 1×1 km grid cells. The benchmark case is computed with initial wages set to one, $w_i^0 = 1$. The outcome of the simulation yields a model-consistent distribution of wages, w_i^*. We then substantially alter the initial conditions for wages and verify whether our fixed-point algorithm still converges to the benchmark solution. We choose the initial wage of each cell w_i^0 to the values either $\underline{w}^0 = 0.2 \min\{w_i^*\}$ and $\overline{w}^0 = 5 \max\{w_i^*\}$. Initial conditions on floorspace prices, share of commercial build-up, population, and employment densities are set as functions of the initial wage vector under uniform taxation, applying equations (1.3.4), (1.3.5), (1.3.6), (1.3.10), and (1.3.18). We assume uniform productivity A_j and uniform G_i for the initial guess. These exercises are computationally intensive. Because of computing time and memory constraints, we restrict the number of grid cells by keeping one cell out of every four cells. [10] We repeat this exercise with the tax differences defined in the chapter.

Four types of initial wage vectors are tested. Initial conditions (1) to (5) randomize wages between $\underline{w}^0$ and $\overline{w}^0$ with a probability equal to 1/2. Initial condition (6) sets wages to $\overline{w}^0$ in potential subcenters and to $\underline{w}^0$ elsewhere. We chose two symmetric subcenters located 40 km away from the geographical center of the economy. The radius of each of the subcenters is equal to 30 km. Initial conditions (7) to (9) set wages to $\overline{w}^0$ in a ring-shaped donuts located at distances from 20 to 40, from 40 to 60, and from 60 to 75 km respectively from the center and at the boundary of the disk, and $\underline{w}^1$ elsewhere.

Tables 1.G.8 and 1.G.9 report the number of iterations K, the uniform norm (sup-norm) convergence indicator, $\|w_i^K - w_i^{K-1}\|_\infty$, the statistics of wages and floorspace prices in the last iteration K. It can be verified that none of the initial conditions converges to a solution different from the benchmark, and that all deviations in numbers are within the machine precision.

[10] This restriction furthermore parallels the properties of our calibrated model on the set of active cells.

	Benchmark	(1)	(2)	(3)	(4)	(5)	(6)	(7)	(8)	(9)
Iterations K		202	202	202	224	202	205	207	231	254
$\|w_i^K - w_i^{K-1}\|_\infty$	2.16711×10^{-9}	1.76633×10^{-9}	1.2006×10^{-9}	1.25203×10^{-9}	6.8858×10^{-10}	1.43566×10^{-9}	1.0778×10^{-9}	3.97786×10^{-9}	1.53106×10^{-9}	1.31334×10^{-10}
$\|q_i^K - q_i^{K-1}\|_\infty$	9.45025×10^{-6}	1.5281×10^{-6}	2.7461×10^{-6}	2.55959×10^{-6}	3.32929×10^{-6}	1.97565×10^{-6}	1.34852×10^{-6}	8.6301×10^{-6}	2.84053×10^{-6}	7.74735×10^{-7}
$\min_i w_i^K$	0.104135158	0.104135112	0.104135112	0.104135112	0.104135147	0.104135112	0.10413512	0.104135121	0.104135152	0.10413514
mean w_i^K	0.099970625	0.099970596	0.099970596	0.099970596	0.09997063	0.099970596	0.099970604	0.099970605	0.099970635	0.099970624
$\max_i w_i^K$	0.098900733	0.098900704	0.098900704	0.098900704	0.098900738	0.098900704	0.098900712	0.098900713	0.098900743	0.098900732
$\min_i q_i^K$	101.8057697	101.8058651	101.8058649	101.8058647	101.8057531	101.8058650	101.8058394	101.8058356	101.8057371	101.8057751
mean q_i^K	96.88661374	96.88670487	96.88670476	96.88670453	96.88659827	96.88670482	96.88668042	96.88667683	96.88658307	96.88661928
$\max_i q_i^K$	74.90646373	74.90655001	74.90654994	74.90654976	74.90646620	74.90654998	74.90653079	74.90652787	74.90645432	74.90648275

Table 1.G.8: Robustness check w.r.t. initial conditions - seamless geography, equal taxes.

	Benchmark	(1)	(2)	(3)	(4)	(5)	(6)	(7)	(8)	(9)
Iterations K		217	217	217	253	217	220	230	245	239
$\|w_i^K - w_i^{K-1}\|_\infty$	3.0095×10^{-9}	8.47174×10^{-10}	6.37057×10^{-10}	6.43142×10^{-10}	4.01282×10^{-10}	7.39164×10^{-10}	2.40723×10^{-10}	1.26539×10^{-9}	4.453×10^{-11}	4.23955×10^{-10}
$\|q_i^K - q_i^{K-1}\|_\infty$	1.31982×10^{-5}	1.0172×10^{-6}	5.24669×10^{-7}	5.4134×10^{-7}	1.5353×10^{-6}	7.63913×10^{-7}	8.56382×10^{-7}	3.74044×10^{-6}	9.58894×10^{-7}	3.85421×10^{-7}
$\min_i w_i^K$	0.104135158	0.104135148	0.104135148	0.104135148	0.104135158	0.104135148	0.104135151	0.104135161	0.104135161	0.104135151
mean w_i^K	0.100743831	0.100743821	0.100743821	0.100743821	0.100743831	0.100743821	0.100743824	0.100743834	0.100743834	0.100743825
$\max_i w_i^K$	0.099139493	0.099139483	0.099139483	0.099139483	0.099139493	0.099139483	0.099139486	0.099139496	0.099139496	0.099139487
$\min_i q_i^K$	112.6815803	112.681617	112.6816169	112.6816169	112.6815805	112.681617	112.6816056	112.6815699	112.6815702	112.681604
mean q_i^K	97.31370871	97.31373934	97.31373929	97.31373921	97.3137078	97.31373931	97.31372946	97.31369866	97.31369886	97.31372809
$\max_i q_i^K$	74.29305848	74.29310291	74.29310288	74.29310282	74.29307845	74.29310290	74.29309527	74.29307141	74.29307153	74.29309420

Table 1.G.9: Robustness check w.r.t. initial conditions - seamless geography, unequal taxes.

Chapter 2

Welfare Effects of Congestion in Luxembourg and the Greater Region

This chapter is based on the joint work with Pierre M. Picard.

2.1 Introduction

Congestion is a major spatial friction and cost for commuters. It increases travel time and commuting expenses, but it can also limit the inflow of new workers to central areas by reducing access to high-productivity labor markets. This barrier may protect the advantages of existing residents and workers, who could face net welfare losses if congestion is reduced. This chapter examines how highway congestion shapes economic outcomes in Luxembourg, where more than half of the labor force commutes daily from abroad. It uses new empirical evidence to assess how the effects of congestion differ across regions, who bears the costs, and where these costs are most concentrated.

To address these questions, we estimate average speed losses during rush hours using a multi-period difference-in-differences framework. Using highway camera data from Luxembourg, together with the hub-and-spoke structure of its highways and directional asymmetries in traffic flows, we measure rush-hour effects across routes. We then build a travel time matrix to quantify regional exposure to congestion and examine how travel time losses are distributed across space. Using this matrix, we calibrate a quantitative spatial urban model to evaluate aggregate and local impacts of congestion on consumer welfare. We introduce counterfactual scenarios in which congestion is eliminated by setting travel speeds to free-flow levels. The calibrated model translates travel time changes into utility and wage equivalents, providing an intuitive measure of welfare losses or gains.

Our empirical results reveal substantial heterogeneity in congestion effects. French highways are the most affected, with additional bottlenecks at border crossings and motorway exits in Esch, Dudelange, and Bettembourg. The model simulations complement these findings, showing that while congestion lowers welfare and production in most areas outside Luxembourg, residents of Luxembourg City benefit for two main reasons. First, most work locally and rely on public transport, including the congestion-free tram, which limits their exposure to highway traffic. Second, higher commuting costs from abroad reduce competition in the city's labor market, easing pressure on both jobs and housing rents. Removing congestion leads to a short-run welfare loss of €1,140 per person per year for Luxembourg City residents, which turns into a welfare gain of €3,490 in the long run with population reallocation. When migration inflows from the broader economy are considered, the welfare effect becomes a loss of €8,110 per resident per year.

This study contributes to the literature in three ways. First, it uses detailed data on population, employment, and travel times to measure congestion effects at a 1×1 km scale. Second, it shows the asymmetric nature of congestion: intensity can differ between inbound and outbound traffic on the same road segment within the same time window, affecting welfare measurement and willingness-to-pay estimates. Third, in a multi-country setting, it quantifies the fiscal impact of removing congestion. The estimated fiscal gain for Luxembourg is €2.50 billion per year in the short run, €1.18 billion in the long run, and €7.04 billion with migration inflows. The short-run gain alone could finance the expansion of 35% of Luxembourg's highways by adding one lane in each direction.

For more than a decade, urban economies have been studied using quantitative spatial models that incorporate geography, mixed land use, trade, and commuting (Ahlfeldt et al., 2015; Allen & Arkolakis, 2014; Delventhal et al., 2022; Monte et al., 2018a; Redding, 2016; Redding & Rossi-Hansberg, 2017; Tsivanidis, 2019). Our study fits within this literature, focusing on congestion and its effects on firms and residents. This approach requires highly detailed data on prices, population, and employment, which we construct using disaggregation techniques. Price data

are predicted with kriging methods that capture spatial correlation (Cressie, 1988; Wackernagel, 2003), high-resolution population data are assembled by combining administrative sources with satellite imagery, and property prices are obtained through web scraping from the largest real estate aggregator in Luxembourg and its surrounding region.

The paper also connects to the broader transport economics literature on congestion. Foundational work by Pigou (1920), Knight (1924), and Vickrey (1963) established the principles of congestion externalities and peak-load pricing, with further formalization by Walters (1961), Small (1992), and Small and Verhoef (2007). More recent contributions have documented induced demand from road capacity expansion (Duranton & Turner, 2011; Hymel et al., 2010) and evaluated large-scale congestion relief and management policies, such as the Stockholm and London experiments (Börjesson et al., 2012; Eliasson, 2009; Leape, 2006).

Our work draws on both the transport economics tradition and the empirical (Ahlfeldt & Feddersen, 2018; Akbar et al., 2023; Couture et al., 2018; Duranton & Turner, 2012; Heblich et al., 2020) and theoretical (Anas, 2012; Duranton & Turner, 2011; Rotemberg, 1985) literature on transport infrastructure and congestion. At the same time, since transportation theory shows that expanding road capacity rarely eliminates congestion, our model is not intended as a forecasting tool. Instead, we use it to measure the ex-ante willingness-to-pay for changes in travel time in a controlled setting, treating the results as a thought experiment rather than a policy prescription, and we therefore set aside issues of optimal network design and endogenous traffic responses (Allen & Arkolakis, 2022; Fajgelbaum & Schaal, 2020).

Our study is closely related to Seidel and Wickerath (2020) in both spirit and methodology. Their paper examines a German setting using a quantitative spatial model that includes trade but omits the housing market, studying how congestion relief affects the spatial distribution of economic activity. They find that lower travel times increase urbanization, aggregate welfare, and average labor productivity. We extend their work in three ways. First, we introduce a floorspace market with both commercial and residential floorspace use to capture the general equilibrium response of both sectors to transport improvements, which is especially relevant in Luxembourg. Second, we conduct the analysis on a 1×1 km grid, allowing us to capture localized congestion effects and measure welfare losses at a fine spatial scale. Third, we consider a multi-country setting with land, labor, and VAT taxation, enabling us to capture the fiscal feedback loop whereby transport improvements raise tax revenues, which, in turn, could help finance future infrastructure. Finally, we appraise a potential congestion relief measure in the spirit of Hörcher and Graham (2024).

This chapter builds on the model and data introduced in Chapter 1. To avoid repetition, only key elements are briefly recalled where needed, with details provided in Chapter 1. The chapter is structured as follows. Section 2.2 presents stylized facts on cross-border mobility and congestion in Luxembourg's commuting region. Section 2.3 outlines the identification strategy for estimating rush-hour effects on average speed across highways and camera pairs. Section 2.4 summarizes the model from Chapter 1. Section 2.5 introduces additional data sources. Section 2.6 provides parameter estimates. Section 2.7 reports comparative statics in a stylized geography. Section 2.8 presents counterfactual results. Section 2.9 concludes the chapter.

2.2 Stylized facts

This section presents stylized facts on cross-border mobility in Luxembourg and the Greater Region. We begin by outlining the structure of the road network, showing that Luxembourg's highways have a radial layout with Luxembourg City at the center. We then provide summary statistics on observable covariates for cross-border and domestic work commutes. Cross-border commutes are, on average, longer, start and end earlier, and account for more than half of all work-related trips. Finally, we show that the number of cross-border commutes rises sharply after 06:00, which we define as the start of rush hour in the Greater Region.

2.2.1 Highway system of Luxembourg

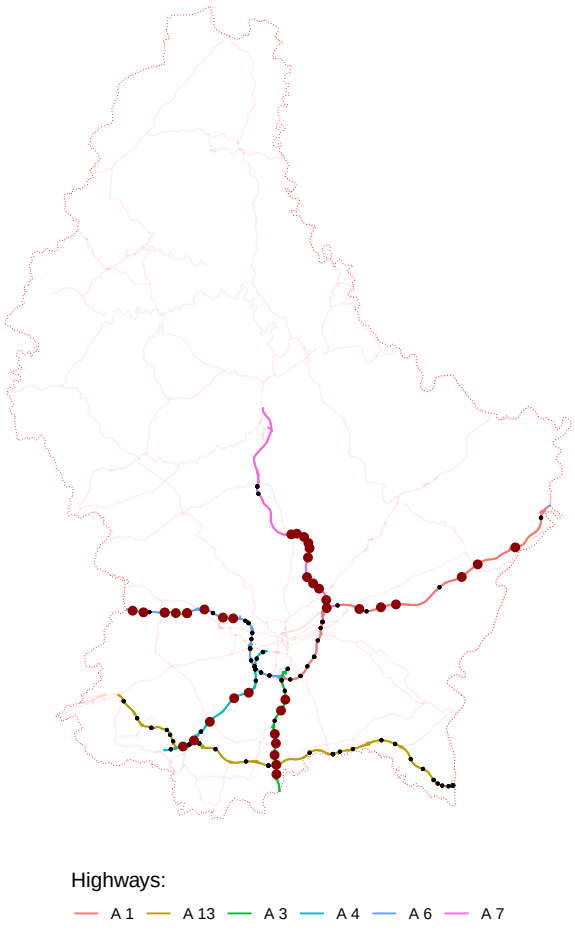

Note: Each highway (*autoroute*) is shown in a unique color. The A1 links Luxembourg City to Germany. The A3 and A4 connect Luxembourg City to France via Dudelange and Esch-sur-Alzette, respectively. The A6 and A7 connect Luxembourg City to Belgium via Arlon and Gouvy, while the A13 links Germany with Belgium and France through southern Luxembourg. Other roads (internal highways, national roads, and other primary roads) are shown in pale red. Camera pairs are marked in black, with those used in the analysis highlighted by large red circles. The selection criteria are described in Section 2.3.2.

Figure 2.2.1: Cross-border highways of Luxembourg.

Luxembourg hosts the largest cross-border commuting labor market in the EU, with more than 500,000 daily commuters. Most travel into the Grand Duchy for work, underscoring its role as a regional economic hub. Luxembourg City is the main destination, serving as the financial

center with a high concentration of banks, multinational firms, and key European institutions, including the Court of Justice, Eurostat, the European Investment Bank, the European Stability Mechanism, and the Secretariat of the European Parliament. This makes the city a central workplace for both domestic employees and cross-border professionals.

The city's connectivity is central to sustaining its large cross-border commuting network. Luxembourg City is linked to the rest of the country and neighboring regions through a dense road system. Direct connections include Belgium (A6, A7, A13), France (A3, A4), and Germany (A1, A13). The layout of these highways within the national motorway system is shown in Figure 2.2.1.

Car traffic is monitored through more than 160 camera pairs installed along the main highways. This network covers key transport corridors and provides real-time data. CITA, the agency in charge, records average speed, traffic volume, and density separately for inbound (toward Luxembourg City) and outbound (leaving Luxembourg City) flows, with data collected at five-minute intervals.

2.2.2 Commuting patterns

This subsection describes commuting patterns within Luxembourg and across borders. The main data source is the 2017 "LuxMobil" survey conducted by the Ministry of Transport of Luxembourg. The survey provides a representative sample of commuters in the Luxembourg area and features 82,000 weighted individual observations. It reports information on trip origins and destinations, transport mode, distance, duration, time of day, and selected commuter characteristics. The survey covers 217 origins and destinations, most of which are within Luxembourg.

We focus on work-related car commutes, which make up 30% of the sample. Cross-border commutes are defined as trips starting outside Luxembourg and ending within the country. Commutes with both origin and destination outside Luxembourg are excluded, as only 20 such cases appear in the data. Summary statistics are shown in Table 2.2.1.

	In Luxembourg	**Cross-border**
Number of commuters	133,000	145,225
Distance, km	19.2	41.5
Duration, min	28.4	54.0
Departure time, hrs	8.7	7.4
Arrival time, hrs	9.2	8.3
Share, by car	0.87	0.85

Note: We restrict the sample to work-related car commutes. Domestic commutes are those starting and ending in Luxembourg, while cross-border commutes start abroad and end in Luxembourg. Commutes that do not end in Luxembourg are excluded. The total number of commuters is computed by summing survey weights. **Source:** "LuxMobil" survey, 2018.

Table 2.2.1: Summary statistics on work-related commutes, by category.

First, the share of cross-border commuters is approximately the same as that of commuters working within Luxembourg, highlighting the distinct nature of its labor market. Second, cross-border commutes are longer in both distance and duration. Third, cross-border commuters typically leave home and arrive at work about an hour earlier than domestic commuters. Finally, while most commuters in both groups use cars, cross-border commuters are slightly more likely to rely on buses or trains.

2.2.3 Traffic flow patterns

This subsection highlights key stylized facts on congestion and cross-border flows in Luxembourg. Two points are most relevant for the analysis: the stability of cross-border flows and the radial pattern of work commutes centered on Luxembourg City.

Figure 2.2.2 shows daily traffic volumes at all highway and national road entry points to Luxembourg: seven from France, ten from Germany, and nine from Belgium. The vertical axis plots daily traffic flows for each weekday in 2019, while the horizontal axis shows the hours of the day. Flows are highly stable across the year, with only small deviations from the hourly average, indicated by the red dashed line. Inbound traffic rises sharply at 06:00.

Figure 2.2.3 uses 2017 commuting flow data for France and Luxembourg to illustrate work-related car commutes. It covers all Luxembourgish municipalities and French municipalities within 50 km of the border where at least 1% of workers commute to Luxembourg. The left panel shows high cross-border commuting from France: in some border municipalities, more than 60% of the workforce is employed in Luxembourg. The right panel displays the conditional probability of commuting to Luxembourg City, given employment in Luxembourg. This share is highest in Luxembourg City and in French municipalities along the highway corridor, where more than half of cross-border commuters work in the capital. This pattern confirms the radial structure of commuting flows converging on Luxembourg City, supported by the highway network.

In summary, daily inbound car traffic to Luxembourg is highly stable, accounts for most work-related commutes, follows a radial pattern centered on Luxembourg City, and rises sharply at 06:00. Building on these patterns, the next section estimates highway congestion severity using the temporal stability and spatial radiality of flows for identification.

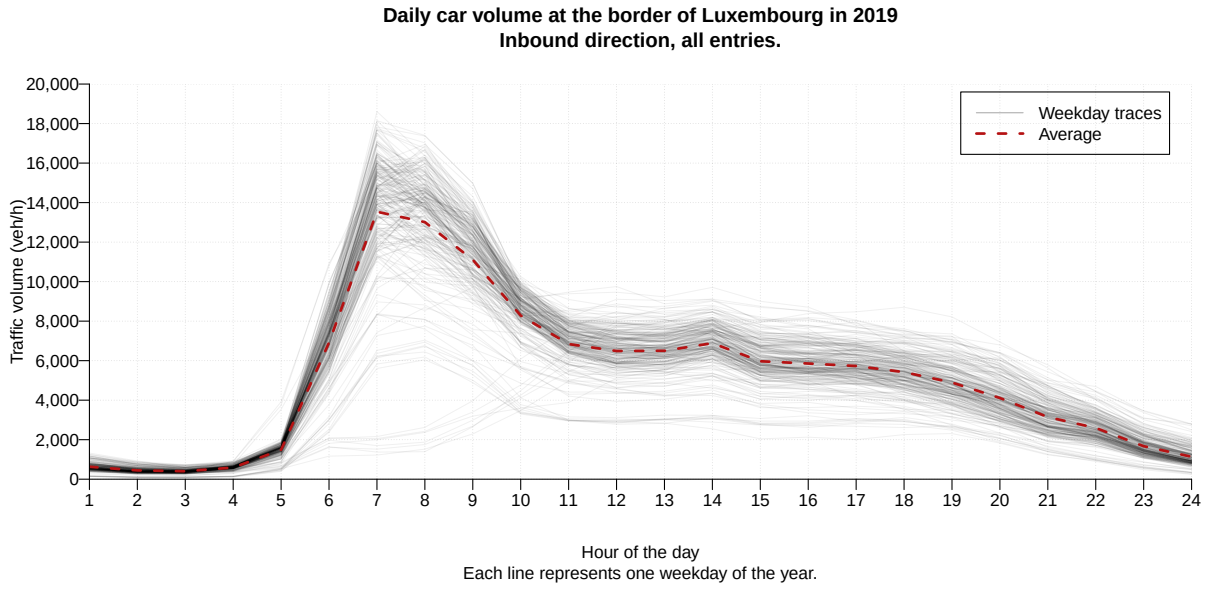

Note: Each black line shows total inbound traffic at Luxembourg's borders for one weekday in 2019: 7 entry points from France, 10 from Germany, and 9 from Belgium. The red dashed line marks the mean flow. **Source:** CITA and Administration des ponts et chaussées, 2019.

Figure 2.2.2: Distribution of traffic volume by hour of the day at border crossings.

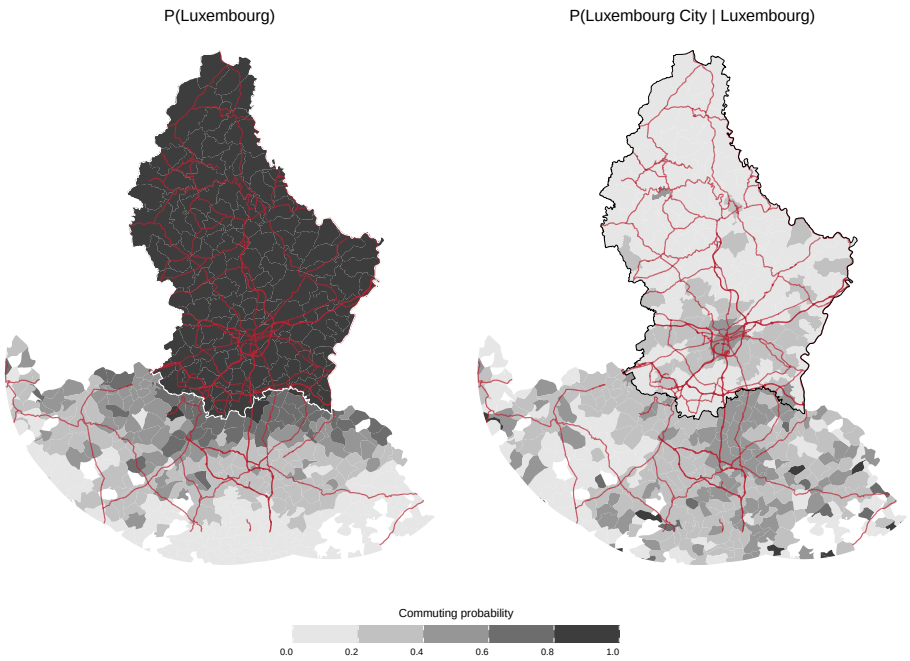

Note: Highways and primary roads are shown in red. Luxembourg's border is marked in white (left) and black (right). Data are shown only for Luxembourg and France due to limited granularity for Belgium and Germany. French municipalities with less than 1% commuting probability to Luxembourg or located more than 50 km from the border are excluded. Only work-related car commutes are considered. **Source:** "LuxMobil" survey and INSEE, 2018.

Figure 2.2.3: Commuting probability to Luxembourg (left) and commuting probability to Luxembourg City conditional on commuting to Luxembourg (right).

2.3 Empirical evidence

This section estimates the effect of the morning rush hour on average travel speed using a multi-period difference-in-differences strategy. The analysis exploits two features of the setting: the stable start and end times of the workday, which define rush hours, and the radial structure of Luxembourg's highway network with Luxembourg City as the main destination.

The method uses within-camera pair variation in speed data. For each pair, the inbound camera (toward Luxembourg City) is treated during the morning rush hour, while the outbound camera serves as a control. Comparing changes in average speed between the treated and control cameras over time identifies the causal impact of rush hour congestion on traffic speed. The strategy is applied in two steps: first, estimating average speed losses at the highway level to capture heterogeneity across routes; second, applying the method at the camera-pair level to detect spatial variation. Cameras with the largest speed reductions are identified as network choke points.

2.3.1 Data

The analysis relies on traffic data from more than 160 camera pairs installed along Luxembourg's main highways. Managed by CITA[11], the cameras record average speed, traffic volume, and density separately for inbound (toward Luxembourg City) and outbound (from Luxembourg City) traffic. We use data from November 25 to December 13, 2019, before the COVID-19

[11] The Luxembourg agency Contrôle et Information du Trafic sur Autoroute (CITA) provides data on highway traffic speeds.

outbreak. Observations are recorded every five minutes, but to address irregular coverage across cameras, we average them to the hourly level. The analysis focuses on the radial highways connecting to Luxembourg City.

2.3.2 Highway congestion

This subsection outlines the regression specification used to estimate the causal effect of the morning rush hour on average highway speeds in Luxembourg. The identification strategy rests on two observations about cross-border traffic. First, most organizations in the Greater Region follow stable work schedules: the day typically starts between 08:00 and 09:00 and ends between 17:00 and 18:00. As shown earlier, cross-border commuters usually begin their trips one to two hours before work, with traffic volumes rising sharply from 06:00. We use 2019 data, before COVID-19 and the widespread shift to remote work, so teleworking can be excluded as a factor affecting congestion.

The second observation is that Luxembourg City is the main commuter destination. Thus, highways are expected to experience inbound congestion during rush hours, while outbound traffic remains relatively free-flowing. The radial layout of the highway network supports a clear distinction between inbound and outbound flows. To avoid contamination from outbound cameras that may still capture inbound traffic near the city center, we exclude cameras within 5 km of Luxembourg City. In addition, two highways, B40 and A13, do not follow the radial pattern and are excluded from the main analysis. As a robustness check (Appendix 2.A), we show that these non-radial highways display no significant inbound–outbound speed differences.

The identification strategy is straightforward: we compare the average speeds recorded by the same camera pair before and after the morning rush hour. Road characteristics, capacity, and speed limits are identical in both directions, as paired cameras are typically less than 10 meters apart. The only systematic difference is demand: during the morning rush hour, inbound traffic is much heavier than outbound. Thus, one camera in each pair measures congested segments, while the other measures uncongested segments, allowing us to isolate the effect of rush hour on average speed.

We estimate a multi-period difference-in-differences model with simultaneous treatment, defining 06:00 as the start of rush hour. All observations from 06:00 onward are treated. Although the rush hour ends at 10:00, we assume an absorbing treatment and plot highway-specific coefficients across post-treatment periods to show the gradual convergence of speeds between treated and control cameras. The regression uses a logarithmic specification, consistent with transportation studies employing travel speeds as outcomes (Akbar et al., 2023; Ang et al., 2020; Cook et al., 2025). As a robustness check, Appendix 2.A presents results from a linear specification, confirming that the parallel trends assumption holds in both cases, and that findings are robust to functional form. The baseline model is specified as follows:

$$\log speed_{cphdt} = \alpha + \delta_{pdt} + \sum_{t=-4, t\neq 0}^{7} \beta_{ht} \times inbound_c \times rush_t + \varepsilon_{cphdt}. \tag{2.3.1}$$

Here, c indexes a camera in pair p on highway h, with observations taken on day d at time t. The inbound camera is treated, while the outbound camera serves as the control. The treatment indicator $inbound_c$ equals one for inbound cameras, and the rush-hour indicator $rush_t$ equals one for observations after 06:00. δ_{pdt} denotes pair–day–hour fixed effects, capturing all variation across pairs, so identification relies only on within-pair differences in average speeds.

The heterogeneous effect β_{ht} varies by time of day and is interpreted as the log difference in average speeds between inbound and outbound cameras within the same pair.

Dependent variable:	Average speed, log					
	All	A1	A3	A4	A6	A7
inbound × rush$_{-4}$	-0.038**	-0.057	-0.015	-0.153	-0.009	-0.015
	(0.018)	(0.034)	(0.044)	(0.101)	(0.015)	(0.016)
inbound × rush$_{-3}$	-0.026	-0.042	0.007	-0.160	0.020	-0.035
	(0.017)	(0.032)	(0.050)	(0.091)	(0.013)	(0.019)
inbound × rush$_{-2}$	0.003	0.003	0.081	-0.084	0.067**	-0.086
	(0.026)	(0.034)	(0.053)	(0.100)	(0.023)	(0.076)
inbound × rush$_{-1}$	0.029	0.046	0.118*	-0.126	0.078***	-0.024
	(0.022)	(0.038)	(0.057)	(0.102)	(0.018)	(0.039)
inbound × rush$_1$	-0.404***	-0.104	-0.759***	-0.993**	-0.461***	-0.088
	(0.068)	(0.059)	(0.162)	(0.264)	(0.041)	(0.069)
inbound × rush$_2$	-0.721***	-0.344**	-0.888***	-1.165**	-0.887***	-0.529**
	(0.081)	(0.108)	(0.095)	(0.379)	(0.097)	(0.175)
inbound × rush$_3$	-0.621***	-0.223*	-0.843***	-1.042***	-0.779***	-0.431**
	(0.072)	(0.115)	(0.127)	(0.257)	(0.064)	(0.153)
inbound × rush$_4$	-0.189***	0.043	-0.414***	-0.406**	-0.236***	-0.080
	(0.045)	(0.041)	(0.115)	(0.145)	(0.039)	(0.096)
inbound × rush$_5$	-0.037	0.015	-0.069	-0.085	0.039**	-0.099
	(0.032)	(0.042)	(0.055)	(0.134)	(0.015)	(0.090)
inbound × rush$_6$	-0.023	0.021	0.025	-0.079	0.027	-0.104
	(0.030)	(0.035)	(0.045)	(0.112)	(0.018)	(0.090)
inbound × rush$_7$	-0.038	-0.030	0.012	-0.058	0.018	-0.115
	(0.033)	(0.054)	(0.049)	(0.114)	(0.015)	(0.097)
Observations	38,665	7,225	7,136	4,692	9,464	10,148
R^2	0.627	0.446	0.804	0.723	0.789	0.444
Within R^2	0.385	0.180	0.604	0.548	0.706	0.212
Pair × Day × Hour FE	X	X	X	X	X	X

Note: We report estimation results from the multi-period difference-in-differences specification (2.3.1). Standard errors, clustered at the camera-pair level, are shown in parentheses. All models include pair–day–hour fixed effects. Treated cameras are those facing inbound traffic, while cameras within 5 km of Luxembourg City are excluded. Rush hour is defined as starting at 06:00. We assume an absorbing treatment and classify 10:00–13:00 as treated to show convergence of estimates to zero. **Source:** CITA.
* $p < 0.1$, ** $p < 0.05$, *** $p < 0.01$.

Table 2.3.1: Event study difference-in-difference coefficients for the average speed during congestion time.

Table 2.3.1 reports the results. Before rush hour, average speeds in inbound and outbound directions do not differ significantly. Coefficients for the pre-treatment period (02:00–05:00) are small and statistically insignificant, supporting the parallel trends assumption, with the slight exception of the A6, which shows earlier congestion. After 06:00, coefficients indicate large speed reductions. For example, Column 1 shows a drop of –0.404 (-33%) at 07:00, with the effect peaking at –0.721 (-51%) at 08:00. These effects are large and statistically significant, and significant negative coefficients through 10:00 show that congestion is persistent rather than short-lived.

The size of congestion effects differs markedly across highways. A4 shows the largest reductions

in average speed, with coefficients of –0.993 (–62%) at 07:00 and –1.165 (–68%) at 08:00. A1 displays smaller and less consistent effects, with –0.104 (–10%) at 07:00 and –0.344 (–29%) at 08:00. A6 shows intermediate effects, with –0.461 (–37%) at 07:00 and –0.887 (–59%) at 08:00. Overall, the results highlight strong heterogeneity across the network, with A3 and A4, both leading to France, as the most affected routes. After 10:00, the coefficients become largely insignificant, indicating no meaningful differences between inbound and outbound speeds and marking the end of the morning rush hour, as expected.

Appendix 2.A reports four robustness checks. First, using absolute speeds, we confirm parallel trends and robustness to functional form. Second, applying the model to excluded non-radial highways (A13, B40) shows no significant pre/post differences. Third, weekend data reveal no inbound-outbound differences. Fourth, estimating the evening rush hour (from 16:00) with outbound traffic treated confirms parallel trends; the smaller coefficients reflect greater dispersion in evening travel.

2.3.3 Spatial distribution of highway congestion

This subsection examines the spatial distribution of rush hour congestion across camera pairs on Luxembourg's highways, identifying locations with more severe inbound congestion. The regression specification is:

$$\log speed_{cphdt} = \alpha + \delta_{pdt} + \sum_{t=-4, t\neq 0}^{4} \beta_{pt} \times inbound_c \times rush_t + \varepsilon_{cphdt}. \tag{2.3.2}$$

Here, the heterogeneous effect β_{pt} varies by camera pair and time of day. Figure 2.3.1 shows the estimates. The effect differs across pairs and times: on highways to Belgium and Germany it is relatively uniform, while on highways to France it is strongest near exits serving large population centers such as Esch-sur-Alzette, Dudelange, and Bettembourg.

In conclusion, cross-border congestion is spatially heterogeneous. It is fairly uniform on routes to Belgium and Germany but concentrated near entry points to large towns on routes to France.

2.3.4 Congestion times

This subsection examines average commuting times to and from Luxembourg City's central business district, defined as the densest pixel within the city's administrative boundary, located near the central railway station. We focus on the functional area around Luxembourg, covering the entire country and extending 50 km into France, Belgium, and Germany. The analysis is conducted on a 1 × 1 km grid over this area. To concentrate on urban clusters and reduce computational load, we exclude cells with residential and employment densities below 100 persons per km^2, leaving 3,182 urbanized cells (Figure 2.3.2).

We use OpenStreetMap (OSM) data to construct an asymmetric, distance-weighted road network. OSM provides road classes (motorway, primary, secondary, tertiary, and others) and speed limits; missing limits are imputed with the class median. To capture directional congestion, we build two networks: one for pre-rush hour (05:00) and one for rush hour (08:00). For highway segments, average speeds are taken from model (2.3.2), with inbound estimates applied for the morning rush hour. Other road classes are assigned speeds equal to 80% of the official speed limit, which are constant across periods. Highway segments without camera coverage (e.g., the ring road or highways outside Luxembourg) are assigned the speed of the nearest

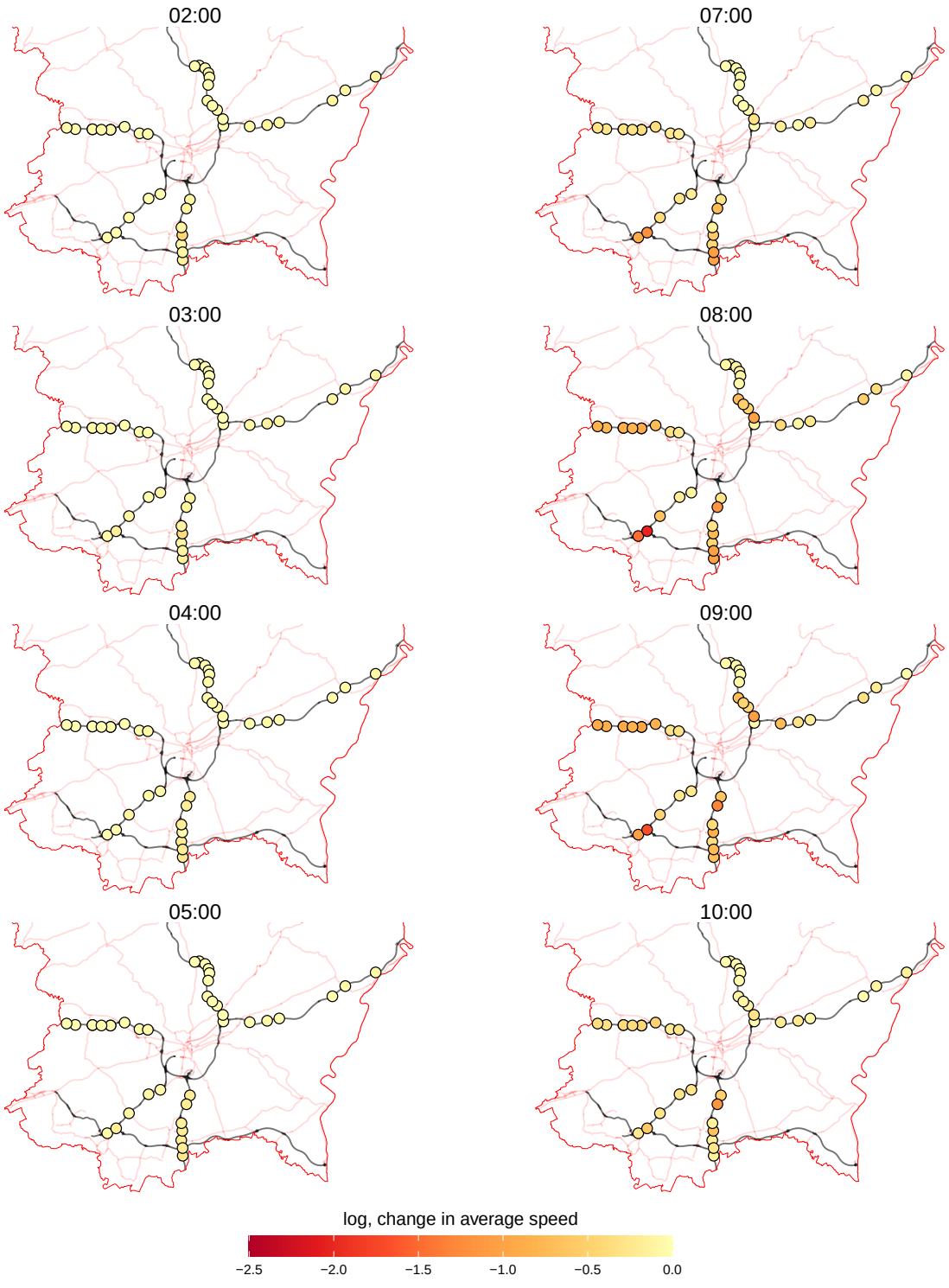

Note: The plotted effect is the log change in average speed in the inbound direction (toward Luxembourg City) during rush hour, relative to cameras in the outbound direction. Luxembourg's borders are shown in red, and highways are denoted by black lines.

Figure 2.3.1: Heterogeneity in congestion effects across camera pairs in the event study difference-in-differences specification.

observed camera pair based on road distance. Each highway segment, including those within Luxembourg, is matched to its closest camera pair. Using these assignments, we compute rush and non-rush travel time matrices between grid cells based on the shortest paths from Dijkstra's algorithm.

Figure 2.3.2 shows commuting times. The left panel plots travel time differences to Luxembourg City before and after rush hour, while the right panel shows differences from the city. On average, the duration of outbound trips from Luxembourg City increases by 9% (3 minutes) during rush hour, whereas the duration of inbound trips increases by 33% (13 minutes). This highlights the asymmetric impact of morning congestion.

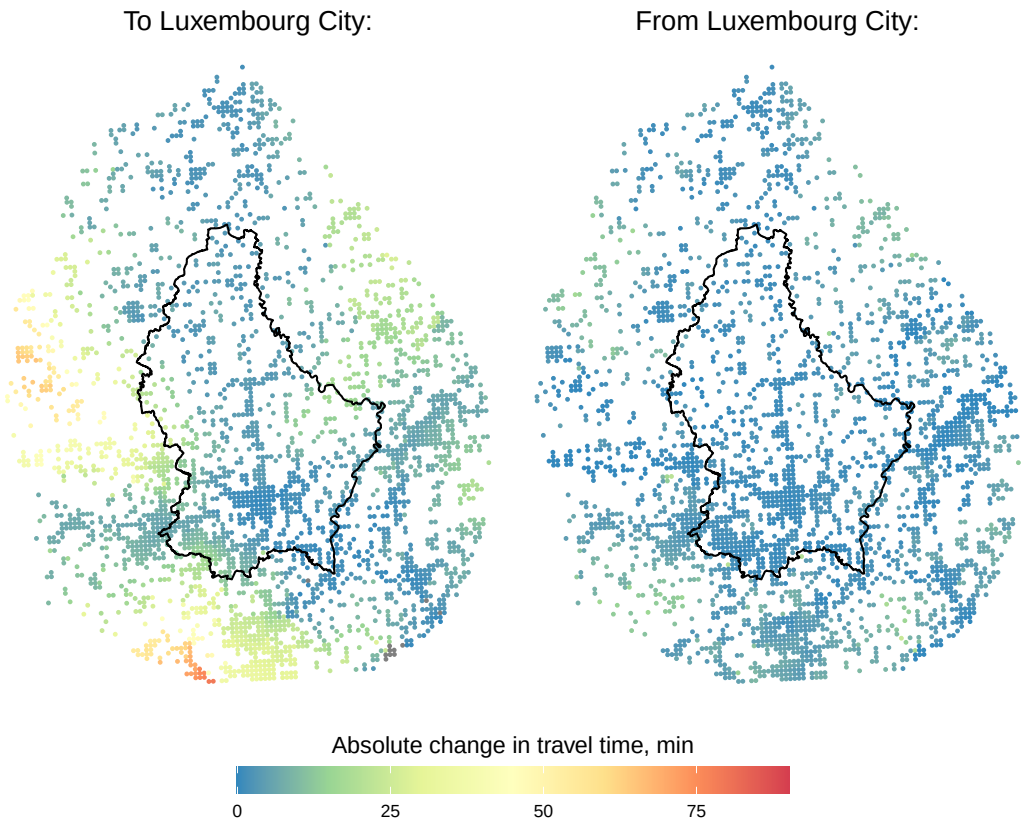

Note: Absolute changes in travel time to Luxembourg City (left) and from Luxembourg City (right) after rush hour, in minutes. Inbound and outbound speeds are imputed from estimates of (2.3.2); secondary road speeds are set at 80% of the limit. **Source:** CITA, OSM, and own calculations.

Figure 2.3.2: Commuting time differences between congested and free flow to and from Luxembourg City.

The largest increases in travel time from Luxembourg City occur within the city itself, suggesting that outbound commuters are mainly affected by congestion inside city limits. Beyond the city, outbound roads remain largely uncongested. In contrast, inbound travel times rise sharply, by 33% on average. In some areas – particularly in France, around Arlon in Belgium, and in southern Luxembourg – commuting times to the city during rush hour can double.

2.4 Model

This chapter builds on the model introduced in Section 1.3. To avoid repetition, only the main components are briefly recalled. The model features workers who choose residence and workplace locations, firms that produce with Cobb-Douglas technology, a competitive construction sector, and governments that collect taxes and provide local amenities. Workers face commuting disutility, housing and goods taxes, and derive utility from local amenities; firms face labor and property taxes. Labor and housing markets clear, and governments balance their budgets.

The only difference from Section 1.3 is that location-specific productivity A_j and residential amenities B_j are treated as exogenous; in Chapter 1 they were endogenous. For full details on preferences, firm optimization, government budgets, and equilibrium conditions, see Section 1.3 and Appendix 1.A.

2.5 Data

This chapter uses the same data sources and constructions as Chapter 1, including commuting flows, population and employment densities, floorspace prices, and wages for the Luxembourg functional area. We therefore provide only a brief summary here, highlighting the one difference from Chapter 1 – the travel time matrix. Summary statistics for the other data sources are reported in Table 1.3.

2.5.1 Travel flows and times

We use the 2017 "Luxmobil" survey (Ministry of Mobility and Public Works) and the 2017 "Population Census – Mobility Flow" database from INSEE for the French departments bordering Luxembourg (Meuse, Moselle, Meurthe-et-Moselle) to construct commuting flows between 447 Luxembourgish and non-Luxembourgish municipalities within a 50 km border band. Municipality pairs with no observed commutes are assigned zero flows, yielding a sparse origin–destination matrix.

The novelty relative to Chapter 1 is that travel times are recomputed using a new cell-to-cell travel time matrix that incorporates asymmetric congestion effects. Municipality-to-municipality times are then aggregated from cell-level times, weighted by population at the origin and employment at the destination. Updated summary statistics are shown in Table 2.5.1.

	Mean	SD	Min	Max	Observations
Number of commuters	2.5	46.0	0.0	12,249	113,569
Travel time (min)	64.1	29.0	0	188.0	113,569
Number of commuters (non-zero flow)	31.4	160	1	12,249	9,073
Travel time (min, non-zero flow)	37.4	23.1	0	156.2	9,073

Note: The data cover commuter counts and travel times for municipality pairs within Luxembourg and up to 50 km beyond its border. Commuter counts are taken from the 2017 "LuxMobil" survey and the French Population Census. Travel times are computed using a matrix aggregated from cell-to-cell times. The construction procedure is described in Section 2.3.

Table 2.5.1: Summary statistics for commuting data within 50 km of Luxembourg's border.

2.5.2 Tax rates

The tax rates used in the model are summarized in Table 2.5.2. We use data from OECD Tax Statistics (2017). Labor tax is defined as the tax wedge, i.e., the ratio between taxes paid by an average single worker (a single person earning 100% of the average wage, without children) and the total labor cost to the employer. Real property taxes are defined as property tax payments as a percentage of the private capital stock.

Tax	Corporate	Labor	Goods (VAT)	Property
Luxembourg	0.260	0.382	0.17	0.0005
France	0.344	0.476	0.20	0.0125
Belgium	0.296	0.527	0.21	0.0055
Germany	0.298	0.495	0.19	0.0020

Note: The table reports effective tax rates. Labor tax is defined as the tax wedge, i.e., the ratio between taxes paid by an average single worker (a single person earning 100% of the average wage, without children) and the total labor cost to the employer. Real property taxes are defined as property tax payments as a percentage of the private capital stock. **Source:** OECD Tax Statistics (2017).

Table 2.5.2: Tax rates in the Greater Region.

2.6 Estimation of parameters

Table 2.6.1 summarizes the values and sources of the parameters used in the analysis. The first two rows report parameters estimated from our data, while the remaining rows present parameters taken from the literature. These parameters are used in the model inversion described above. The detailed estimation procedure is provided in Appendix 2.C.

Parameter	Description	Value	Source
ε	Residence-workplace heterogeneity	3.6	Appendix 2.C
κ	Commuting disutility	0.027	Appendix 2.C
α	Firms' labor expenditure share	0.7	Valentinyi and Herrendorf (2008)
$1-\beta$	Consumers' housing expenditure share	0.33	Combes et al. (2019)
μ	Housing capital expenditure share	0.65	Combes et al. (2021)
ζ	Public good production	0.25	Fajgelbaum et al. (2019)

Table 2.6.1: Parameters.

2.7 Congestion in stylized geographies

To highlight the main economic mechanisms, we abstract from the spatial details of the studied geography. This section therefore examines general equilibrium effects in a stylized area: a disk with a 50 km radius, divided into hexagonal cells of 5 km diameter (Figure 2.7.1). The geography is symmetric and featureless, with residential fundamentals, production fundamentals, and development density uniformly set to one across all locations. The model is solved for the open-city equilibrium, allowing population migration into the area.

The stylized economy is divided into two regions: the center and the periphery. The first region occupies the area within 25 km of the center, while the second covers the surrounding zone (Figure 2.7.1). Each jurisdiction collects taxes from firms and residents and redistributes them

only to residents. Tax rates are assumed to be exogenous, equal across regions, and set to the average values reported in Table 2.5.2. The structural parameters are the same as in Table 2.6.1. The stylized transport network consists of six straight highways radiating from the center, which are subject to congestion, and secondary roads connecting adjacent hexagons along their edges. Commuters use the fastest route, determined by Dijkstra's shortest-path algorithm.

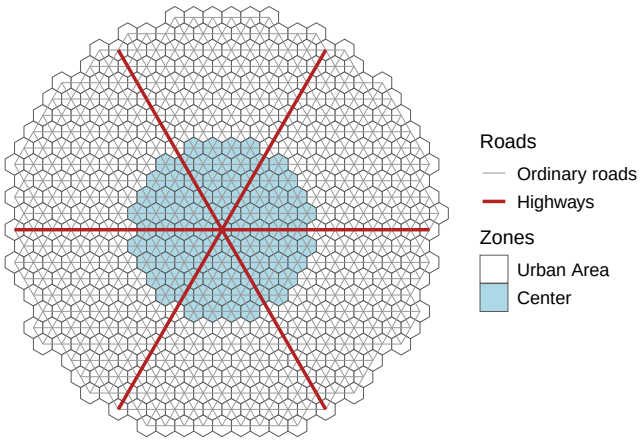

Note: The central jurisdiction is shown in blue. Secondary roads (30 km/h) are in gray, while highways with asymmetric congestion are in dark red. The border of the central jurisdiction is marked in black. The stylized geography assumes unit productivities, amenities, and development densities, with equal taxes on labor, goods, and property. The travel time matrix is computed from a graph with asymmetric weights.

Figure 2.7.1: The geographic outline of the stylized economy.

In the baseline scenario, highway travel speed is set at 120 km/h in both directions, corresponding to free-flow conditions in Luxembourg, while secondary roads are set uniformly at 30 km/h in both directions, reflecting urban speed limits. This scenario establishes the benchmark spatial equilibrium distribution of economic activity. The only parameter that varies is the travel speed on the six radial highways.

In the counterfactual scenario, congestion is introduced asymmetrically: outbound highway speed remains 120 km/h, while inbound speed is reduced to 60 km/h, a 50% cut consistent with the estimates in Section 2.3. We focus on morning commutes when simulating the model, assuming that evening congestion mirrors morning patterns in magnitude and direction – i.e., if inbound traffic is congested in the morning, outbound traffic is equally congested in the evening.

We focus on two measures: residential commuting market access (RCMA) and firm commuting market access (FCMA). As shown in Tsivanidis (2019), these measures serve as sufficient statistics for evaluating the effects of road infrastructure improvements.

We begin with residential demand:

$$H_{Ri} = \sum_{j \in S} \pi_{ij} H = \frac{H B_i^{\varepsilon} G_i^{\varepsilon}}{\Phi (t_i^c)^{\beta\varepsilon} (t_i^q Q_i)^{(1-\beta)\varepsilon}} \sum_{j \in S} \frac{w_j^{\varepsilon}}{d_{ij}^{\varepsilon}}. \tag{2.7.1}$$

Define

$$\Phi_i^R = \sum_{j \in S} \frac{w_j^{\varepsilon}}{d_{ij}^{\varepsilon}},$$

which we call residential commuting market access (RCMA). This measure captures the attractiveness of job opportunities for residents of i, combining wage levels and commuting costs. From labor market clearing, labor demand at firm location j can be written as

$$H_{Mj} = \sum_{i \in S} \pi_{ij|i} H_{Ri} = \sum_{i \in S} \frac{w_j^{\varepsilon} d_{ij}^{-\varepsilon}}{\sum_{s \in S} w_s^{\varepsilon} d_{is}^{-\varepsilon}} H_{Ri} \tag{2.7.2}$$
$$= w_j \sum_{i \in S} \frac{H_{Ri}}{\Phi_i^R} d_{ij}^{-\varepsilon} = w_j \Phi_j^F .$$

Here,

$$\Phi_j^F = \sum_{i \in S} \frac{H_{Ri}}{\Phi_i^R} d_{ij}^{-\varepsilon}$$

denotes a firm's commuting market access (FCMA). This measure captures how effectively firms in j can draw from the citywide pool of workers. The weighting places greater emphasis on residents in locations with low RCMA, since they have fewer outside options and are more likely to accept jobs in j.

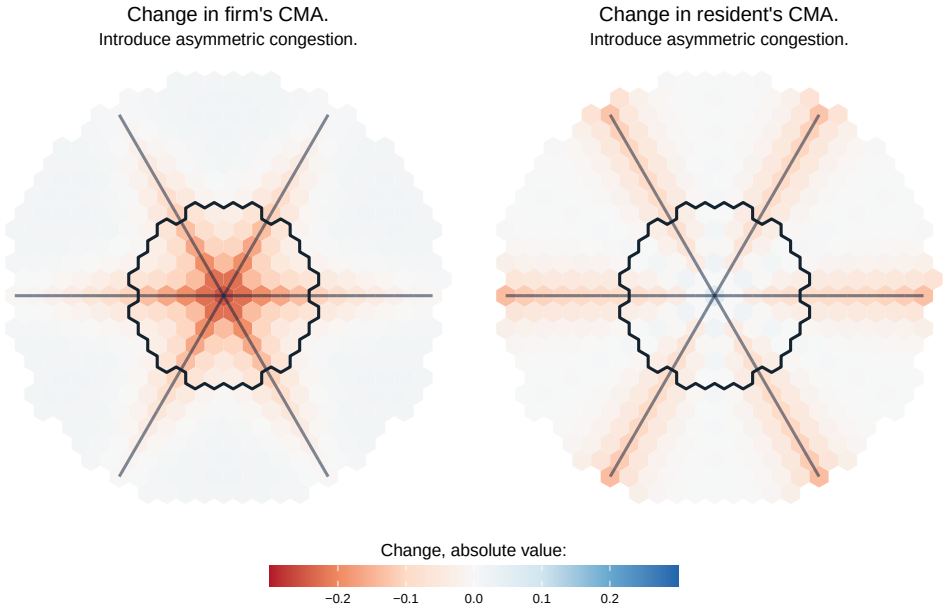

Note: Tax levels are set to the average rate in the data. The border of the central jurisdiction is shown in black, and highways are indicated by black dotted lines.

Figure 2.7.2: Change in residential commuting market access (right) and firm's commuting market access (left) in the new equilibrium with asymmetric congestion.

This formulation isolates the effects of transportation costs in two compact expressions, making it easier to discuss infrastructure improvements in terms of residential and firm market access. The results are shown in Figures 2.7.2 and 2.7.3.

The right panel of Figure 2.7.2 shows changes in RCMA under the asymmetric congestion scenario. Residential commuting market access falls at the periphery, with stronger effects along highways. The farther a location is from the core, the larger the decline. By contrast, RCMA rises at the core of the central jurisdiction. This occurs because central workers either also work

in the core—where wages increase after asymmetric congestion – or commute outbound along uncongested routes and are thus unaffected.

The left panel of Figure 2.7.2 shows changes in FCMA under the asymmetric congestion scenario. FCMA falls in the core of the central jurisdiction but remains largely unchanged in the periphery. This illustrates a key implication of asymmetric travel speeds: FCMA declines in the core, while RCMA declines in the periphery.

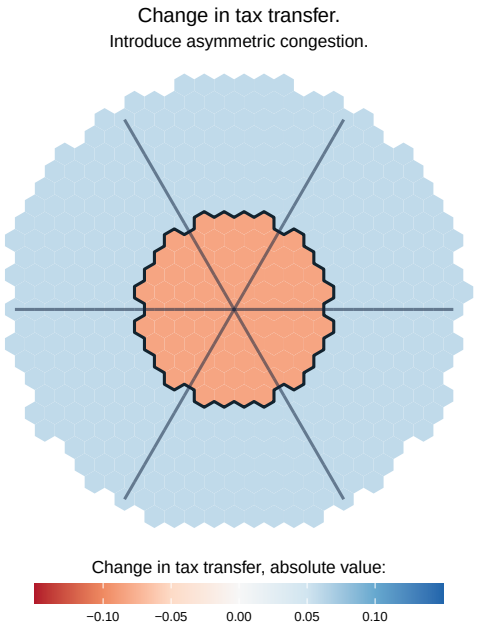

Note: Tax levels are set to the average rate in the data. The border of the central jurisdiction is shown in black, and highways are indicated by black dotted lines.

Figure 2.7.3: Change in public good provision in new equilibrium with asymmetric congestion.

Finally, Figure 2.7.3 shows changes in public good provision at the core and periphery. Asymmetric congestion reduces tax revenue in the core but increases it in the periphery. The reason is that congestion lowers cross-border commuting: living in the periphery and working in the core becomes too costly, reducing tax inflows from the periphery to the core.

In summary, asymmetric congestion produces three main effects. First, residential market access rises in the center but falls in the periphery. Second, firm market access falls in the center and stays largely unchanged in the periphery. Third, tax revenue in the central jurisdiction declines relative to the no-congestion baseline. In the counterfactual with congestion relief, the opposite occurs: residential market access falls in the core and rises in the periphery, firm market access rises in the core, and tax revenue in the central jurisdiction increases.

Appendix 2.E analyzes changes in other endogenous model outcomes. These follow patterns similar to commuting market access: wages, floorspace rents, commercial build-up share, and employment show a star-shaped pattern consistent with FCMA, while population changes align with RCMA.

2.8 Welfare analysis

This section analyzes the welfare effects of congestion relief, which restores highway travel speeds to pre-rush-hour levels in both directions. We first define the welfare measure – the ex-post compensating wage variation – used to evaluate monetary gains or losses. We then outline the nested counterfactuals designed to isolate the effect of each endogenous parameter on welfare. Finally, we present the results of these counterfactuals and assess the resulting welfare changes.

To translate model predictions into real economic outcomes, we normalize endogenous values to match observed figures. Wages are normalized to match Luxembourg's 2024 GDP per capita of €118,000[12]. This yields a predicted government tax revenue of €23.7 billion , close to the reported central government revenue of €29.6 billion in 2024. The gap reflects the absence of capital and firm profits in the model. Housing prices per square meter are converted into annual housing costs using the coefficient from Column 8 of Table 2.D.1 in Appendix 2.D.

2.8.1 Individual ex-post compensating wage variation

The compensating variation is defined as the wage change that keeps workers on their baseline indifference curve under the new price ratios. The benchmark utility is

$$u_{ijo}^0 = \frac{B_i G_i^{0\zeta} z_{ijo} w_j^0}{d_{ij}^0 \left(t_i^q Q_i^0\right)^{1-\beta} \left(t_i^c\right)^{\beta}},$$

and the counterfactual utility is

$$u_{ijo}^1 = \frac{B_i G_i^{1\zeta} z_{ijo} w_j^1}{d_{ij}^1 \left(t_i^q Q_i^1\right)^{1-\beta} \left(t_i^c\right)^{\beta}}.$$

For a worker o living in i and employed in j, the compensating wage $\overline{w}_{ij}^1$ is defined by

$$u_{ijo}^0 = \frac{B_i G_i^{1\zeta} z_{ijo} \overline{w}_{ij}^1}{d_{ij}^1 \left(t_i^q Q_i^1\right)^{1-\beta} \left(t_i^c\right)^{\beta}}.$$

This implies

$$\frac{\overline{w}_{ij}^1}{w_j^0} = \widehat{d}_{ij} (\widehat{Q}_i)^{1-\beta} (\widehat{G}_i)^{-\zeta},$$

where $\widehat{x} \equiv x^1/x^0$. The compensating variation for commute (i, j) is then

[12] Source: World Bank, 2024

$$
\begin{aligned}
CV_{ij} &= \overline{w}^1_{ij} - w^1_j \\
&= w^0_j \Big[\widehat{d}_{ij} (\widehat{Q}_i)^{1-\beta} (\widehat{G}_i)^{-\zeta} - \widehat{w}_j \Big].
\end{aligned}
$$

A positive value of CV_{ij} implies that workers would need a wage increase to accept the counterfactual environment, meaning they are worse off. If commuting disutility falls ($\widehat{d}_{ij} < 1$), then, holding other terms fixed, $CV_{ij} < 0$ and workers are better off. Notably, the expression does not depend on the idiosyncratic shock z_{ijo} but only on residential and employment locations. Aggregating over job choices and assuming workers can re-sort, the expected compensating variation at residence i is computed using ex-post choice probabilities:

$$
\begin{aligned}
E^1\big[CV_{ij} \mid i\big] &= \sum_j \pi^1_{ij|i} \overline{w}^1_{ij} - \sum_j \pi^1_{ij|i} w^1_j \\
&= (\widehat{Q}_i)^{1-\beta} (\widehat{G}_i)^{-\zeta} \sum_j \pi^1_{ij|i} w^0_j \widehat{d}_{ij} - \sum_j \pi^1_{ij|i} w^1_j.
\end{aligned}
$$

The first term corresponds to the expected compensating wage at the place of residence, while the second term is the expected counterfactual wage at the place of residence.

The comparative statics are straightforward. An increase in $\widehat{Q}_i$ (housing prices) raises the cost of living in i, increasing the expected compensating variation and making consumers worse off. A higher $\widehat{G}_i$ (per capita tax transfer) raises net income, reducing the required compensating wage and improving welfare. An increase in $\widehat{d}_{ij}$ (commuting disutility) raises the expected compensating variation and lowers welfare. Finally, a higher counterfactual wage w^1_j raises the second term, reduces the compensating variation, and improves welfare.

2.8.2 Structure of counterfactuals

This section conducts a counterfactual exercise where highway congestion is removed by setting travel speeds to those observed at 05:00, consistent with Section 2.3. We implement a sequence of nested counterfactuals (CF0–CF5) that capture short- and long-run adjustments. Nesting isolates the contribution of each endogenous margin: by adding one adjustment at a time, we can trace how much of the overall welfare impact is due to wages, housing markets, commercial land use, residential relocation, or population size.

CF0 is the baseline. CF1 allows wages and workplace employment to adjust to the new travel time matrix. CF2 adds floorspace price adjustments. CF3 incorporates changes in the commercial build-up share. CF4 allows residential relocation, bringing the economy into spatial equilibrium through utility equalization. CF5 introduces free entry, with population growing until expected utility returns to its baseline level.

For tractability, the analysis focuses on seven urban areas within Luxembourg's commuting zone, each with more than 15,000 residents: Luxembourg City, Esch-sur-Alzette, Ettelbruck, and Differdange in Luxembourg; Trier in Germany; Arlon in Belgium; and Thionville in France.

2.8.3 Results

Figure 2.8.1 shows the evolution of endogenous outcomes under the counterfactual simulations. The figure has six panels, each reporting changes for seven cities: Arlon, Differdange, Esch-sur-Alzette, Ettelbruck, Luxembourg City, Thionville, and Trier. Congestion relief raises employment in Luxembourg City but lowers its population, reinforcing its role as the primary work destination in the Greater Region. Other Luxembourgish cities gain both employment and population, suggesting revitalization. Thionville records the largest population increase but a decline in employment, consistent with its role as a major commuter town. Arlon, Trier, and Ettelbruck display mixed dynamics.

Across all counterfactuals, housing prices rise in every city except Ettelbruck and Trier, reflecting utility gains from faster commutes. The largest increases occur in foreign commuter towns and in Esch-sur-Alzette. Expected wages at the place of residence grow in foreign commuter towns but fall in Luxembourgish towns, especially in the capital, due to stronger labor competition and easier worker access for Luxembourg firms. Wages at the place of work decline across the economy. Finally, the share of commercial build-up rises consistently in Luxembourg City, reinforcing its role as the main production center in the Greater Region.

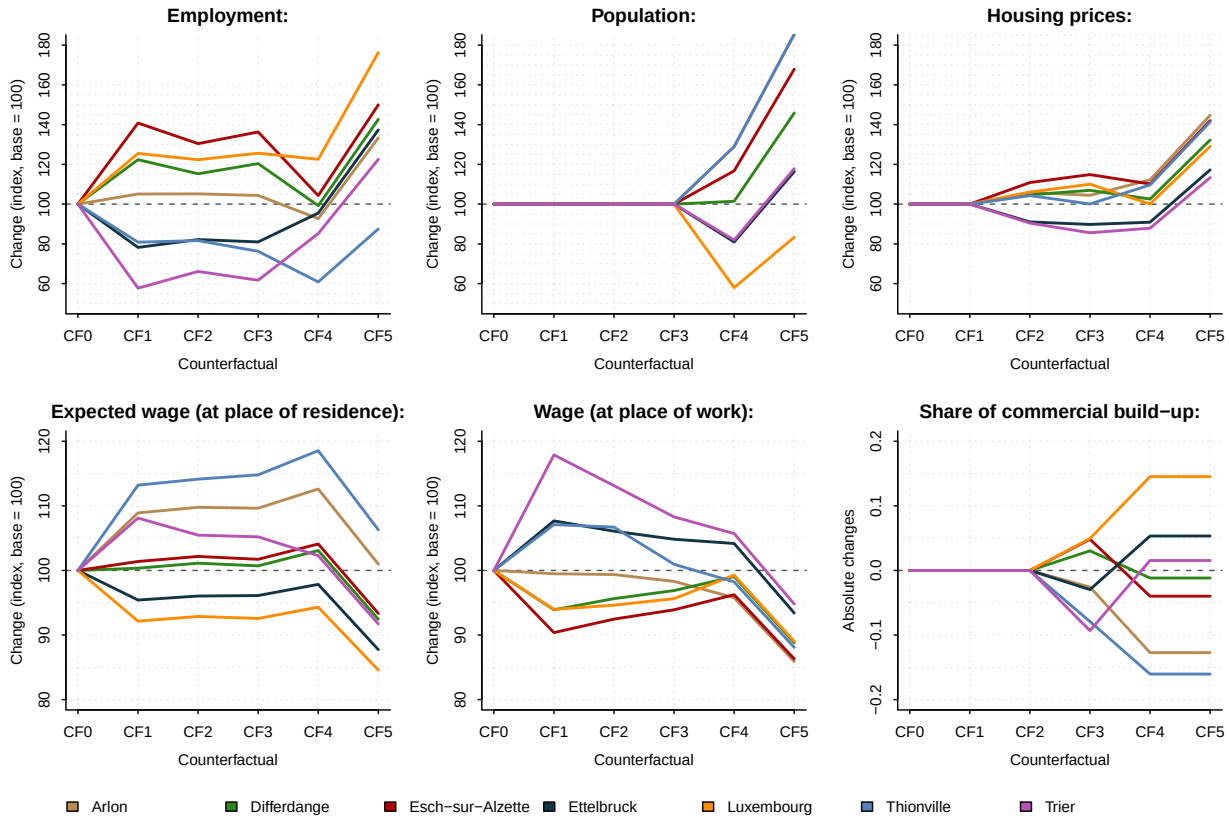

Note: The X-axis labels CF0 - CF5 correspond to sequential counterfactual scenarios. CF0 denotes the baseline. CF1 allows wages and workplace employment to adjust to the new travel time matrix. CF2 adds floorspace price adjustment, CF3 adds commercial build-up share adjustment, CF4 adds residential population adjustment, and CF5 incorporates free entry. This ordering reflects the gradual introduction of adjustment margins in the model.

Figure 2.8.1: Evolution of endogenous variables of the model under different counterfactual scenarios.

Figure 2.8.2 shows the evolution of three welfare measures: total economic output (left panel), expected utility by residence (center panel), and compensating wage variation (right panel). Total output and expected utility are measured relative to baseline levels. The compensating

wage is expressed as expected annual income at the place of residence, with negative values indicating welfare gains and positive values indicating welfare losses.

Economic output rises consistently only in Luxembourg City. In Esch and Differdange, short-run gains vanish in the long run. Output falls in all other cities, driven by stronger competition (Trier) or their transition into commuter towns for Luxembourg City and Esch (Thionville, Ettelbruck). Arlon shows mixed results: output increases in CF1–CF3 but declines once population reallocation is included. The shift toward commuter-town status brings welfare gains for residents, largest in Thionville and Arlon, followed by Differdange, Esch, and Ettelbruck.

Luxembourg City is the only location with a positive compensating wage in the short-run scenario, corresponding to a welfare loss of about €1,140 per resident per year in CF1–CF3. In the long-run scenario with population reallocation, welfare in Luxembourg City rises to about €3,490 per resident per year, despite a 40% population decline relative to the baseline. When migration from the wider economy is included, these gains turn into welfare losses of about €8,110 per resident per year, driven by lower expected wages from stronger labor competition, higher housing costs, and insufficient tax-transfer compensation.

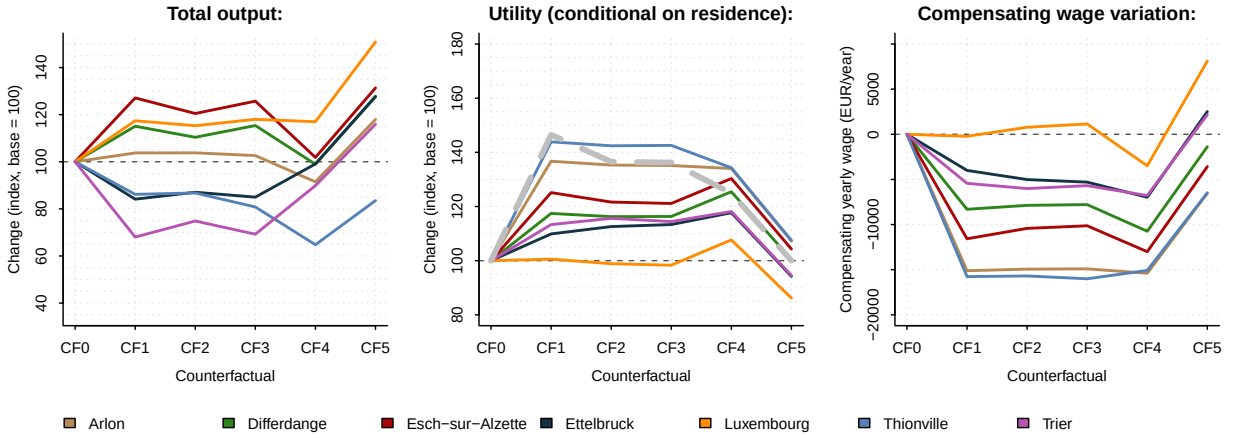

Note: The X-axis labels CF0 - CF5 correspond to sequential counterfactual scenarios. CF0 denotes the baseline. CF1 allows wages and workplace employment to adjust to the new travel time matrix. CF2 adds floorspace price adjustment, CF3 adds commercial build-up share adjustment, CF4 adds residential population adjustment, and CF5 incorporates free entry. This ordering reflects the gradual introduction of adjustment margins in the model.

Figure 2.8.2: Evolution of output and welfare measures.

Overall, only Arlon, Thionville, Esch, and Differdange show consistent welfare gains across all counterfactuals. For the foreign commuter towns, the gains stem solely from easier access to Luxembourg City. For Esch and Differdange, they reflect both improved access to Luxembourg City and local economic revival.

Figure 2.8.3 reports fiscal gains and average compensating wage variation by country. Congestion relief raises tax revenue in Luxembourg, consistent with theory. Fiscal gains are about €1.18 billion in the closed-city counterfactual. With government revenue at €29.6 billion in 2024, this equals a 4% budget increase. If all additional revenue were allocated to highway construction, the conservative long-run estimate (excluding migration) corresponds to 118 km of new highway lanes each year[13]. Given Luxembourg's highway network of 165 km, this revenue would cover adding one lane in each direction on 35% of the network.

[13] Highway construction cost estimated at €10 million per km-lane. **Source:** www.globalhighways.com

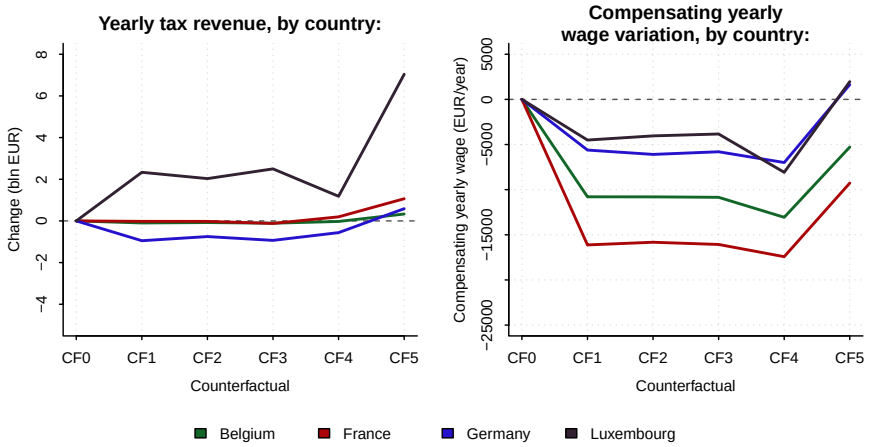

Note: The X-axis labels CF0 - CF5 correspond to sequential counterfactual scenarios. CF0 denotes the baseline. CF1 allows wages and workplace employment to adjust to the new travel time matrix. CF2 adds floorspace price adjustment, CF3 adds commercial build-up share adjustment, CF4 adds residential population adjustment, and CF5 incorporates free entry. This ordering reflects the gradual introduction of adjustment margins in the model.

Figure 2.8.3: Total tax revenue gains and average compensating wage variation, by country.

Belgium and France show smaller fiscal benefits, as VAT gains offset labor tax losses. Germany is the only country with significant fiscal losses: €0.56 billion in the closed-city case. With migration, however, all countries record fiscal gains due to new arrivals and a larger tax base.

For compensating wage variation, Germany and Luxembourg experience welfare losses with migration, while Belgium and France see substantial gains, reflected in negative values in the right panel of Figure 2.8.3. Without migration, all countries show welfare gains: about €17,450 per resident in France, €13,100 in Belgium, and €7,500 in both Germany and Luxembourg. The only location with short-run welfare losses is Luxembourg City.

Congestion relief increases economic output in Luxembourg City and, to a smaller extent, in Esch, while output declines elsewhere. In the short run, welfare rises in all cities except Luxembourg City, where it falls due to lower expected wages from stronger labor inflows and higher housing costs driven by commercial demand. With population reallocation, welfare in Luxembourg City turns positive, but only at the cost of a 40% decline in its baseline population.

2.9 Conclusion

This chapter quantifies the economic effects of congestion in Luxembourg, focusing on its magnitude, spatial heterogeneity, and distributional consequences. Evidence from a difference-in-differences design shows persistent reductions in highway speeds during the morning rush, with the sharpest slowdowns on routes to France and at choke points near border crossings and motorway exits in southern Luxembourg.

Counterfactual simulations with free-flow traffic show that congestion relief increases aggregate output in Luxembourg City and, to a lesser extent, in Esch, while output falls elsewhere as surrounding towns shift toward commuter status. Welfare effects diverge: all locations except Luxembourg City gain in the short run, with the largest gains in foreign commuter towns such as Thionville and Arlon. In Luxembourg City, congestion relief produces a welfare loss of €1,140 per resident per year in the short run, which turns into a gain of €3,490 in the long run once population reallocation is considered. With migration inflows from the wider economy, however,

the welfare effect for city residents becomes strongly negative, at €8,110 per person per year.

At the regional scale, congestion relief has redistributive consequences. Luxembourg captures the efficiency gains in production and fiscal revenues—estimated at €2.50 billion per year in the short run, €1.18 billion in the long run, and €7.04 billion with migration inflows—while neighboring regions benefit mainly through welfare improvements for their residents.

A key limitation of the framework is that congestion is treated as exogenous. The analysis does not allow for modal shifts or the endogenous adjustment of traffic to policy interventions. Extending the model to incorporate endogenous congestion dynamics would enhance its predictive value and is a priority for future research.

Appendix

2.A Robustness checks for difference-in-differences

Dependent variable:	Average speed, km/h					
	All	A1	A3	A4	A6	A7
inbound × $rush_{-4}$	-4.841***	-4.499	-5.710	-12.795	-0.339	-5.504
	(1.628)	(3.715)	(4.300)	(7.777)	(1.441)	(3.131)
inbound × $rush_{-3}$	-3.758*	-3.271	-2.431	-12.090	1.273	-6.288
	(1.967)	(3.716)	(4.202)	(7.471)	(1.490)	(5.361)
inbound × $rush_{-2}$	-1.784	-0.709	4.150	-9.413	2.749	-7.479
	(2.297)	(3.693)	(3.771)	(7.759)	(1.691)	(6.828)
inbound × $rush_{-1}$	-0.918	1.598	5.842	-7.811	4.723**	-9.508
	(2.696)	(3.729)	(4.321)	(8.636)	(1.591)	(8.046)
inbound × $rush_1$	-23.004***	-4.675	-48.047***	-55.901***	-22.780***	-7.140
	(3.941)	(5.393)	(8.592)	(12.183)	(1.642)	(4.894)
inbound × $rush_2$	-40.902***	-22.839**	-56.092***	-66.262***	-52.639***	-23.551***
	(4.154)	(7.613)	(6.572)	(16.248)	(3.010)	(7.194)
inbound × $rush_3$	-38.694***	-16.564*	-54.829***	-61.716***	-54.329***	-21.136**
	(4.164)	(7.843)	(5.603)	(12.950)	(3.407)	(6.949)
inbound × $rush_4$	-15.802***	2.617	-31.208***	-32.826***	-21.016***	-7.914
	(3.003)	(4.689)	(6.696)	(7.055)	(2.257)	(5.622)
inbound × $rush_5$	-2.080	3.277	-6.863	-8.391	4.135*	-5.972
	(2.259)	(3.484)	(4.483)	(9.235)	(2.025)	(5.809)
inbound × $rush_6$	-1.403	1.749	0.779	-5.458	2.785	-7.231
	(2.183)	(3.585)	(4.374)	(8.739)	(1.770)	(5.875)
inbound × $rush_7$	-1.920	0.015	1.427	-4.233	1.605	-7.644
	(2.259)	(3.699)	(4.794)	(9.152)	(1.677)	(6.089)
Observations	20,054	4,072	3,600	2,389	4,753	5,240
R^2	0.763	0.664	0.895	0.848	0.928	0.565
Within R^2	0.427	0.221	0.722	0.610	0.865	0.199
Pair × Day × Hour FE	X	X	X	X	X	X

Note: We present estimation results from a multi-period difference-in-differences regression specification (2.3.1) where the average speed is taken as the dependent variable. Standard errors, clustered at the camera-pair level, are reported in parentheses. All specifications include pair-day-hour fixed effects. Treated cameras are those positioned in the inbound direction. The rush hour period includes 06:00. We assume an absorbing treatment and define the time period from 10:00 to 13:00 as treated in order to demonstrate the convergence of estimates to zero. **Source:** CITA.
* $p < 0.1$, ** $p < 0.05$, *** $p < 0.01$.

Table 2.A.1: Event study difference-in-difference coefficients for the average speed during morning rush hour.

Dependent variable:	Average speed, log		
	All	A13	B40
inbound × $rush_{-4}$	-0.063*	-0.042	-0.070
	(0.034)	(0.043)	(0.044)
inbound × $rush_{-3}$	-0.063*	-0.074	-0.058
	(0.035)	(0.039)	(0.046)
inbound × $rush_{-2}$	-0.039	-0.057	-0.032
	(0.034)	(0.040)	(0.045)
inbound × $rush_{-1}$	-0.002	-0.034	0.010
	(0.035)	(0.037)	(0.046)
inbound × $rush_1$	-0.030	-0.077	-0.013
	(0.031)	(0.052)	(0.038)
inbound × $rush_2$	-0.082*	-0.064	-0.089
	(0.046)	(0.047)	(0.061)
inbound × $rush_3$	-0.046	-0.047	-0.045
	(0.044)	(0.033)	(0.060)
inbound × $rush_4$	-0.033	-0.036	-0.032
	(0.027)	(0.030)	(0.035)
inbound × $rush_5$	-0.043	-0.018	-0.051
	(0.027)	(0.038)	(0.035)
inbound × $rush_6$	-0.042	-0.025	-0.048
	(0.029)	(0.034)	(0.037)
inbound × $rush_7$	-0.045	-0.020	-0.053
	(0.030)	(0.039)	(0.037)
Observations	9,346	2,370	6,976
R^2	0.857	0.763	0.762
Within R^2	0.051	0.179	0.045
Pair × Day × Hour FE	X	X	X

Note: We present estimation results from a multi-period difference-in-differences regression specification (2.3.1) for non-radial highways A13 and B40. Standard errors, clustered at the camera-pair level, are reported in parentheses. All specifications include pair-day-hour fixed effects. Treated cameras are those positioned in the inbound direction. The rush hour period includes 06:00. We assume an absorbing treatment and define the time period from 10:00 to 13:00 as treated in order to demonstrate the convergence of estimates to zero. **Source:** CITA.
* $p < 0.1$, ** $p < 0.05$, *** $p < 0.01$.

Table 2.A.2: Event study difference-in-difference coefficients for the log of average speed on non-radial highways during morning rush hour.

Dependent variable:	Average speed, log					
	All	A1	A3	A4	A6	A7
inbound × $rush_{-4}$	-0.100	-0.026	-0.070	-0.118	-0.014	-0.243
	(0.060)	(0.033)	(0.041)	(0.081)	(0.012)	(0.215)
inbound × $rush_{-3}$	-0.107	-0.028	-0.068	-0.105	-0.017	-0.274
	(0.070)	(0.033)	(0.042)	(0.074)	(0.014)	(0.254)
inbound × $rush_{-2}$	-0.099	-0.038	-0.013	-0.039	-0.014	-0.304
	(0.072)	(0.033)	(0.049)	(0.038)	(0.014)	(0.266)
inbound × $rush_{-1}$	-0.066	0.002	-0.002	-0.054	0.023	-0.242
	(0.057)	(0.028)	(0.054)	(0.038)	(0.017)	(0.204)
inbound × $rush_1$	-0.062	-0.007	-0.009	-0.094	0.015	-0.191
	(0.053)	(0.031)	(0.043)	(0.062)	(0.013)	(0.191)
inbound × $rush_2$	-0.057	0.010	-0.005	-0.099	0.016	-0.187
	(0.051)	(0.032)	(0.045)	(0.081)	(0.019)	(0.184)
inbound × $rush_3$	-0.047	-0.005	0.001	-0.132	0.029	-0.141
	(0.042)	(0.029)	(0.048)	(0.123)	(0.016)	(0.143)
inbound × $rush_4$	-0.028	0.031	0.036	-0.097	0.015	-0.122
	(0.039)	(0.036)	(0.056)	(0.089)	(0.018)	(0.133)
inbound × $rush_5$	-0.036	0.015	0.009	-0.120	0.015	-0.115
	(0.037)	(0.035)	(0.051)	(0.121)	(0.017)	(0.120)
inbound × $rush_6$	-0.031	0.023	0.003	-0.123	0.022	-0.103
	(0.033)	(0.031)	(0.046)	(0.120)	(0.017)	(0.105)
inbound × $rush_7$	-0.028	0.028	0.002	-0.094	0.029	-0.112
	(0.034)	(0.031)	(0.047)	(0.115)	(0.018)	(0.111)
Observations	6,078	1,224	1,080	750	1,440	1,584
R^2	0.655	0.660	0.947	0.796	0.768	0.498
Within R^2	0.030	0.034	0.037	0.095	0.089	0.084
Pair × Day × Hour FE	X	X	X	X	X	X

Note: We present estimation results from a multi-period difference-in-differences regression specification (2.3.1) for the subset of weekend commutes. Standard errors, clustered at the camera-pair level, are reported in parentheses. All specifications include pair-day-hour fixed effects. Treated cameras are those positioned in the inbound direction. The rush hour period includes 06:00. We assume an absorbing treatment and define the time period from 10:00 to 13:00 as treated in order to demonstrate the convergence of estimates to zero. **Source:** CITA.
* $p < 0.1$, ** $p < 0.05$, *** $p < 0.01$.

Table 2.A.3: Event study difference-in-difference coefficients for the log of the average speed during morning rush hour. Weekends only.

Dependent variable:	Average speed, log					
	All	A1	A3	A4	A6	A7
inbound × $rush_{-4}$	0.027	-0.007	-0.012	0.064	-0.025	0.108
	(0.030)	(0.039)	(0.042)	(0.110)	(0.016)	(0.093)
inbound × $rush_{-3}$	0.032	0.013	-0.017	0.046	-0.015	0.112
	(0.031)	(0.039)	(0.045)	(0.111)	(0.015)	(0.096)
inbound × $rush_{-2}$	0.036	0.004	0.021	0.050	-0.012	0.104
	(0.029)	(0.039)	(0.057)	(0.113)	(0.015)	(0.085)
inbound × $rush_{-1}$	0.015	0.041	-0.119**	-0.028	-0.004	0.115
	(0.032)	(0.058)	(0.050)	(0.131)	(0.017)	(0.085)
inbound × $rush_1$	-0.158***	-0.047	-0.509***	-0.502*	-0.176***	0.138
	(0.054)	(0.044)	(0.092)	(0.200)	(0.018)	(0.098)
inbound × $rush_2$	-0.245***	-0.051	-0.597***	-0.646**	-0.358***	0.101
	(0.058)	(0.043)	(0.081)	(0.201)	(0.023)	(0.095)
inbound × $rush_3$	-0.200***	-0.021	-0.630***	-0.292	-0.334***	0.101
	(0.053)	(0.037)	(0.054)	(0.162)	(0.023)	(0.093)
inbound × $rush_4$	-0.044	0.039	-0.376***	-0.011	-0.092***	0.136
	(0.047)	(0.032)	(0.037)	(0.129)	(0.020)	(0.131)
inbound × $rush_5$	0.059	0.044	0.020	0.066	0.002	0.144
	(0.045)	(0.034)	(0.038)	(0.128)	(0.013)	(0.158)
Observations	16,725	3,400	2,999	2,006	3,922	4,398
R^2	0.607	0.647	0.845	0.596	0.851	0.497
Within R^2	0.104	0.026	0.611	0.228	0.690	0.087
Pair × Day × Hour FE	X	X	X	X	X	X

Note: We present estimation results from a multi-period difference-in-differences regression specification (2.3.1) for the evening rush hour. Standard errors, clustered at the camera-pair level, are reported in parentheses. All specifications include pair-day-hour fixed effects. Treated cameras are those positioned in the outbound direction. The rush hour period includes 16:00. We assume an absorbing treatment and define the time period from 16:00 to 21:00 as treated in order to demonstrate the convergence of estimates to zero. **Source:** CITA.
* $p < 0.1$, ** $p < 0.05$, *** $p < 0.01$.

Table 2.A.4: Event study difference-in-difference coefficients for the average speed during evening rush hour.

2.B Equilibrium definition

Here, we provide a detailed definition of spatial general equilibrium.

Given parameters $\{\alpha, \beta, \mu, \varepsilon, \kappa\}$, location characteristics $\{\varphi, L, \xi, \tau\}$, productivity and amenities $\{A, B\}$, reservation utility $\bar{U}$, and tax multipliers $\{t^c, t^q, t^w\}$, the spatial general equilibrium is given by the scalar H and the vectors $\{\pi_M, \pi_R, Q, q, w, \theta, g\}$ that solve the following system of equations:

$$\bar{U} = \Gamma_0 \left[\sum_{i\in\mathcal{I}} \sum_{j\in\mathcal{I}} (d_{ij}(t_i^q Q_i)^{1-\beta}(t_i^c)^{\beta})^{-\varepsilon}(B_i G_i w_j)^{\varepsilon} \right]^{\frac{1}{\varepsilon}},$$

$$\begin{aligned}
\pi_{Ri} &= \frac{\sum_{s\in\mathcal{I}} (d_{is}(t_i^q Q_i)^{1-\beta}(t_i^c)^{\beta})^{-\varepsilon}(B_i G_i w_s)^{\varepsilon}}{\sum_{r\in\mathcal{I}}\sum_{s\in\mathcal{I}} (d_{rs}(t_r^q Q_r)^{1-\beta}(t_r^c)^{\beta})^{-\varepsilon}(B_r G_r w_s)^{\varepsilon}}, \quad \forall i \in \mathcal{I}. \\
\pi_{Mj} &= \frac{\sum_{r\in\mathcal{I}} (d_{rj}(t_r^q Q_r)^{1-\beta}(t_r^c)^{\beta})^{-\varepsilon}(B_r G_r w_j)^{\varepsilon}}{\sum_{r\in\mathcal{I}}\sum_{s\in\mathcal{I}} \left(d_{rs}(t_r^q Q_r)^{1-\beta}(t_r^c)^{\beta}\right)^{-\varepsilon}(B_r G_r w_s)^{\varepsilon}}, \quad \forall j \in \mathcal{I}.
\end{aligned}$$

$$q_j = \frac{(1-\alpha)A_j^{\frac{1}{1-\alpha}}}{t_j^q}\left(\frac{\alpha}{w_j t_j^w}\right), \quad \forall j \in \mathcal{I}.$$

$$\begin{cases}
P_i = q_i \text{ and } \theta_i = 0 & \text{if } q_i > Q_i, \\
P_i = q_i \text{ and } \theta_i \in [0,1] & \text{if } q_i = Q_i, \\
P_i = Q_i \text{ and } \theta_i = 1 & \text{if } q_i < Q_i.
\end{cases}$$

$$\begin{aligned}
\theta_j \phi_j L_j^{1-\mu} &= A_j^{\frac{1}{\alpha}}\left(\frac{1-\alpha}{q_j t_j^q}\right)^{\frac{1}{\alpha}} H\pi_{Mj}, \quad \forall j \in \mathcal{I}. \\
(1-\theta_i)\phi_i L_i^{1-\mu} &= (1-\beta)\left(\sum_{s\in\mathcal{I}} \frac{(w_s/d_{is})^{\varepsilon}}{\sum_r^S (w_r/d_{ir})^{\varepsilon}} w_s\right)\frac{H\pi_{Ri}}{t_i^q Q_i}, \quad \forall i \in \mathcal{I}.
\end{aligned}$$

$$\begin{aligned}
g_i &= \frac{t_n^c - 1}{t_n^c}\beta \frac{\sum_{i\in\mathcal{I}_n} \mathbb{E}[w|i]H_{Ri}}{\sum_{i\in\mathcal{I}_n} H_{Ri}} + \frac{t_n^q - 1}{t_n^q}(1-\beta)\frac{\sum_{i\in\mathcal{I}_n} \mathbb{E}[w|i]H_{Ri}}{\sum_{i\in\mathcal{I}_n} H_{Ri}} \\
&\quad + (t_n^w - 1)\frac{\sum_{j\in\mathcal{I}_n} w_j H_{Mj}}{\sum_{i\in\mathcal{I}_n} H_{Ri}} + (t_n^q - 1)\frac{\sum_{j\in\mathcal{I}_n} q_j S_{Mj}}{\sum_{i\in\mathcal{I}_n} H_{Ri}}, \quad \forall i \in \mathcal{I}_n. \\
G_i &= g_i^{\zeta}, \quad \forall i \in \mathcal{I}_n.
\end{aligned}$$

2.C Parameter estimation

2.C.1 Semi-elasticity of commuting

The parameter ν is estimated using the data on work travels by car in Luxembourg and surrounding countries provided by the Luxembourgish LuxMobil survey and French census. We use the equation for the unconditional commuting probability (1.3.4) and write it as

$$\log \pi_{ij} = -\nu\tau_{ij} + \xi_i + \zeta_j + \varepsilon_{ij} \tag{2.C.1}$$

Here, ξ_i represents origin-specific fixed effects, such as amenities and floor space prices, while ζ_j captures destination-specific fixed effects. The origin-specific and destination-specific variables are absorbed by fixed effects.

Dependent variable:	Commuting flows, log		
	LuxMobil	INSEE	Both
OSRM Travel Time, min	-0.111***	-0.087***	-0.098***
	(0.005)	(0.003)	(0.002)
Origin FE	Yes	Yes	Yes
Destination FE	Yes	Yes	Yes
R^2	0.818	0.835	0.840
Observations	13,225	44,908	107,226
Country of origin:	LU	FR	LU+FR
Country of destination:	LU	FR	LU+FR

Note: Departure communes are within 50 km from the state border of Luxembourg. Robust standard errors in parentheses. * p < 0.1, ** p < 0.05, *** p < 0.01.

Table 2.C.1: Commuting elasticity estimation.

To estimate this regression model, we associate the work travel by car provided by the Luxembourgish LuxMobil survey and the French census with the above-computed travel times. To balance municipality sizes in Luxembourg and France, we consider French municipalities with more than 2,000 residents. Results are presented in Table 2.C.1. We use the Poisson Pseudo-Maximum-Likelihood (PPML) regression model to account for the count nature and the zeros in commuting flows.

Columns 1 to 3 present PPML estimates for the baseline regression based on different subsamples. Column 1 uses LuxMobil Survey data only. Column 2 uses data from the INSEE commuting survey only. Column 3 uses a combined commuting survey. In the subsequent analysis, we use the results in Column 3 with the estimate $\nu = 0.098$.

2.C.2 Residence and workplace preferences

We choose the Fréchet parameter ϵ that produces wage dispersion closest to the observed one (Ahlfeldt et al. (2015)). More formally, we minimize the absolute difference between the variances of the logarithm of the observed wages and the wages simulated by the model, $|\text{var}(\log w_m^{data}) - \text{var}(\log w_m^{sim}(\varepsilon))|$. The net wage w_m^{data} are observed at the municipal level and

the simulated wages $w_m^{sim}(\varepsilon)$ are computed for each cell from the labor market conditions (1.3.17) and then aggregated for each municipality. We find the minimizer $\epsilon = 3.6$, which yields the value of κ 0.027 (Figure 2.C.1).

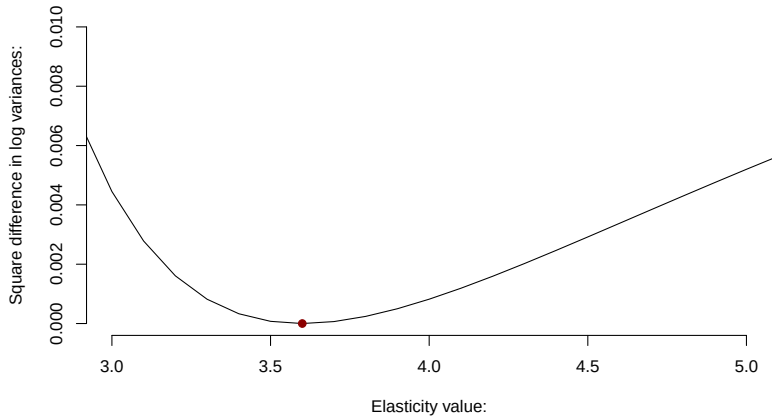

Figure 2.C.1: Optimal value of ε.

2.D Rental and purchase prices

Table 2.D.1 compares the hedonic price regressions for rental prices (columns 1 and 5) and purchase prices (columns 2 and 6) without and with cell fixed effects. It also displays the results from the merger of rental and purchase listings, with a dummy control for a purchase in Luxembourg (columns 3 and 7) and a dummy control for a purchase (versus rental) (columns 4 and 8).

	Without cell fixed effects				With cell fixed effects			
	Separate		Pooled		Separate		Pooled	
	Rent, log	Price, log	Rent, log	Rent, log	Rent, log	Price, log	Rent, log	Rent, log
log, Surface	-0.112***	-0.049***	-0.130***	-0.093***	-0.156***	-0.239***	-0.165***	-0.165***
	(0.005)	(0.015)	(0.004)	(0.006)	(0.004)	(0.007)	(0.003)	(0.003)
Number of Rooms	-0.079***	-0.110***	-0.045***	-0.108***	-0.004	-0.016***	-0.018***	-0.018***
	(0.006)	(0.004)	(0.002)	(0.003)	(0.006)	(0.002)	(0.002)	(0.002)
Number of Bedrooms	0.003	0.001	-0.002*	0.003*	0.000	-0.001	-0.001*	-0.001*
	(0.003)	(0.002)	(0.001)	(0.002)	(0.002)	(0.001)	(0.001)	(0.001)
Number of Bathooms	0.008	0.007*	0.003	0.010***	0.004	-0.002	-0.001	-0.001
	(0.005)	(0.004)	(0.002)	(0.003)	(0.004)	(0.002)	(0.002)	(0.002)
Furnished	0.085***	0.009	0.024***	0.021**	0.039***	-0.008	0.006	0.002
	(0.013)	(0.012)	(0.007)	(0.009)	(0.010)	(0.006)	(0.005)	(0.005)
Age, decade	0.016***	0.008***	0.004***	0.007***	0.007**	0.004***	0.004***	0.004***
	(0.005)	(0.001)	(0.001)	(0.001)	(0.004)	(0.000)	(0.000)	(0.000)
Age^2, decade 10^{-3}	0.092***	-0.004***	-0.002***	-0.004***	0.059**	-0.002***	-0.002***	-0.002***
	(0.034)	(0.001)	(0.000)	(0.001)	(0.027)	(0.000)	(0.000)	(0.000)
Balcony surface	0.003	0.009***	0.005***	0.009***	-0.003	0.002***	0.002***	0.002***
	(0.003)	(0.001)	(0.001)	(0.001)	(0.003)	(0.001)	(0.001)	(0.001)
Year not defined	-0.028	0.015	-0.011	0.020**	-0.019	-0.035***	-0.026***	-0.022***
	(0.019)	(0.012)	(0.007)	(0.010)	(0.016)	(0.005)	(0.006)	(0.006)
Purchase: Lux			6.035***				5.919***	
			(0.010)				(0.009)	
Purchase: Not Lux			4.862***				5.516***	
			(0.012)				(0.017)	
Purchase				5.685***				5.837***
				(0.014)				(0.008)
Type FE	Yes	Yes	Yes	Yes	Yes	Yes	Yes	Yes
Type FE × Rooms	Yes	Yes	Yes	Yes	Yes	Yes	Yes	Yes
Insulation FE	Yes	Yes	Yes	Yes	Yes	Yes	Yes	Yes
Buy FE	No	No	No	Yes	No	No	No	Yes
Buy FE × Lux	No	No	Yes	No	No	No	Yes	No
Cell FE	No	No	No	No	Yes	Yes	Yes	Yes
R^2	0.590	0.488	0.983	0.965	0.820	0.926	0.992	0.992
Observations	4,149	8,916	13,065	13,065	4,149	8,916	13,065	13,065

Table 2.D.1: Hedonic regression outcomes for purchase prices and rents.

2.E Stylized economy: other endogenous variables

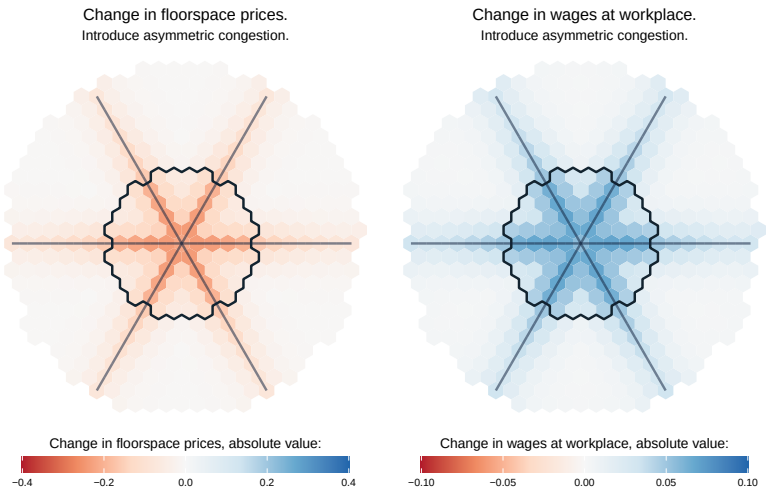

Note: Tax levels are assumed to be equal to the average tax rate in the data. The border of the central jurisdiction is in black. Highways are denoted by black dotted lines.

Figure 2.E.1: Change in floorspace prices (right) and wages at workplace (left) in the new equilibrium with asymmetric congestion.

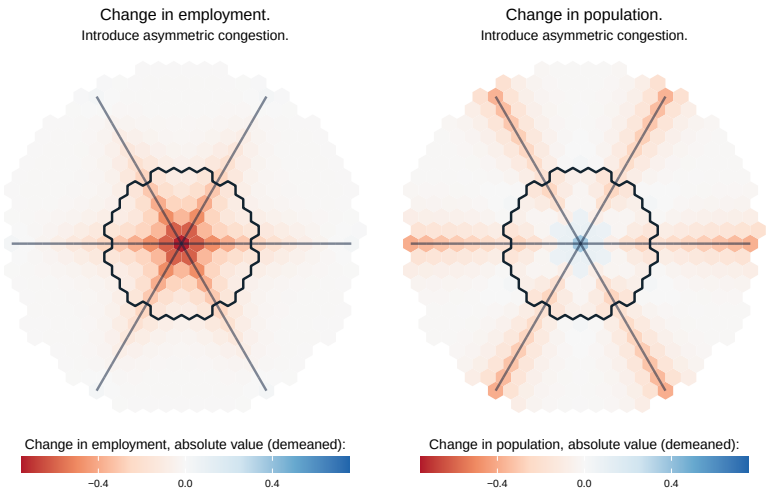

Note: Tax levels are assumed to be equal to the average tax rate in the data. The border of the central jurisdiction is in black. Highways are denoted by black dotted lines.

Figure 2.E.2: Change in employment (right) and residential population (left) in the new equilibrium with asymmetric congestion.

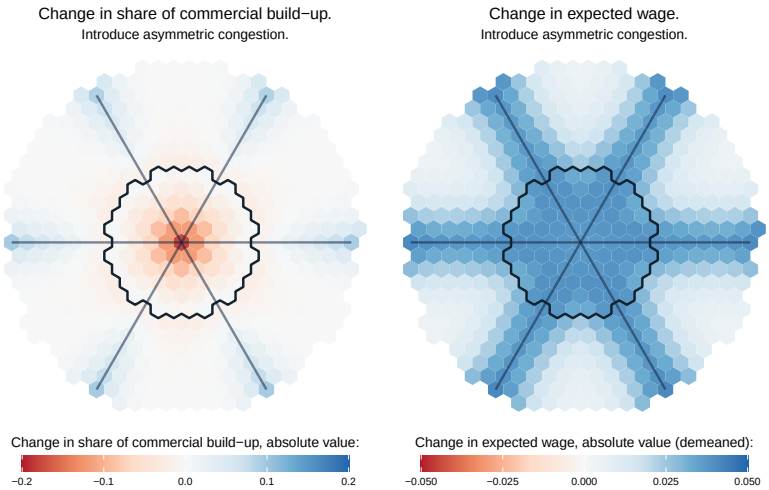

Note: Tax levels are assumed to be equal to the average tax rate in the data. The border of the central jurisdiction is in black. Highways are denoted by black dotted lines.

Figure 2.E.3: Change in share of commercial build-up (right) and expected wages at the place of residence (left) in the new equilibrium with asymmetric congestion.

Chapter 3

A Radiation Model of Cross-Border Commuting and Residential Location

This chapter is based on joint work with Michał Burzyński and Bertrand Verheyden.

3.1 Introduction

Cross-border labor mobility is a defining feature of regional economic integration, especially in compact territories where national borders intersect with functional labor markets. In such settings, permanent migration is only part of the story; short-distance cross-border commuting – workers residing in one jurisdiction and working in another – creates complex spatial interactions between wages, local amenities, and congestion externalities. The Greater Region around Luxembourg, with its intense daily flows from Belgium, France, and Germany, clearly illustrates these dynamics. Despite free public transport initiatives and high incomes, commuting times, and the concentration of high-skilled employment generate persistent tensions between where workers live and where they work. Understanding these tensions requires a framework that captures job search and commuting mechanics, incorporates residential congestion feedback into residential location choice, and reflects realistic behavioral frictions in how workers discover and accept jobs.

We propose a spatial general equilibrium model of commuting that incorporates a radiation-style sequential job search within an economic geography setting, characterized by endogenous wages and density-dependent disamenities. The core innovation of this chapter is to take the radiation class of human mobility models — originally developed by Simini et al. (2012) and later widely adopted in geography and epidemiology — and to endow it with economic microfoundations. Workers search outward from their place of residence, evaluating potential jobs sequentially in order of increasing travel time and stopping when they encounter the first option that yields a marginal improvement in expected utility. This "first-better" stopping rule embeds search frictions and limited consideration directly, contrasts with conventional gravity-type formulations that assume a global comparison of all opportunities, and naturally generates spatial attenuation via intervening satisfactory opportunities. A central implication is that reducing commuting times need not lower wages: if the resulting expansion of the opportunity set intensifies competition for mobile labor between firms, both wages and employment at a destination can rise simultaneously, as we find for Luxembourg in the counterfactual analysis.

Crucially, the model enhances the basic radiation mechanism by introducing heterogeneity in match quality, which is endogenous to local labor market thickness, wages, and amenities. This provides a clear economic interpretation of the key dispersion parameter, which governs both the dispersion of job matches and the elasticity of commuting flows to wages at the destination. Residential location decisions interact with commuting and job matching through density-dependent congestion forces.

The model is calibrated using granular data from Luxembourg and the surrounding regions in Belgium, France, and Germany. Luxembourg's small geography, occupational specialization in managerial and professional work, and linguistic openness make it a compelling laboratory. Large cross-border commuter shares and long commuting times create a setting where the trade-offs between commuting and migration are economically significant. By combining administrative commuting flows, wage and occupation data, and travel time measures, we uncover how infrastructure and congestion jointly shape labor market outcomes, commuting patterns, and residential allocation.

Our study is at the intersection of three strands of literature: human mobility and radiation models, spatial equilibrium and agglomeration economics, and labor market search with bounded consideration. The radiation model of human mobility explains flows across space using intervening opportunities along with distance decay. Its success in geography and epidemiology (Jia et al., 2020; Nilforoshan et al., 2023; Schläpfer et al., 2021; Simini et al., 2021) stems from

minimal data requirements and relatively good predictive quality. However, this literature has typically abstracted from the economic incentives and endogenous feedbacks that characterize real labor markets. We adapt the "first-better" search logic underlying radiation flows and embed it into an equilibrium environment with wages and density-dependent disamenities, thereby providing an economic foundation and closing the loop between search behavior and aggregate spatial outcomes.

The spatial economics literature has long emphasized how economic activity organizes itself over space through mechanisms such as sharing, learning, and matching (Duranton & Puga, 2004). Much of the recent quantitative spatial equilibrium work uses gravity-like structures for interaction and trade in space (Ahlfeldt et al., 2015; Allen & Arkolakis, 2014; Monte et al., 2018b; Redding & Rossi-Hansberg, 2017), with matching and sorting arising from observable fundamentals and cost structures. We extend this by making matching itself a primitive with frictions: the availability and realization of good job matches depend on the sequence of search encounters and the stochastic nature of match quality. In doing so, we offer a complement to the dominant knowledge spillover paradigm, showing that spatial agglomeration can emerge endogenously from job matching.

The behavioral foundation for the radiation-style search is grounded in the labor economics literature on sequential search, reservation wages, and limited consideration. The canonical models of Stigler (1961) and McCall (1970) formalize the idea that workers sample opportunities one at a time and optimally stop when the current offer exceeds a reservation threshold, which is derived from the indifference condition between accepting the current wage and searching further. This generates "first-better" acceptance behavior rather than global optimization. Subsequent search-and-matching theory (Mortensen & Pissarides, 1994; Rogerson et al., 2005) embeds these dynamics in a general equilibrium framework. In this chapter, we assume that an individual's domestic utility draw acts as a reservation wage, and they accept the first offer for which the commuting-weighted wage exceeds the domestically drawn reservation wage.

The rest of the chapter is organized as follows. Section 3.2 presents the theoretical framework, demonstrating how the congestion-inclusive radiation search operates in a spatial general equilibrium with endogenous density-dependent disamenities and wages. Section 3.3 describes the data and calibration. Section 3.4 utilizes counterfactual simulations to assess the effects of congestion relief on the spatial distribution of employment, wages, and population. Section 3.5 concludes and outlines directions for extending the framework, notably by introducing a fully endogenous housing market.

3.2 Theoretical model

To provide a realistic overview of the Greater Region's economy, our theoretical approach develops a spatial general equilibrium model in which labor market frictions and population density interact. The connection between the two arises from individual decisions regarding commuting and migration within the region, which explicitly consider the region's geography, the existing network of road connections, and the distribution of job opportunities by occupation. We define the region's geography as a set of discrete residential ($i \in 1,\ldots,J$) and employment ($j \in 1,\ldots,J$) locations that are connected by the road network defined by the travel time matrix τ_{ij} between every origin i and destination j. We assume that individuals are characterized by their occupations, denoted by $o = 1,\ldots,N$. In our model, agents cannot change occupations, but they can change job locations j within the same occupation o.

3.2.1 Labor markets

In each pixel $j = 1,\ldots,J$, there exists a competitive firm endowed with a Cobb-Douglas production technology that depends on the fixed total factor productivity A_j, capital K_j, and a CES labor composite, where the labor demand for each occupation ($o = 1,\ldots,N$) is denoted by L_{jo}:

$$Y_j = A_j K_j^{\rho} \left(\sum_{o'=1}^{N} \theta_{jo'} L_{jo'}^{\frac{\sigma-1}{\sigma}} \right)^{\frac{(1-\rho)\sigma}{\sigma-1}}. \tag{3.2.1}$$

Here, θ_{jo} is a cell-specific relative productivity factor of occupation o (such that $\sum_o \theta_{jo} = 1$), $\rho \in [0,1]$ is the share of capital in the firm's expenditure, and $\sigma > 1$ represents the elasticity of substitution across all occupations. Firms rent capital at a constant rate r and take the price of the output as one. They choose K_j and $\{L_{jo}\}_{o=1}^{N}$ to maximize profits

$$\Pi_j \;=\; Y_j \;-\; r\,K_j \;-\; \sum_{o'=1}^{N} w_{jo'}\,L_{jo'}. \tag{3.2.2}$$

The marginal products of labor and capital are equal to

$$w_{jo} = (1-\rho) A_j K_j^{\rho}\, \theta_{jo} \left(\sum_{o'=1}^{N} \theta_{jo'} L_{Mjo'}^{\frac{\sigma-1}{\sigma}} \right)^{\frac{(1-\rho)\sigma}{\sigma-1}} L_{Mjo}^{-1/\sigma} \tag{3.2.3}$$

and

$$r = \rho A_j K_j^{\rho-1} \left(\sum_{o'=1}^{N} \theta_{jo'} L_{Mjo'}^{\frac{\sigma-1}{\sigma}} \right)^{\frac{(1-\rho)\sigma}{\sigma-1}}. \tag{3.2.4}$$

Here, L_{Mjo} is the firm's optimal demand for labor in occupation o at location j.

3.2.2 Consumers

Each individual with the occupation o is endowed with a matching shock $\tilde{z}_{jo}$[14] for each matching opportunity she encounters. The random variable $\tilde{z}_{jo}$ is independently distributed with a Fréchet cumulative distribution function $\mathbb{P}(\tilde{z}_{jo} < z) = e^{-z^{-\gamma}}$ and a shape parameter γ that measures the inverse of the dispersion (i.e., homogeneity) of matching shocks. We assume that the same distribution applies to all occupations o. Each individual consumer locally consumes a numeraire good c, supplies the same amount of labor equal to 8 hours per day, and solves the following optimization problem:

$$\max_{c_{io}} \frac{B_{io}\,\tilde{z}_{jo}\,c_{io}^{\alpha_o}}{d_{ij}} \quad \text{s.t. } c_{io} = w_{jo}. \tag{3.2.5}$$

Here, d_{ij} represents commuting disutility, B_{io} denotes an occupation-specific local amenity, and w_{jo} denotes the wage at the job location. A larger occupation-specific parameter $\alpha_o \in (0,1]$ implies a stronger decreasing marginal utility from consumption and, therefore, from income. Commuting disutility increases with commuting time and is assumed to be given by

[14] Throughout the chapter, we denote random variables with tildes.

$d_{ij} = \left(1 - t_{ij}\right)^{-\beta_o}$, where $t_{ij} = \tau_{ij}/480$ is the share of commuting time τ_{ij} relative to the work time in minutes, and β_o is an occupation-specific elasticity of utility with respect to leisure time. The individual's indirect utility is, therefore, given by

$$U_{ijo} = \frac{B_{io}\,\tilde{z}_{jo}\,w_{jo}^{\alpha_o}}{d_{ij}} = B_{io}\,\tilde{z}_{jo}\,w_{jo}^{\alpha_o}\,(1 - t_{ij})^{\beta_o}. \tag{3.2.6}$$

3.2.3 Job search and matching

Each resident searches for a job by visiting the cells surrounding her home cell i and sequentially increasing her commuting distance until she finds the *first* cell j that offers better utility than her home location. Each visited cell k provides a number μ_{ko} of job matching opportunities, which we treat as exogenous. Each job matching opportunity implies an independent random draw $\tilde{z}_{ko}$ that multiplies her utility from work, which is given by

$$U_{iko} = \tilde{z}_{ko} v_{iko}, \text{ where } v_{iko} = B_{io} w_{ko}^{\alpha_o}/d_{ik}. \tag{3.2.7}$$

The best offer in k delivers $\tilde{U}_{iko} = \max_{1,\ldots,\mu_{ko}}\{\tilde{z}_{ko} v_{iko}\}$. The probability that the utility derived from the best domestic offer is lower than z is, therefore, equal to

$$\mathbb{P}[\tilde{U}_{iio} < z] = \exp(-\mu_{io} v_{iio}^{\gamma} z^{-\gamma}). \tag{3.2.8}$$

Equation 3.2.8 defines the distribution of the reservation wage obtained at the home location. The probability that the utility derived from the best offer in j is greater than z is equal to

$$\mathbb{P}[\tilde{U}_{ijo} > z] = 1 - \exp\left(-\mu_{jo}\, v_{ijo}^{\gamma}\, z^{-\gamma}\right). \tag{3.2.9}$$

The probability that the utility derived from the best offer is lower than z for every intermediate k equals

$$\prod_{k \in \mathcal{S}_{ijo}} \mathbb{P}[\tilde{U}_{iko} < z] = \exp\Big(-\sum_{k \in \mathcal{S}_{ijo}} \mu_{ko}\, v_{iko}^{\gamma}\, z^{-\gamma}\Big), \tag{3.2.10}$$

where $\mathcal{S}_{ijo}$ is the set of visited cells $k \neq i, j$ with a commuting time smaller than that between i and j, that is

$$\mathcal{S}_{ijo} = \{k : \tau_{ij} > \tau_{kj} > 0\}.$$

The probability of a worker of type o choosing the residence-workplace pair (i, j) is therefore given by

$$\pi_{j|i}^{o} = \int_0^{\infty} (1 - \mathbb{P}[\tilde{U}_{ijo} < z]) \prod_{k \in \mathcal{S}_{ijo}} \mathbb{P}[\tilde{U}_{iko} < z] \frac{d}{dz}(\mathbb{P}[\tilde{U}_{iio} < z])\, dz. \tag{3.2.11}$$

The expression above describes the probability of finding a better job match at j and not finding better job matches in other visited locations $\mathcal{S}_{ijo}$ for all possible draws in the home location i. In Appendix 3.A.1 we show that the resulting commuting probability is equal to

$$\pi^{o}_{j|i} = \mu_{io}\, v^{\gamma}_{iio}\left[\frac{1}{\sum\limits_{k\in S_{ijo}\cup\{i\}} \mu_{ko}\, v^{\gamma}_{iko}} - \frac{1}{\sum\limits_{k\in S_{ijo}\cup\{i,j\}} \mu_{ko}\, v^{\gamma}_{iko}}\right] \quad (j \neq i). \tag{3.2.12}$$

Define $\pi^{o}_{i|i} = 1 - \sum\limits_{j\neq i} \pi^{o}_{j|i}$. It implies that the probability of staying at i is equal to the probability that the best offer at the home location delivers the highest utility among all other locations; that is (see Appendix 3.A.2)

$$\pi^{o}_{i|i} = \frac{\mu_{io}\, v^{\gamma}_{iio}}{\sum\limits_{k=1}^{J} \mu_{ko}\, v^{\gamma}_{iko}}. \tag{3.2.13}$$

If $v_{iko} = 1$ for all $i, k \in J$ and $o \in N$, then Equation 3.2.12 parallels the collision probability in the radiation model for physical particles, where each cell k contains the number μ_{ko} of other particles. The economic improvement with respect to this model lies in the fact that any cell k with a higher wage w_{ko} or a better matching opportunity μ_{ko} is more likely to generate a successful job match.

3.2.4 Expected utility

The expected utility of living in location i is defined as

$$\mathbb{E}[U_{io}] = \sum_{j\in J} \int_0^{\infty} z(1-\mathbb{P}[\tilde{U}_{ijo} < z]) \prod_{k\in S_{ijo}} \mathbb{P}[\tilde{U}_{iko} < z] \frac{d}{dz}(\mathbb{P}[\tilde{U}_{iio} < z])\, dz. \tag{3.2.14}$$

In Appendix 3.A.3 we demonstrate that this expression simplifies to

$$\mathbb{E}[U_{io}] = \Gamma_0 \mu_{io}^{1/\gamma} B_{io} w_{io}^{\alpha_o} (1-(\pi^{o}_{i|i})^{\frac{\gamma-1}{\gamma}}), \text{ where } \Gamma_0 = \Gamma\left(\frac{\gamma-1}{\gamma}\right). \tag{3.2.15}$$

Here, $\Gamma_0\, \mu_{io}^{1/\gamma}$ captures the effect of local market size on utility, $B_{io}\, w_{io}^{\alpha_o}$ captures the utility derived from amenities and wages in the domestic market, and $\left(1-(\pi^{o}_{i|i})^{\frac{\gamma-1}{\gamma}}\right)$ is the market access component of utility. In the spirit of Rosen (1979) and Roback (1982), we assume that, in equilibrium, utility is equalized across space for each occupation. Therefore, the utility equalization condition implies that

$$\Gamma_0 \mu_{io}^{1/\gamma} B_{io} w_{io}^{\alpha_o} (1-(\pi^{o}_{i|i})^{\frac{\gamma-1}{\gamma}}) = \bar{U}^{o}. \tag{3.2.16}$$

As in Monte et al. (2015), the expected utility from residing in i decreases with the share of domestic commuting. This formulation of expected utility implies that, under utility equalization across space, we must observe a higher share of domestic employment in areas with more job opportunities, higher wages, or a greater level of domestic amenities.

3.2.5 Amenity

We define amenity as

$$B_{io} = b_{io} L_{Ri}^{-\eta}, \tag{3.2.17}$$

where b_{io} is an occupation-specific fundamental amenity term, and $L_{Ri} = \sum_{o'} L_{Rio'}$ is a total population density. The elasticity of amenity with respect to population density, $\eta > 0$, introduces congestion forces into the model.

3.2.6 General equilibrium definition

Given the vector of parameters $\{\alpha_o, \beta_o, \gamma, \eta, \rho, \sigma\}$ and the exogenous inputs $\{\mu_{jo}, A_j, \theta_{jo}, L_o, t_{ij}, b_{io}, r\}$, a spatial general equilibrium of the model is a vector of endogenous variables $\{L_{Rio}, L_{Fjo}, \pi^o_{j|i}, v_{ijo}, w_{jo}, B_{io}, K_j, \bar{U}^o\}$, such that for every origin cell i, destination cell j, and occupation o:

1. Labor market clears:

$$L_{Fjo} = \sum_{i \in J} \pi^o_{j|i} L_{Rio}, \tag{3.2.18}$$

where:

$$\pi^o_{j|i} = \begin{cases} \mu_{io} v_{iio}^{\gamma} \left[\dfrac{1}{\sum\limits_{k \in S_{ijo} \cup \{i\}} \mu_{ko} v_{iko}^{\gamma}} - \dfrac{1}{\sum\limits_{k \in S_{ijo} \cup \{i,j\}} \mu_{ko} v_{iko}^{\gamma}} \right], & j \neq i, \\ \dfrac{\mu_{io} v_{iio}^{\gamma}}{\sum\limits_{k=1}^{J} \mu_{ko} v_{iko}^{\gamma}}, & j = i, \end{cases} \tag{3.2.19}$$

$$v_{iko} = B_{io} w_{ko}^{\alpha_o} (1 - t_{ik})^{\beta_o}, \tag{3.2.20}$$

$$S_{ijo} = \{k : \tau_{ij} > \tau_{ik} > 0\}.$$

2. The price of each factor is its marginal product for every location i and occupation o:

$$w_{jo} = (1-\rho) A_j K_j^{\rho} \theta_{jo} \left(\sum_{o'=1}^{N} \theta_{jo'} L_{Fjo'}^{\frac{\sigma-1}{\sigma}} \right)^{\frac{(1-\rho)\sigma}{\sigma-1}} L_{Fjo}^{-1/\sigma}, \tag{3.2.21}$$

$$r = \rho A_j K_j^{\rho-1} \left(\sum_{o'=1}^{N} \theta_{jo'} L_{Fjo'}^{\frac{\sigma-1}{\sigma}} \right)^{\frac{(1-\rho)\sigma}{\sigma-1}}. \tag{3.2.22}$$

3. The residential amenity is equal to

$$B_{io} = b_{io} L_{Ri}^{-\eta}, \text{ where } L_{Ri} = \sum_{o'} L_{Rio'}. \tag{3.2.23}$$

4. Utility equalizes across space for every occupation o:

$$\Gamma_0 \mu_{io}^{1/\gamma} B_{io} w_{io}^{\alpha_o} (1 - (\pi_{i|i}^o)^{\frac{\gamma-1}{\gamma}}) = \bar{U}^o \text{ for all } i \in J. \tag{3.2.24}$$

5. Population and employment counts are equal for every occupation o:

$$\bar{L}^o = \sum_i L_{Rio} = \sum_j L_{Fjo} \text{ for all } o \in N. \tag{3.2.25}$$

Together, conditions (3.2.18) - (3.2.25) define eight equations that establish a model equilibrium consistent with calibrated fundamentals and parameter values.

3.3 Data and calibration

This section describes the data sources, imputations, and parameter calibration used in the model. The model is implemented on a 1×1 km grid covering over 15,000 cells in the Greater Region, each containing information on the resident population and local employment. Individuals are grouped into eight occupations: managers, professionals, technicians and associate professionals, clerical support workers, service and sales workers, skilled agricultural, forestry, and fishery workers, craft and related trades workers, plant and machine operators and assemblers, and elementary occupations. In the first subsection, we describe the imputation procedures for the data used to power the model. In the second subsection, we estimate parameters from external data sources, calibrate preference parameters numerically, and invert model fundamentals such as cell-specific productivity, occupation shares, and amenities from the observed equilibrium.

3.3.1 Data inputs

In this subsection, we summarize the data imputation procedures. We proceed as follows: first, we harmonize and impute the data on population and employment by occupation for each pixel. Next, we impute wage rates. Then, we disaggregate the commuting matrices by occupation. Finally, we describe the procedure used to generate the travel time by car between those cells. A detailed description of each step is provided below.

Population data and imputations The process of population and employment imputation consists of four steps. First, commune-level totals of population and employment are combined with a gridded population dataset to produce pixel-level totals. This is accomplished by multiplying each pixel's population by the commune-level employment-to-population ratio, resulting in pixel-level counts for both variables. Each pixel is associated with a commune based on the pixel centroid coordinate. For each municipality, the obtained employment counts at the pixel level are rescaled to match the total employment at the commune level.

Second, population shares by occupation at the place of residence are estimated. For Luxembourg, we use 2021 Census data at the pixel level to estimate pixel-level regressions that relate the total population in each pixel to logit-transformed occupational shares. For other countries, the regression coefficients estimated using Luxembourg data are applied to total pixel populations from the WorldPop Database (Bondarenko et al., 2020) to impute occupational shares. We normalize the predicted occupational shares to ensure they sum to one for each pixel.

Third, employment shares by occupation at the place of work are estimated. For Luxembourg, regressions are estimated at the commune level, and the Luxembourg-based commune-level coefficients are then applied to pixel-level employment totals to obtain imputed shares, which are subsequently normalized to sum to one for each pixel.

Finally, commune-level totals by occupation, along with pixel-level totals and imputed shares, are reconciled using the Iterative Proportional Fitting Procedure (IPFP), which adjusts the pixel-level allocations to ensure they simultaneously match commune-level totals for each occupation and pixel-level totals across all occupations, while remaining as close as possible to the initial shares. The outcome of the algorithm, in principle, depends on the initial shares supplied. We use predicted estimates for employment and population shares by pixel from the previous step as our initial guess, also known as *seed matrix*. The output is a set of pixel-level counts by occupation for both the residential population and employment. A more detailed description of the data inputs and the imputation algorithm is presented in Appendix 3.B.

Wage imputation and the labor market The process of wage imputation consists of three steps. First, using microdata from the Structure of Earnings Survey (SES) by Eurostat, we estimate the following regression specification:

$$\ln wage_{nos} = \alpha_{os} + \beta\, age_n + \gamma\, gender_n + \delta\, educ_n + \varepsilon_{nos}. \tag{3.3.1}$$

Here, we regress the reported wages of individuals n who work in occupations o and sectors s on the occupation-sector fixed effects α_{os}, age groups age_n, a gender dummy variable $gender_n$, and education levels $educ_n$. We restrict the sample to NUTS-1 regions within the Greater Region. For each of these regions, we estimate the regression separately.

Second, we use the estimated country-specific occupation-sector effects $\widehat{\alpha}_{os}$ to impute wages at the commune level. Since detailed occupation-by-sector counts at the commune level are not directly available, we apply the Iterative Proportional Fitting Procedure (IPFP) to the marginal distributions of occupations and sectors as inputs. We use a matrix of ones as our seed matrix for each commune in the sample. We produce a balanced occupation-sector employment matrix whose row and column sums match these margins.

Finally, we compute each commune's imputed wage by combining the cell counts from the matrix with the corresponding estimated fixed effect values.

Commuting flow matrix The commuting data for Luxembourg residents and cross-border commuters originates from the Luxembourgish Ministry of Transport. The matrix for residents of Luxembourg contains an aggregated number of commuters by origin and destination communes. This matrix is then decomposed by occupation using a version of the IPFP that is constrained by the total flows for each origin-destination pair, the marginal distribution of workers by occupation at the destination, and the marginal distribution of residents by occupation at the origin. A detailed procedure, the definition of the seed matrix, and the formal mathematical definition of the optimization problem are outlined in Appendix 3.B.4. Data for commutes that do not originate or end in Luxembourg is not available.

Travel time matrix We derive a 1×1 km pixel-level travel time matrix for the Greater Region by first estimating road segment speeds from motorway camera data and then applying these as weights to a road network extracted from OSM. Rush hour speeds on highways are set at

80% of the speed limit; a speed of 80 km per hour is assigned to highways without a specified speed limit, while other road classes retain the free-flow speed. The network is converted into a weighted graph via the `sfnetworks` package in R, and the shortest travel times between the pixel centroids are calculated using Dijkstra's algorithm on the largest connected component, which covers 99.8% of the nodes.

3.3.2 Parameters of the model

In this subsection, we present the values for the model elasticities $\{\eta, \sigma, \rho\}$ and an exogenous rental rate of capital r, as derived from the literature. The summary is provided in Table 3.3.1:

Parameter	Description	Value	Source
σ	Elasticity of substitution for labor inputs	1.50	Katz and Murphy (1992)
ρ	Share of capital in production	0.33	Gollin (2002)
η	Congestion elasticity	0.32	Desmet et al. (2018)
r	Capital rental rate	0.05	Piketty (2014)

Table 3.3.1: Parameter values from the literature.

3.3.3 Model calibration

In this subsection, we invert the model fundamentals $\{\mu_{jo}, A_j, \theta_{jo}, b_{io}\}$ and calibrate the preference parameters $\{\alpha^o, \beta^o, \gamma\}$ from the observed data under the assumption that the data represent an equilibrium outcome of the model. These parameters can be divided into two groups: the first group consists of parameters that can be relatively easily inverted from the production side of the model and the available data, while the second group includes parameters that require numerical calibration. The former parameters are cell-specific productivities and occupation shares for the production function. The inversion strategy for these parameters is outlined below.

Cobb-Douglas parameters

Note that the first-order condition on wages implies for any occupations o and $o' \in N$:

$$\frac{w_{jo}}{w_{jo'}} = \frac{\theta_{jo} L_{Fjo}^{-1/\sigma}}{\theta_{jo'} L_{Fjo'}^{-1/\sigma}} \Longrightarrow \frac{\theta_{jo}}{\theta_{jo'}} = \frac{w_{jo} L_{Fjo}^{1/\sigma}}{w_{jo'} L_{Fjo'}^{1/\sigma}}.$$

Since $\sum_{o' \in O} \theta_{jo'} = 1$, we identify θ_{jo} from data on employment and wages. First-order conditions imply that

$$A_j K_j^{\rho} = \frac{w_{jo} L_{Fjo}^{1/\sigma}}{(1-\rho)\theta_{jo} \left(\sum_{o'=1}^{N} \theta_{jo'} L_{Fjo'}^{\frac{\sigma-1}{\sigma}} \right)^{\frac{\sigma}{\sigma-1}}}, \tag{3.3.2}$$

$$A_j K_j^{\rho-1} = \frac{r}{\rho \left(\sum_{o'=1}^{N} \theta_{jo'} L_{Fjo'}^{\frac{\sigma-1}{\sigma}} \right)^{\frac{\sigma}{\sigma-1}}}. \tag{3.3.3}$$

By dividing (3.3.2) by (3.3.3), we obtain

$$K_j = \frac{\rho w_{jo} L_{Fjo}^{1/\sigma}}{(1-\rho) r \theta_{jo}}. \tag{3.3.4}$$

Note that the cell-specific capital use, K_j, can be computed using only the available data and previously obtained values for θ_{jo}. Thus, we can invert the productivity A_j from Equation 3.3.3. As a result, A_j and θ_{jo} can be inverted using data on wages w_{jo}, capital rent r, employment L_{Fjo}, and the values of the parameters σ and ρ.

Preference parameters

Some parameters of the model cannot be inverted directly from the model and, therefore, must be calibrated using numerical optimization techniques. In this subsection, we present the calibration strategy for the preference exponents $\{\alpha^o, \beta^o, \gamma\}$, as well as for the occupation-specific opportunity shifters μ_{jo}.

The algorithm features two distinct loops: the inner loop that solves for the optimal parameter values $\{\alpha^o, \beta^o, \gamma\}$ given μ_{jo}, and the outer loop that solves for μ_{jo} given the parameter values obtained in the inner loop. The outer loop repeats until the maximum change in any μ_{jo} falls below a prescribed threshold.

In the outer loop, a radiation-style probability matrix is computed on the cell grid for every origin cell i and every destination cell j while holding $\{\alpha^o, \beta^o, \gamma\}$ fixed. Multiplying the obtained conditional commuting probability matrix $\pi^o_{j|i}$ by the resident count and summing over the origins yields a predicted employment figure for each cell. The relative difference between observed and predicted employment defines an error term by cell, and each μ_{jo} is updated proportionally: under-predicted cells are up-weighted, while over-predicted cells are down-weighted.

In the inner loop, for a given matching opportunity value $\hat{\mu}_{jo}$ obtained in the outer loop, the three exponents are recalibrated as follows: simulated pixel-level commuting flows are aggregated at the commune level to produce model-implied commune-by-commune flow matrices, $N_{ijo}\left(\alpha_o, \beta_o, \gamma \mid w_{jo}^{data}, \hat{\mu}_{jo}, t_{ij}\right)$. Then, for each commune-level origin-destination pair $i, j \in C \times C$ where $i \neq j$ and occupation o, we define the moment condition as a difference between simulated and observed flows:

$$g_{ijo} = N_{ijo}\left(\alpha_o, \beta_o, \gamma \mid w_{jo}^{data}, \hat{\mu}_{jo}, t_{ij}\right) - N_{ijo}^{data}. \tag{3.3.5}$$

Finally, we choose α_o, β_o and γ that minimize

$$\min_{\alpha_o, \beta_o, \gamma} G_o\left(\alpha_o, \beta_o, \gamma \mid N_{ij}^{data}, w_{jo}^{data}, \hat{\mu}_{jo}, t_{ij}\right) = \sqrt{\sum_{j \in C} \sum_{i \in C} g_{ijo}^2}. \tag{3.3.6}$$

For each occupation, the algorithm outputs the calibrated cell-level matching opportunities μ_{jo} and the occupation-specific exponents $\{\alpha^o, \beta^o, \gamma\}$. As shown in (3.2.19), parameter γ enters the model multiplicatively with respect to α^o and β^o. Thus, we normalize γ to one for every occupation o. The summary of the estimated parameter values is presented in Table 3.3.2:

	Occupations							
	(1)	(2)	(3)	(4)	(5)	(6)	(7)	(8)
α_o	0.85	0.85	0.85	0.85	0.85	0.75	0.70	0.70
β_o	2.30	2.00	2.25	2.30	2.30	2.00	2.20	1.80

Note: Column 1 provides calibrated values for managers, Column 2 – for professionals, Column 3 – for technicians and associate professionals, Column 4 – for clerical support workers, Column 5 – for service and sales workers, Column 6 – for skilled agricultural, forestry and fishery workers, as well as for craft and related trades workers, Column 7 – for plant and machine operators, and assemblers, Column 8 – for elementary occupations. The value of parameter γ is normalized to one for all occupations. We report rounded values.

Table 3.3.2: Rounded calibrated parameter values, by occupation.

Amenity inversion

In the previous step, we calibrated the values for the matching opportunity parameter, μ_{jo}. Now, from the equalization of utility across space, we can infer the values of b_{io} up to normalization. We choose to normalize the amenity by the occupation-specific geometric mean. We denote the geometric means of variables with a bar over the symbol.

Recall that for every occupation o and residential cell i, the utility equalization implies that:

$$b_{io} L_{Ri}^{-\eta} = \frac{\bar{U}^o}{\Gamma_0 \mu_{io}^{1/\gamma} w_{io}^{\alpha_o} ((1-(\pi^o_{i|i})^{\frac{\gamma-1}{\gamma}})}. \tag{3.3.7}$$

Denote $M_{io} = (1-(\pi^o_{i|i})^{\frac{\gamma-1}{\gamma}})$. Then, we obtain that

$$\frac{b_{io}}{\bar{b}_o} = \left[\frac{L_{Rio}}{\bar{L}_{Ro}}\right]^{\eta} \left[\frac{\mu_{io}}{\bar{\mu}_o}\right]^{-1/\gamma} \left[\frac{w_{io}}{\bar{w}_o}\right]^{-\alpha_o} \left[\frac{M_{io}}{\bar{M}_o}\right]^{-1}. \tag{3.3.8}$$

Thus, we invert occupation and cell-specific amenities b_{io} up to normalization.

3.3.4 Average commuting time and conditional commuting probability

In this section, we evaluate the model output by plotting two quantities. First, for each origin pixel i, we plot the conditional probability of working in Luxembourg $\sum_{j \in Lux} \pi_{j|i}$. Second, for each origin i, we plot the average travel time to work, weighted by the conditional probability of working at each destination $\sum_{j \in J} \pi_{j|i} t_{ij}$. Results are aggregated across all occupations. The plots are shown in Figure 3.3.1.

Within Luxembourg's borders, the conditional probability of working in Luxembourg approaches 100%, indicating minimal outward commuting flows to neighboring regions, which is consistent with empirical daily commuting data. As the distance from the state border increases, the probability decreases. In the main commuter towns of Arlon and Thionville, the average share of residents commuting to Luxembourg is between 40% and 60%, as illustrated in the top left panel of Figure 3.3.1.

The model predicts average travel times to work ranging from 5 to 60 minutes, as shown in the top right panel of Figure 3.3.1. Within Luxembourg City, the economic core of the Greater Region, the mean commute is under 10 minutes, implying that most city residents work locally. Beyond the city, locations fall into two groups: those with relatively high average

commuting times (reflecting a greater propensity to commute to Luxembourg) and those with lower average times (indicating predominantly local employment). The bottom panel of Figure 3.3.1 displays the distribution of probabilities for working in one's commune of residence. The modal probability of remaining in the home commune is 5%, while the mean is 20%.

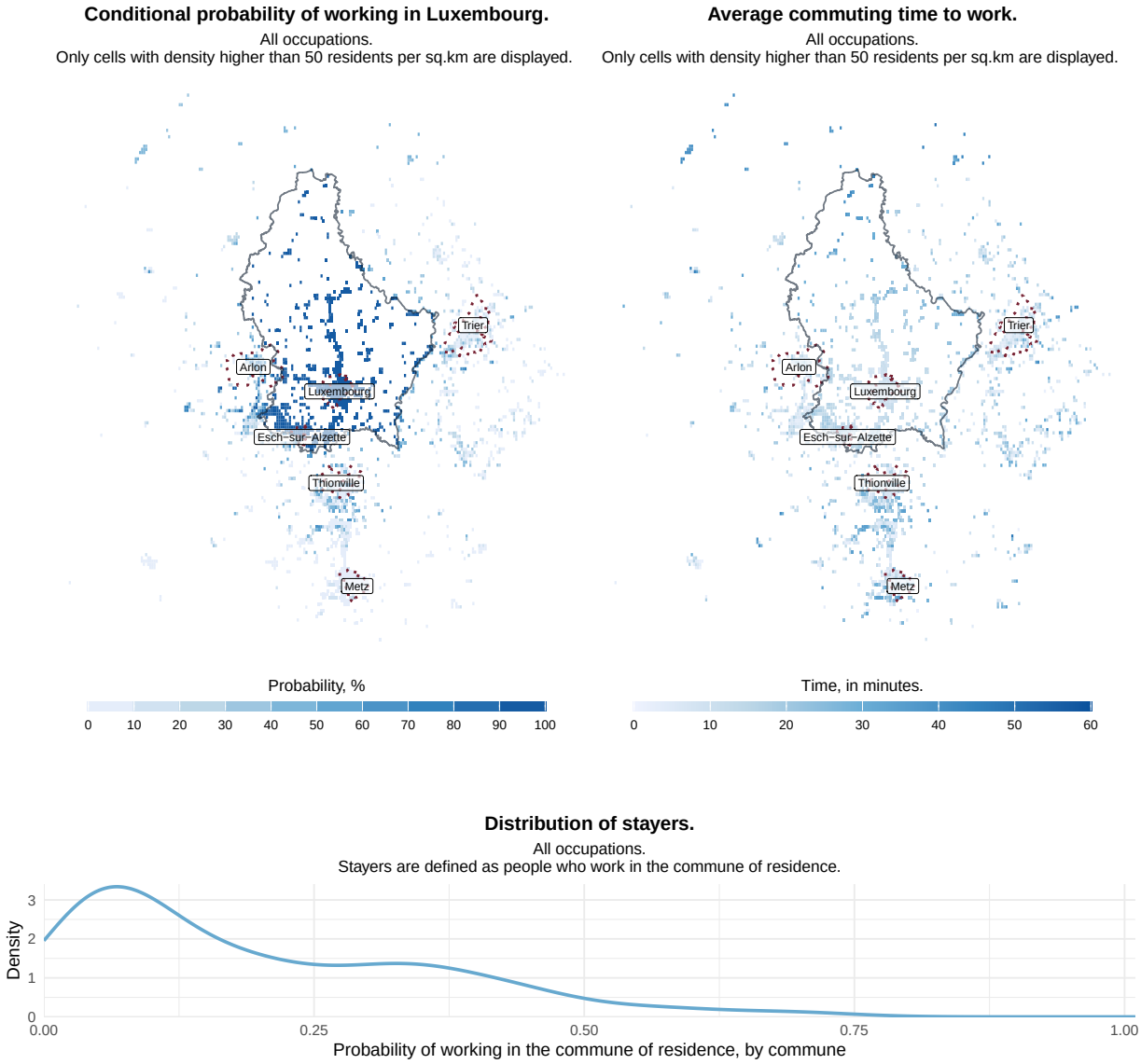

Note: Only pixels with population density higher than 50 people per km^2 are displayed. The state border of Luxembourg is displayed in black solid line. Commune boundaries for communes with more than 25,000 residents are displayed in red dotted line.

Figure 3.3.1: Calibrated conditional probability of commuting to Luxembourg (top left panel), probability-weighted average travel time to workplace in the Greater Region (top right panel), and the distribution of probabilities of working in the same commune as the commune of residence, by commune (bottom panel).

3.4 Simulation results

High labor demand draws thousands of daily cross-border commuters from France, Belgium, and Germany, who accept peak-hour motorway congestion and longer travel times in exchange for higher wages. To address congestion, the government has proposed expanding capacity on the main inbound corridors. This prompts the question: under a hypothetical free-flow transport regime, what would be the equilibrium distribution of residents and workers in the Greater Region and the resulting welfare outcomes? The following subsections analyze this scenario. More formally, we define the problem of finding a counterfactual equilibrium allocation as follows:

Definition of a counterfactual: Given the model parameters $\{\alpha_o, \beta_o, \gamma, \eta, \rho, \sigma\}$, exogenous inputs $\{\mu_{jo}, A_j, \theta_{jo}, L_o, b_{io}, r\}$, and the counterfactual travel time matrix τ'_{ij}, find the counterfactual values for the endogenous variables of the model $\{L_{Rio}, L_{Fjo}, \pi^o_{j|i}, v_{ijo}, w_{jo}, B_{io}, K_j, \bar{U}^o\}$ such that the equilibrium conditions (3.2.18) - (3.2.25) hold. The detailed procedure is outlined in Appendix 3.C.

3.4.1 Change in commuting patterns

In Figure 3.4.1, we break down this effect by occupation. For each commune and occupational group, we plot the distribution of stayers in both the baseline and the counterfactual (medians are shown as dashed lines). The changes vary significantly: service and sales workers exhibit the largest shift, from a median stay rate of 17% down to 8%, while technicians and associate professionals show the smallest change, under 2 percentage points. These results imply that congestion relief measures yield uneven benefits across occupations. Although every group experiences a reduction in local commuting, service and sales workers benefit the most, owing to greater access to external opportunities. In contrast, technicians, associate professionals, and agricultural and forestry workers experience the smallest shifts, suggesting that, while they also save travel time, they have fewer new job options to capitalize on.

On average, the median probability of staying decreases from 19.5% in the baseline to 17.5% in the counterfactual. The 2 p.p. drop in the probability of working in the commune of residence reflects increased out-commuting and indicates aggregate utility gains.

In Figure 3.4.2, we observe changes in both the conditional probability of working in Luxembourg and the average probability-weighted travel time to work. In the left panel, the probability of commuting to Luxembourg remains virtually unchanged for locations within Luxembourg itself, reflecting an initial share close to 100%. In contrast, most cross-border areas register substantial increases – often exceeding 20 percentage points – in their likelihood of sending commuters to Luxembourg, with the largest gains found in neighboring French and German regions. Notably, there is a small cluster of negative changes around the Longwy-Athus tri-point (where Belgium, France, and Luxembourg meet); however, this effect is confined to border-adjacent cells.

Overall, the magnitude of change diminishes with distance from Luxembourg, indicating that proximity amplifies the impact of recent policy or infrastructural adjustments on cross-border commuting patterns, which is consistent with the radiation-style job search and matching model.

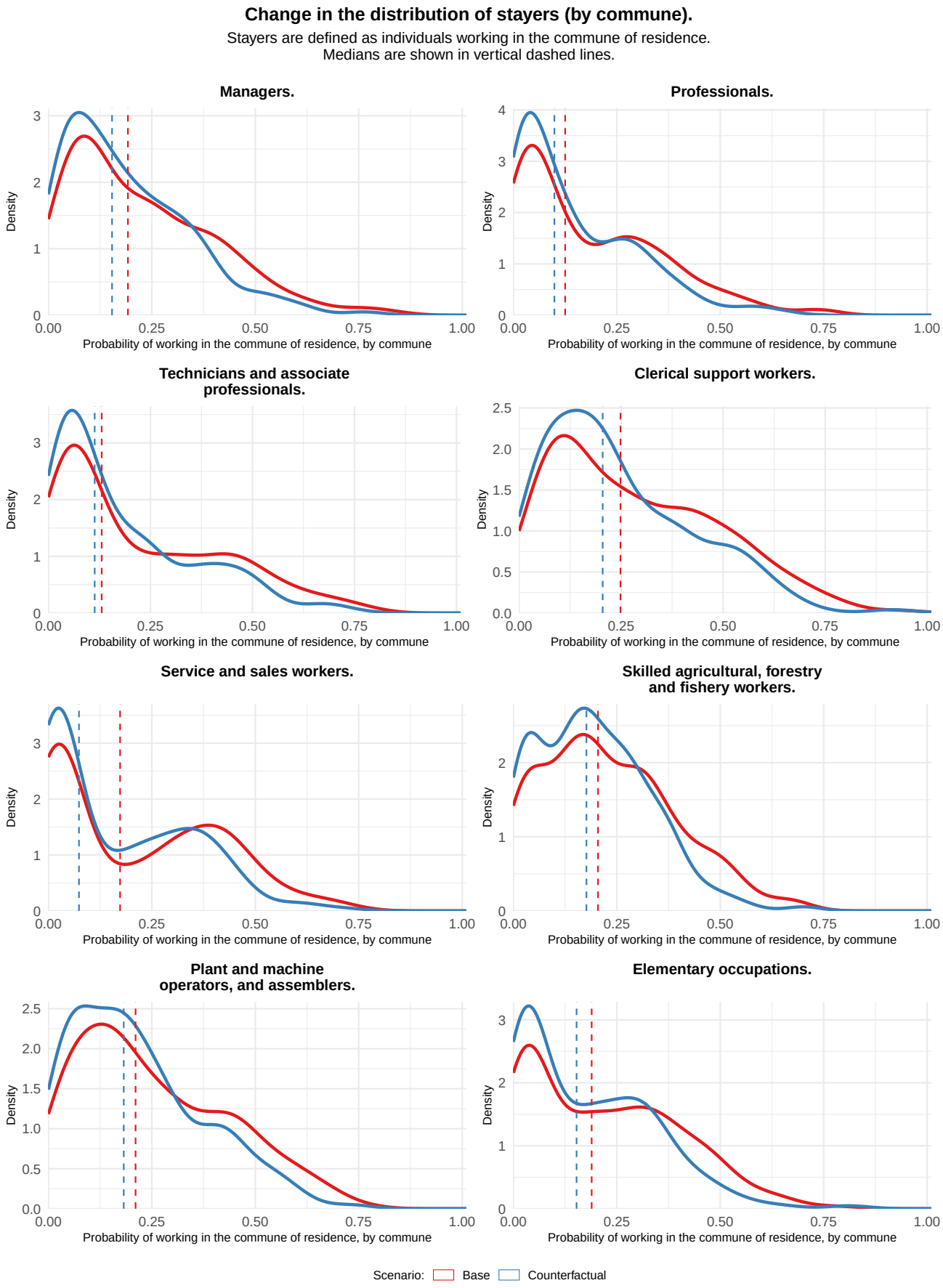

Figure 3.4.1: Change in the distribution of the probability of working in the commune of residence, by occupation.

In the right panel, the average travel time to work decreases across nearly all origin locations, implying a broad benefit from congestion relief interventions. In southern Luxembourg, along Belgium's highway corridors to Luxembourg, and around Thionville in France, reductions reach up to 10 minutes, suggesting that commuters maintain their preferred destinations while enjoying faster journeys. Conversely, a few outlier points, such as Trier and the aforementioned tri-point area, show increases in average travel time. This suggests a shift toward more distant or higher-quality employment opportunities that were previously inaccessible, reflecting an expanded effective labor market following improved cross-border connectivity.

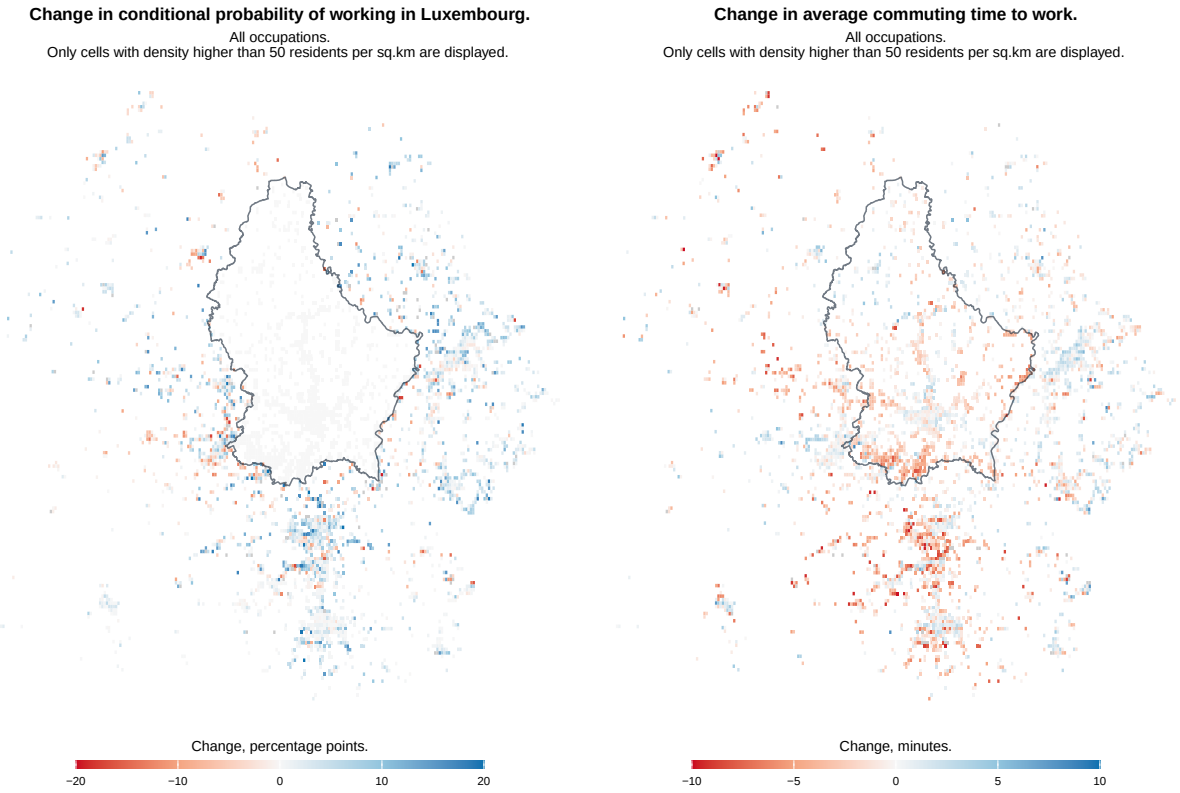

Note: Changes in conditional probability are in percentage point changes, changes in travel time are in minutes. Only pixels with population or employment density higher than 50 people per km^2 are displayed. The state border of Luxembourg is displayed in black solid line.

Figure 3.4.2: Change in conditional probability of working in Luxembourg (left panel) and average travel time to workplace (right panel).

3.4.2 Changes in wages, population and employment

Table 3.4.1 reports the simulated changes in employment, mean wages, and population across four countries for each of the eight occupations. These changes reflect general equilibrium effects following improvements in accessibility and labor mobility. In terms of counterfactual employment, white-collar occupations, such as professionals and technicians, experience smaller changes relative to the total, while blue-collar occupations show more variability. In France, for example, clerical support workers (+7.85%) and service and sales workers (+6.10%) experience employment growth well above the aggregate rate, while the same groups decline sharply in Germany. Wages adjust as workers relocate and firms respond to shifts in local labor supply and demand. On average, Germany shows the strongest wage increase (+1.77%), followed by Belgium (+0.28%) and Luxembourg (+0.13%), while France experiences a modest decline (– 0.81%). However, there is significant heterogeneity across occupations.

	Luxembourg	Belgium	France	Germany
Total employment change, %	0.61	-1.27	3.08	-5.53
Mean wage change, %	0.13	0.28	-0.81	1.77
Total population change, %	-2.07	-0.64	4.88	-3.80
Employment changes by occupation:				
Managers	0.38	-2.91	1.18	-6.44
Professionals	1.38	-2.17	0.92	-6.17
Technicians	0.94	-2.33	4.33	-7.59
Clerical support workers	-1.87	-1.55	7.85	-5.80
Service and sales	-1.00	-1.90	6.10	-8.51
Agriculture and forestry	0.66	0.44	0.23	-1.85
Machinery	1.10	0.05	0.10	-1.69
Elementary occupations	1.62	1.15	1.54	-1.52
Wage changes by occupation:				
Managers	0.68	1.30	0.24	2.23
Professionals	-0.22	0.77	0.43	2.10
Technicians	-0.81	0.95	-1.80	3.16
Clerical support workers	1.93	0.30	-3.92	1.85
Service and sales	0.08	0.71	-2.91	4.01
Agriculture and forestry	-1.40	-0.62	0.43	-0.29
Machinery	-1.69	-0.36	0.51	-0.41
Elementary occupations	-1.58	-1.11	-0.44	-0.52
Population changes by occupation:				
Managers	-2.38	-0.70	4.12	-2.97
Professionals	-0.62	-0.04	3.61	-3.03
Technicians	-2.78	-1.02	6.82	-5.89
Clerical support workers	-6.38	-1.06	11.23	-4.75
Service and sales	-4.28	-1.95	7.74	-7.21
Agriculture and forestry	-0.81	-0.07	1.12	-0.56
Machinery	-0.68	-0.34	0.66	-0.61
Elementary occupations	-1.05	-0.18	1.60	-0.99

Table 3.4.1: Employment, population, and employment-weighted wage changes by occupation and country, in %).

The fact that both Luxembourgish wages and employment increase as a result of congestion relief measures deserves further elaboration. This pattern is specific to the radiation model. In more traditional gravity setups, a decrease in commuting times yields an increase in employment, along with a decrease in wages due to the usual compensating differentials logic. However, in the radiation-style commuting probability expression, a decrease in travel times along highways alters another important parameter of the model: the search set $\mathcal{S}_{ijo}$. Its expansion decreases the conditional probability of working in j as per (3.2.19). On one hand, workers spend less time commuting and require smaller compensation, which pushes wages at the destination downward. On the other hand, a transportation improvement expands the opportunity set $\mathcal{S}_{ijo}$ for a given i, which forces firms at the destination to compete for labor with firms located in $k \in \mathcal{S}_{ijo}$ by increasing wages. In the case of Luxembourg, the latter effect dominates, which explains the simultaneous increase in both employment and wages at the destination.

This effect is also pronounced for certain occupations outside Luxembourg. For example, the dominance of the opportunity channel over the compensating differential is evident for managers, professionals, and workers with elementary occupations residing in France, as well as for German blue-collar workers.

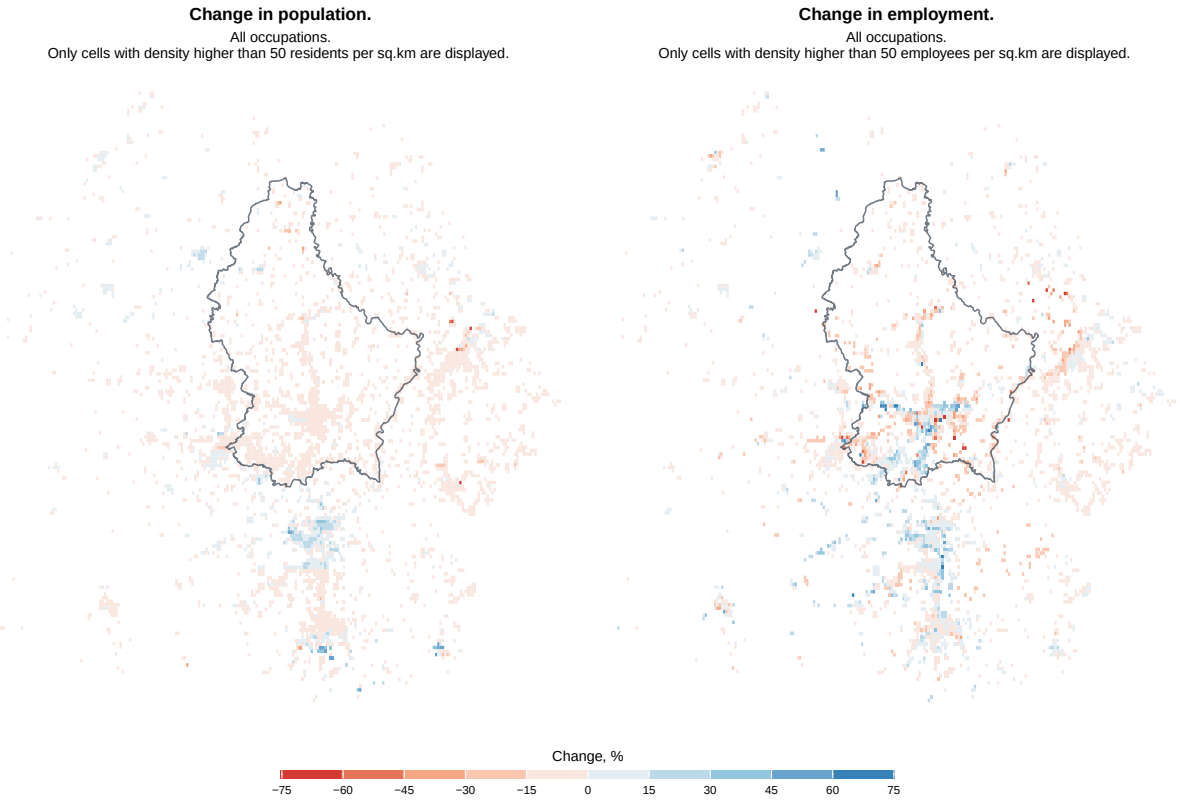

Note: All values expressed in percentage changes from the baseline. Only pixels with population or employment density higher than 50 people per km^2 are displayed. The state border of Luxembourg is displayed in black solid line.

Figure 3.4.3: Changes in population (left panel) and employment (right panel) in the counterfactual free-flow scenario for all occupation groups.

Figure 3.4.3 illustrates the spatial clustering of changes in both employment and population. On the population side, the most notable shifts occur in Thionville and nearby areas in France, which become more accessible to Luxembourg. These areas experience population increases of up to 45%, suggesting an increase in residential demand. In terms of employment, growth is concentrated along major highways and is especially pronounced around Luxembourg City; however, it is notably less so in the south of Luxembourg, which experiences a decline in employment. The French side also shows signs of revitalization: employment increases are observed in both Thionville and areas closer to the Luxembourg border, particularly in locations with good access to the highway.

Overall, the counterfactual free-flow scenario results in greater cross-border commuting, a decline in the share of residents working in their commune of residence, and occupation-specific differences in mobility gains. Luxembourg experiences simultaneous increases in both wages and employment, driven by the expansion of workers' opportunity sets, while effects in neighboring countries vary by occupation and location. Population and employment growth concentrate in accessible French border areas and along major transport corridors, while some regions, including parts of southern Luxembourg, experience declines.

3.5 Conclusion

This chapter develops a spatial general equilibrium model of commuting that integrates a radiation-style sequential job search mechanism into a quantitative spatial framework with endogenous wages, amenities, and density-dependent disamenity. The framework reproduces observed commuting patterns in the Greater Region around Luxembourg and allows for counterfactual simulations of transport policy. By explicitly modeling the search set and intervening opportunities, it captures an important margin absent from gravity-type models: lower commuting times can raise, rather than lower, wages at a destination if the expansion of the worker's opportunity set compels firms to compete more aggressively for labor. The results for Luxembourg illustrate this mechanism clearly, with simultaneous increases in both employment and wages driven by the dominance of the opportunity effect over the compensating differential channel.

Overall, the model retains the tractability of quantitative spatial models while embedding a more realistic frictional labor market in which workers face bounded option sets and heterogeneous match quality. This combination permits a detailed assessment of spatial heterogeneity in responses to transport improvements. In the free-flow scenario, the gains are unevenly distributed across space and occupations: population and employment expand most in accessible French border areas and along major transport corridors, while some regions, including parts of southern Luxembourg, experience declines. Occupational patterns also differ sharply, with service and sales workers benefiting disproportionately from improved access, while technical occupations show smaller shifts.

Several avenues for future research follow naturally. Most importantly, the current model abstracts from modeling the housing market. Introducing a fully endogenous housing market with dynamic adjustments of housing supply and rents would allow for a richer characterization of long-run spatial equilibria and policy effects. Other extensions could incorporate trade, explicit modal choice in commuting, and richer cross-border institutional features. These additions would further enhance the model's ability to serve as a predictive and policy-relevant tool for evaluating the joint effects of transport, housing, and labor market interventions in integrated cross-border regions.

Appendix

3.A Proofs

3.A.1 Radiation probability

The expression is as follows:

$$\pi^{o}_{j|i} = \int_0^\infty (1 - \mathbb{P}[\tilde{U}_{ijo} < z]) \prod_{k \in \mathcal{S}_{ijo}} \mathbb{P}[\tilde{U}_{iko} < z] \frac{d}{dz} (\mathbb{P}[\tilde{U}_{iio} < z])\, dz \tag{3.A.1}$$

Where:

$$\mathbb{P}[\tilde{U}_{iio} < z] = \exp(-\mu_{io} v^{\gamma}_{iio} z^{-\gamma}) \tag{3.A.2}$$

$$\mathbb{P}[\tilde{U}_{ijo} > z] = 1 - \exp(-\mu_{jo} v^{\gamma}_{ijo} z^{-\gamma}) \tag{3.A.3}$$

$$\prod_{k \in \mathcal{S}_{ijo}} \mathbb{P}[\tilde{U}_{iko} < z] = \exp\left(- \sum_{k \in \mathcal{S}_{ijo}} \mu_{ko} v^{\gamma}_{iko} z^{-\gamma} \right) \tag{3.A.4}$$

Additionally:

$$\frac{d}{dz} \mathbb{P}[\tilde{U}_{iio} < z] = \frac{d}{dz} \exp(-\mu_{io} v^{\gamma}_{iio} z^{-\gamma}) = \gamma z^{-\gamma-1} \mu_{io} v^{\gamma}_{iio} \exp(-\mu_{io} v^{\gamma}_{iio} z^{-\gamma}) \tag{3.A.5}$$

We split integral in two, and each part of the integral is a known formula for the probability:

$$\int_0^\infty (1 - \exp(-\mu_{jo} v^{\gamma}_{ijo} z^{-\gamma})) \exp\left(- \sum_{k \in \mathcal{S}_{ijo}} \mu_{ko} v^{\gamma}_{iko} z^{-\gamma} \right) \gamma z^{-\gamma-1} \mu_{io} v^{\gamma}_{iio} \exp(-\mu_{io} v^{\gamma}_{iio} z^{-\gamma})\, dz =$$

$$\int_0^\infty \exp\left(- \sum_{k \in \mathcal{S}_{ijo} \cup \{i\}} \mu_{ko} v^{\gamma}_{iko} z^{-\gamma} \right) \gamma z^{-\gamma-1} \mu_{io} v^{\gamma}_{iio}\, dz -$$

$$- \int_0^\infty \exp\left(- \sum_{k \in \mathcal{S}_{ijo} \cup \{i,j\}} \mu_{ko} v^{\gamma}_{iko} z^{-\gamma} \right) \gamma z^{-\gamma-1} \mu_{io} v^{\gamma}_{iio}\, dz =$$

$$= \frac{\mu_{io} v^{\gamma}_{iio}}{\sum_{k \in \mathcal{S}_{ijo} \cup \{i\}} \mu_{ko} v^{\gamma}_{iko}} - \frac{\mu_{io} v^{\gamma}_{iio}}{\sum_{k \in \mathcal{S}_{ijo} \cup \{i,j\}} \mu_{ko} v^{\gamma}_{iko}} = \mu_{io} v^{\gamma}_{iio} \left[\frac{1}{\sum_{k \in \mathcal{S}_{ijo} \cup \{i\}} \mu_{ko} v^{\gamma}_{iko}} - \frac{1}{\sum_{k \in \mathcal{S}_{ijo} \cup \{i,j\}} \mu_{ko} v^{\gamma}_{iko}} \right]$$

3.A.2 Probability of staying

The probability of commuting to j from i is defined as:

$$\pi^o_{j|i} = \mu_{io}\nu^\gamma_{iio}\left[\frac{1}{\sum\limits_{k\in\mathcal{S}_{ijo}\cup\{i\}}\mu_{ko}\nu^\gamma_{iko}} - \frac{1}{\sum\limits_{k\in\mathcal{S}_{ijo}\cup\{i,j\}}\mu_{ko}\nu^\gamma_{iko}}\right]$$

Now, consider $j' = j+1$, i.e the work location immediately after j. For this location:

$$\mathcal{S}_{ij'o} = \{k : \tau_{ij'} > \tau_{kj'} > 0\} = \mathcal{S}_{ijo}\cup\{j\}$$

And:

$$\pi^o_{j'|i} = \mu_{io}\nu^\gamma_{iio}\left[\frac{1}{\sum\limits_{k\in\mathcal{S}_{ij'o}\cup\{i\}}\mu_{ko}\nu^\gamma_{iko}} - \frac{1}{\sum\limits_{k\in\mathcal{S}_{ij'o}\cup\{i,j'\}}\mu_{ko}\nu^\gamma_{iko}}\right] =$$

$$= \mu_{io}\nu^\gamma_{iio}\left[\frac{1}{\sum\limits_{k\in\mathcal{S}_{ijo}\cup\{i,j\}}\mu_{ko}\nu^\gamma_{iko}} - \frac{1}{\sum\limits_{k\in\mathcal{S}_{ij'o}\cup\{i,j'\}}\mu_{ko}\nu^\gamma_{iko}}\right]$$

Now, note that for j and $j' = j+1$, $\pi^o_{j|i} + \pi^o_{j'|i}$ is just:

$$\pi^o_{j|i}+\pi^o_{j'|i} = \mu_{io}\nu^\gamma_{iio}\left[\frac{1}{\sum\limits_{k\in\mathcal{S}_{ij'o}\cup\{i\}}\mu_{ko}\nu^\gamma_{iko}} - \cancel{\frac{1}{\sum\limits_{k\in\mathcal{S}_{ij'o}\cup\{i,j'\}}\mu_{ko}\nu^\gamma_{iko}}} + \cancel{\frac{1}{\sum\limits_{k\in\mathcal{S}_{ijo}\cup\{i,j\}}\mu_{ko}\nu^\gamma_{iko}}} - \frac{1}{\sum\limits_{k\in\mathcal{S}_{ij'o}\cup\{i,j'\}}\mu_{ko}\nu^\gamma_{iko}}\right] =$$

$$= \mu_{io}\nu^\gamma_{iio}\left[\frac{1}{\sum\limits_{k\in\mathcal{S}_{ij'o}\cup\{i\}}\mu_{ko}\nu^\gamma_{iko}} - \frac{1}{\sum\limits_{k\in\mathcal{S}_{ij'o}\cup\{i,j'\}}\mu_{ko}\nu^\gamma_{iko}}\right]$$

We obtained **telescopic summation**. So:

$$\sum_{m=1}^{J}\pi_{m|i} = \mu_{io}\nu^\gamma_{iio}\left[\frac{1}{\mu_{io}\nu^\gamma_{iio}} - \frac{1}{\sum\limits_{k\in J}\mu_{ko}\nu^\gamma_{iko}}\right] = 1 - \frac{\mu_{io}\nu^\gamma_{iio}}{\sum\limits_{k\in J}\mu_{ko}\nu^\gamma_{iko}}$$

And since we defined $\pi^o_{i|i} = 1 - \sum\limits_{m=1}^{J}\pi_{m|i}$, we get that:

$$\pi^o_{i|i} = \frac{\mu_{io}\nu^\gamma_{iio}}{\sum\limits_{k\in J}\mu_{ko}\nu^\gamma_{iko}}.$$

3.A.3 Expected utility

The expression for the expected utility is defined as:

$$E[U_{io}] = \sum_{j \in J} E[U_{ijo}] = \sum_{j \in J} \int_0^\infty z(1 - \mathbb{P}[\tilde{U}_{ijo} < z]) \prod_{k \in \mathcal{S}_{ijo}} \mathbb{P}[\tilde{U}_{iko} < z] \frac{d}{dz}(\mathbb{P}[\tilde{U}_{iio} < z])\, dz$$

First, we deal with the expression under the integral sign

$$E[U_{ijo}] = \int_0^\infty z(1 - \mathbb{P}[\tilde{U}_{ijo} < z]) \prod_{k \in \mathcal{S}_{ijo}} \mathbb{P}[\tilde{U}_{iko} < z] \frac{d}{dz}(\mathbb{P}[\tilde{U}_{iio} < z])\, dz =$$

$$\int_0^\infty \exp\left(- \sum_{k \in \mathcal{S}_{ijo} \cup \{i\}} \mu_{ko} \nu_{iko}^\gamma z^{-\gamma} \right) \gamma z^{-\gamma} \mu_{io} \nu_{iio}^\gamma \, dz -$$

$$- \int_0^\infty \exp\left(- \sum_{k \in \mathcal{S}_{ijo} \cup \{i,j\}} \mu_{ko} \nu_{iko}^\gamma z^{-\gamma} \right) \gamma z^{-\gamma} \mu_{io} \nu_{iio}^\gamma \, dz =$$

For the first integral, define $\Phi_i = \sum_{k \in \mathcal{S}_{ijo} \cup \{i\}} \mu_{ko} \nu_{iko}^\gamma$. Then:

$$\int_0^\infty \exp\left(- \sum_{k \in \mathcal{S}_{ijo} \cup \{i\}} \mu_{ko} \nu_{iko}^\gamma z^{-\gamma} \right) \gamma z^{-\gamma} \mu_{io} \nu_{iio}^\gamma \, dz = \frac{\mu_{io} \nu_{iio}^\gamma}{\Phi_i} \int_0^\infty \gamma \Phi_i z^{-\gamma} \exp\left(-\Phi_i z^{-\gamma}\right) \, dz$$

Now, do the substitution: $y = \Phi_i z^{-\gamma}$, and $dy = -\gamma \Phi_i z^{-\gamma-1} dz$, so $dz = -\frac{\Phi_i^{1/\gamma} y^{-1/\gamma} dy}{\gamma y}$:

$$\frac{\mu_{io} \nu_{iio}^\gamma}{\Phi_i} \int_0^\infty \gamma \Phi_i z^{-\gamma} \exp\left(-\Phi_i z^{-\gamma}\right) \, dz =$$

$$= \int_\infty^0 e^{-y} \gamma \frac{y}{\Phi_i} \mu_{io} \nu_{iio}^\gamma \left(-\frac{\Phi_i^{1/\gamma}}{\gamma} y^{-1/\gamma - 1} \, dy \right) = \mu_{io} \nu_{iio}^\gamma \Phi_i^{\frac{1}{\gamma} - 1} \int_0^\infty y^{-1/\gamma} e^{-y} \, dy$$

$$= \mu_{io} \nu_{iio}^\gamma \Phi_i^{\frac{1-\gamma}{\gamma}} \Gamma\left(\tfrac{\gamma-1}{\gamma}\right) = \Gamma\left(\tfrac{\gamma-1}{\gamma}\right) \mu_{io} \nu_{iio}^\gamma \left(\sum_{k \in \mathcal{S}_{ijo} \cup \{i\}} \mu_{ko} \nu_{iko}^\gamma \right)^{\frac{1-\gamma}{\gamma}}$$

Denote $\Gamma_0 = \Gamma\left(\tfrac{\gamma-1}{\gamma}\right)$. By analogy, deal with the second integral. In the end, we obtain that:

$$\int_0^\infty z(1 - \mathbb{P}[\tilde{U}_{ijo} < z]) \prod_{k \in \mathcal{S}_{ijo}} \mathbb{P}[\tilde{U}_{iko} < z] \frac{d}{dz}(\mathbb{P}[\tilde{U}_{iio} < z])\, dz =$$

$$= \Gamma_0 \mu_{io} \nu_{iio}^\gamma \left(\sum_{k \in \mathcal{S}_{ijo} \cup \{i\}} \mu_{ko} \nu_{iko}^\gamma \right)^{\frac{1-\gamma}{\gamma}} - \Gamma_0 \mu_{io} \nu_{iio}^\gamma \left(\sum_{k \in \mathcal{S}_{ijo} \cup \{i,j\}} \mu_{ko} \nu_{iko}^\gamma \right)^{\frac{1-\gamma}{\gamma}} =$$

$$= \Gamma_0 \mu_{io} v_{iio}^{\gamma} \left[\frac{1}{\left(\sum_{k \in \mathcal{S}_{ijo} \cup \{i\}} \mu_{ko} v_{iko}^{\gamma} \right)^{\frac{\gamma-1}{\gamma}}} - \frac{1}{\left(\sum_{k \in \mathcal{S}_{ijo} \cup \{i,j\}} \mu_{ko} v_{iko}^{\gamma} \right)^{\frac{\gamma-1}{\gamma}}} \right] = \Gamma_0 \mu_{io} v_{iio}^{\gamma} \Psi_{ij}$$

We denote the difference by Ψ_{ij}. So, the expected utility is a sum over all j:

$$E[U_{io}] = \Gamma_0 \mu_{io} v_{iio}^{\gamma} \sum_{j \in J} \Psi_{ij} \tag{3.A.6}$$

Note that by the telescopic arguement, for the location immediately after j, which we denote as $j' = j + 1$, we have that $\mathcal{S}_{ij'o} = \mathcal{S}_{ijo} \cup \{j\}$, and so the same expression holds:

$$\Psi_{ij'} = \left[\frac{1}{\left(\sum_{k \in \mathcal{S}_{ij'o} \cup \{i\}} \mu_{ko} v_{iko}^{\gamma} \right)^{\frac{\gamma-1}{\gamma}}} - \frac{1}{\left(\sum_{k \in \mathcal{S}_{ij'o} \cup \{i,j'\}} \mu_{ko} v_{iko}^{\gamma} \right)^{\frac{\gamma-1}{\gamma}}} \right] \tag{3.A.7}$$

Which is the same as:

$$\Psi_{ij'} = \left[\frac{1}{\left(\sum_{k \in \mathcal{S}_{ijo} \cup \{i,j\}} \mu_{ko} v_{iko}^{\gamma} \right)^{\frac{\gamma-1}{\gamma}}} - \frac{1}{\left(\sum_{k \in \mathcal{S}_{ijo} \cup \{i,j,j'\}} \mu_{ko} v_{iko}^{\gamma} \right)^{\frac{\gamma-1}{\gamma}}} \right] \tag{3.A.8}$$

So:

$$\Psi_{ij} + \Psi_{ij'} = \left[\frac{1}{\left(\sum_{k \in \mathcal{S}_{ijo} \cup \{i\}} \mu_{ko} v_{iko}^{\gamma} \right)^{\frac{\gamma-1}{\gamma}}} - \frac{1}{\left(\sum_{k \in \mathcal{S}_{ijo} \cup \{i,j,j'\}} \mu_{ko} v_{iko}^{\gamma} \right)^{\frac{\gamma-1}{\gamma}}} \right] \tag{3.A.9}$$

Finally, we get:

$$\sum_{j \in J} \Psi_{ij} = \frac{1}{\left(\mu_{io} v_{iio}^{\gamma} \right)^{\frac{\gamma-1}{\gamma}}} - \frac{1}{\left(\sum_{k \in J} \mu_{ko} v_{iko}^{\gamma} \right)^{\frac{\gamma-1}{\gamma}}}$$

So, the expected utility is just:

$$E[U_{io}] = \Gamma_0 \mu_{io} v_{iio}^{\gamma} \left[\frac{1}{\left(\mu_{io} v_{iio}^{\gamma}\right)^{\frac{\gamma-1}{\gamma}}} - \frac{1}{\left(\sum_{k \in J} \mu_{ko} v_{iko}^{\gamma}\right)^{\frac{\gamma-1}{\gamma}}} \right] \tag{3.A.10}$$

Or, expressed in a more compact form:

$$E[U_{io}] = \Gamma_0 \mu_{io}^{1/\gamma} v_{iio} \left[1 - \left(\pi_{i|i}^{o}\right)^{\frac{\gamma-1}{\gamma}} \right] \tag{3.A.11}$$

3.B Data Imputation

3.B.1 Data sources

Type	Country	Resolution	Variables	Source
Population	LU	1 × 1 km	At the place of residence: population by occupation, sector, age, gender, education.	STATEC (2021)
Population	All	1 × 1 km	At the place of residence: population by age, gender.	WorldPop (2020)
Population	All	Commune	At the place of residence: population by occupation, sector, age, gender, education.	STATEC, INSEE, BELSTAT, DESTATIS (2021)
Employment	All	Commune	At the place of work: population by occupation, sector, age, gender, education.	STATEC, INSEE, BELSTAT, DESTATIS (2021)
Wages	All	Country	Wages at the place of work by: occupation, sector, age, gender, education	Labor Force Survey (2021)
Commuting flows	LU	Commune	Commuting flows	Luxembourgish Ministry of Transport. (2021)
Commuting flows	BE, FR, GE	Commune	Commuting flows by type: white-collar and blue-collar occupations	IGSS (2021)
Road Network	All	NA	Road network data: highways, primary, secondary, tertiary roads.	OSRM (2022)
Speed data	LU	NA	Speed data by: hour, day, camera, direction	CITA (2019)
Housing price data	All	NA	Geo-coded (long,lat) housing price data, hedonic characteristics	athome.lu (2022)

Table 3.B.1: Data sources used for population and jobs imputation

3.B.2 Population and employment construction algorithm

Step 1: Pixel totals for population and employment

In this section, the inputs are total population and employment by commune (STATEC, BelStat, Insee, Destatis), as well as population by pixel (WorldPop 2020). The outputs are pixel totals

for employment and population.

We construct pixel-level totals by combining commune-level population and employment with a gridded population surface. Let emp_c and pop_c denote commune totals, and pop_p denote the pixel population. The baseline employment per pixel is:

$$\text{emp}_p \;=\; \text{pop}_p \times \frac{\text{emp}_c}{\text{pop}_c}.$$

Algorithm 1: Build pixel totals (population and employment)

Inputs : Commune totals pop_c, emp_c; pixel population pop_p (WorldPop 2020).
Outputs : Pixel totals pop_p (baseline), emp_p.

foreach *commune c* **do**
  compute ratio $r_c \leftarrow \text{emp}_c/\text{pop}_c$;
  set provisional $\text{emp}_p \leftarrow r_c \cdot \text{pop}_p$ for all pixels p in c;
  rescale within c so $\sum_{p\in c} \text{emp}_p = \text{emp}_c$ and $\sum_{p\in c} \text{pop}_p = \text{pop}_c$.

Step 2: Population (residents) shares by occupation, by pixel

In this section, the inputs consist of the total pixel population (WorldPop) and the Luxembourg-only pixel population by occupation for estimation. The output is the resident occupation share per pixel.

For Luxembourg, we estimate a logistic model in which we regress the logit-transformed resident occupation shares based on pixel population on the total population in the cell. We include commune fixed effects:

$$\log\frac{\text{shr}_{cpo}}{1-\text{shr}_{cpo}} = \alpha_o + \gamma_{co} + \beta_o \,\text{pop}_p + \varepsilon_{cpo}.$$

The estimation results are presented in Table 3.B.4. Outside Luxembourg, we impute shares using the fitted logit and normalize to sum to one over occupations in each pixel:

$$\text{shr}_{po} \;=\; \frac{e^{\hat{\alpha}_o+\hat{\beta}_o \,\text{pop}_p}}{1+e^{\hat{\alpha}_o+\hat{\beta}_o \,\text{pop}_p}}, \qquad \widehat{\text{shr}}_{po} \;=\; \frac{\text{shr}_{po}}{\sum_o \text{shr}_{po}}.$$

Algorithm 2: Resident occupation shares (Lux. estimation, external imputation)

Inputs : Luxembourg pixel data on resident occupation shares; pixel totals pop_p.
Outputs : Pixel resident shares $\widehat{\text{shr}}_{po}$ (all geographies).
Estimate (Lux): fit logit of shr_{cpo} on pop_p with commune effects; store (α_o, β_o).
Predict (non-Lux): compute shr_{po} from the logit; normalize $\widehat{\text{shr}}_{po} \leftarrow \text{shr}_{po}/\sum_o \text{shr}_{po}$ per pixel.

Step 3: Employment (workplace) shares by occupation, by pixel

In this section, we use employment by occupation at the commune level (STATEC) and pixel employment from Step 1 as inputs. The output is workplace occupation shares by pixel.

For Luxembourg, we estimate a commune-level logistic regression of workplace occupation shares on employment:

$$\log\frac{\text{shr}_{co}}{1-\text{shr}_{co}} = \alpha_o + \beta_o \,\text{emp}_c + \varepsilon_{co}.$$

The estimation result is presented in Table 3.B.2. For all locations, we impute pixel shares from the fitted logit using pixel employment from Step 1 and normalize over occupations:

$$\text{shr}_{po} \;=\; \frac{e^{\hat{\alpha}_o+\hat{\beta}_o \,\text{emp}_p}}{1+e^{\hat{\alpha}_o+\hat{\beta}_o \,\text{emp}_p}}, \qquad \widehat{\text{shr}}_{po} \;=\; \frac{\text{shr}_{po}}{\sum_o \text{shr}_{po}}.$$

Algorithm 3: Workplace occupation shares (Lux. estimation, general imputation)

Inputs : Luxembourg commune shares by occupation and emp_c; pixel emp_p from Step 1.

Outputs : Pixel workplace shares $\widehat{\text{shr}}_{po}$.

Estimate (Lux): fit logit of shr_{co} on emp_c; store (α_o, β_o).
Predict (all): compute shr_{po} from the logit using emp_p; normalize $\widehat{\text{shr}}_{po}$ over o per pixel.

Step 4: Counts by occupation via IPFP

Given commune-by-occupation totals and the pixel totals and shares above, we reconcile to obtain pixel counts by occupation using IPFP. In the population example, we solve:

$$\max_{\text{pop}_{cpo}\geq 0} \sum_{c,p,o} \text{pop}_{cpo} \log\Big(\frac{\text{pop}_{cpo}}{\text{shr}_{cpo}}\Big) \quad \text{s.t.} \quad \sum_p \text{pop}_{cpo} = \text{pop}_{co}, \;\; \sum_o \text{pop}_{cpo} = \text{pop}_{cp}.$$

The IPFP selects the distribution that satisfies the marginal constraints while maximizing entropy, which ensures that no additional structure is imposed beyond what is implied by the constraints. The outputs are pixel-level counts by occupation for both population and employment.

Algorithm 4: IPFP reconciliation (population or employment)

Inputs : Commune-by-occupation totals; pixel totals from Step 1; pixel shares from Steps 2–3.

Outputs : Pixel-by-occupation counts consistent with commune and pixel margins.

Initialize $x_{cpo} \leftarrow$ (pixel total) × (pixel share);
while *margins not matched within tolerance* **do**
  (i) scale across p to match $\sum_p x_{cpo} =$ (commune by occ. total);
  (ii) scale across o to match $\sum_o x_{cpo} =$ (pixel total).

3.B.3 Regression tables

	Logit-transformed shares in employment, by occupation:							
	Occ.1	Occ.2	Occ.3	Occ.4	Occ.5	Occ.6	Occ.7	Occ.8
Intercept	-2.962***	-1.323***	-1.765***	-2.652***	-1.884***	-1.595***	-3.704***	-1.858***
	(0.049)	(0.038)	(0.028)	(0.039)	(0.042)	(0.054)	(0.288)	(0.035)
Employment, ths.	0.006*	0.010***	-0.001	0.006**	-0.004	-0.016***	0.004	-0.006***
	(0.003)	(0.003)	(0.002)	(0.003)	(0.003)	(0.004)	(0.019)	(0.002)
Observations	100	100	100	100	100	100	100	100
R^2	0.031	0.151	0.003	0.062	0.022	0.167	0.001	0.068

Note: The included groups are managers (Occ1), professionals (Occ2), technicians (Occ3), office support workers (Occ4), service and sales workers (Occ5), skilled agricultural, craft and trade workers (Occ6), plant and machine operators, and assemblers (Occ7), elementary occupations (Occ8).

Table 3.B.2: Occupation shares at the place of work as functions of the total employment at the commune level.

	Logit-transformed shares in popluation, by occupation:							
	Occ.1	Occ.2	Occ.3	Occ.4	Occ.5	Occ.6	Occ.7	Occ.8
Intercept	-2.899***	-0.889***	-1.695***	-2.243***	-1.920***	-2.107***	-3.125***	-2.182***
	(0.041)	(0.047)	(0.014)	(0.015)	(0.030)	(0.047)	(0.049)	(0.042)
Population, ths.	0.012*	0.011	-0.010***	-0.004	-0.008*	-0.017**	-0.014*	0.004
	(0.006)	(0.007)	(0.002)	(0.002)	(0.005)	(0.007)	(0.007)	(0.006)
Observations	100	100	100	100	100	100	100	100
R^2	0.035	0.025	0.182	0.027	0.033	0.059	0.036	0.003

Note: The included groups are managers (Occ1), professionals (Occ2), technicians (Occ3), office support workers (Occ4), service and sales workers (Occ5), skilled agricultural, craft and trade workers (Occ6), plant and machine operators, and assemblers (Occ7), elementary occupations (Occ8).

Table 3.B.3: Occupation shares at the place of residence as functions of the total population at the commune level.

	Logit-transformed shares in population, by occupation:							
	Occ.1	Occ.2	Occ.3	Occ.4	Occ.5	Occ.6	Occ.7	Occ.8
Intercept	-8.431***	-4.419**	-7.726***	-7.903***	-5.967***	-1.622	-8.168***	-4.684**
	(2.021)	(1.810)	(1.898)	(2.023)	(1.985)	(1.931)	(2.100)	(2.058)
Population, ths.	3.833***	1.558***	2.541***	3.670***	3.056***	2.209***	4.906***	3.305***
	(0.504)	(0.452)	(0.474)	(0.505)	(0.495)	(0.482)	(0.524)	(0.514)
Observations	1562	1562	1562	1562	1562	1562	1562	1562
R^2	0.155	0.099	0.084	0.094	0.090	0.088	0.134	0.110

Note: The included groups are managers (Occ1), professionals (Occ2), technicians (Occ3), office support workers (Occ4), service and sales workers (Occ5), skilled agricultural, craft and trade workers (Occ6), plant and machine operators, and assemblers (Occ7), elementary occupations (Occ8).

Table 3.B.4: Occupation shares at the place of residence as functions of the total population at the pixel level.

3.B.4 Construction of occupation-specific commuting matrices

Let $T_{ij} \geq 0$ denote the aggregate number of commuters from origin i to destination j, summed over all occupations. Let $O_i^k \geq 0$ denote the number of residents of occupation k at origin i,

and $D_j^k \geq 0$ the number of employees of occupation k at destination j. We seek a tensor $x_{ij}^k \geq 0$ such that:

$$\sum_j x_{ij}^k = O_i^k, \qquad \forall (i,k), \tag{3.B.1}$$

$$\sum_i x_{ij}^k = D_j^k, \qquad \forall (j,k), \tag{3.B.2}$$

$$\sum_k x_{ij}^k = T_{ij}, \qquad \forall (i,j). \tag{3.B.3}$$

If the marginal totals are consistent,

$$\sum_{i,k} O_i^k = \sum_{j,k} D_j^k = \sum_{i,j} T_{ij},$$

and the supports are compatible ($T_{ij} = 0 \implies x_{ij}^k = 0$), there exists a unique solution that minimises the Kullback–Leibler divergence to a prior tensor Q_{ij}^k:

$$\min_{x_{ij}^k \geq 0} \sum_{i,j,k} x_{ij}^k \log \frac{x_{ij}^k}{Q_{ij}^k} \quad \text{s.t.} \quad (3.B.1)\text{–}(3.B.3). \tag{3.B.4}$$

In the absence of additional prior information, we take $Q_{ij}^k \propto T_{ij}$.

The problem is solved by a three-way Iterative Proportional Fitting Procedure (IPFP). Initial values may be set as

$$x_{ij}^k \leftarrow T_{ij} \cdot \frac{O_i^k}{O_i} \cdot \frac{D_j^k}{D_j}, \quad O_i = \sum_j T_{ij}, \quad D_j = \sum_i T_{ij}.$$

At each iteration, the following multiplicative adjustments are applied cyclically until convergence:

1. Scale over (i,k) to satisfy (3.B.1):

$$x_{ij}^k \leftarrow x_{ij}^k \cdot \frac{O_i^k}{\sum_{j'} x_{ij'}^k}.$$

2. Scale over (j,k) to satisfy (3.B.2):

$$x_{ij}^k \leftarrow x_{ij}^k \cdot \frac{D_j^k}{\sum_{i'} x_{i'j}^k}.$$

3. Scale over (i,j) to satisfy (3.B.3):

$$x_{ij}^k \leftarrow x_{ij}^k \cdot \frac{T_{ij}}{\sum_{k'} x_{ij}^{k'}}.$$

With strictly positive feasible marginals, the sequence converges to the unique maximum-entropy solution satisfying all constraints.

3.B.5 Travel time matrix construction

Next, we compute the travel time matrix across all the 1x1 km pixel pairs in the GR. The construction of this matrix involves two parts. First, we estimate the weights using different data sources. Second, we use GIS software to construct a network from the data using specialized software packages. To estimate the weights, we use data from the Luxembourgish Agency for Road Traffic Control (CITA). The dataset aggregates information from 186 cameras on the motorways (A1, A3, A4, A6, A7, A13, B40) between 19/11/2019 and 26/12/2019. We observe the number of cars, traffic density, and average speed at each of the 186 cameras at 5-minute intervals. Each camera captures data for two directions: inbound (towards Luxembourg City) and outbound (from Luxembourg City). To estimate changes in average speed throughout the day, we run the following regression specification:

$$speed_{htrdc} = \phi_d + \psi_c + \alpha_{htr} + \varepsilon_{htrdc}, \tag{3.B.5}$$

where h denotes highway, t denotes time of day (in hours), r denotes direction (outbound or inbound), d denotes day, and c denotes each individual camera. We use the estimated values of α_{htr}, which is a highway-hour-direction fixed effect, to analyze the decrease in speed throughout the day. We plot these values for the inbound direction in Figure 3.B.1.

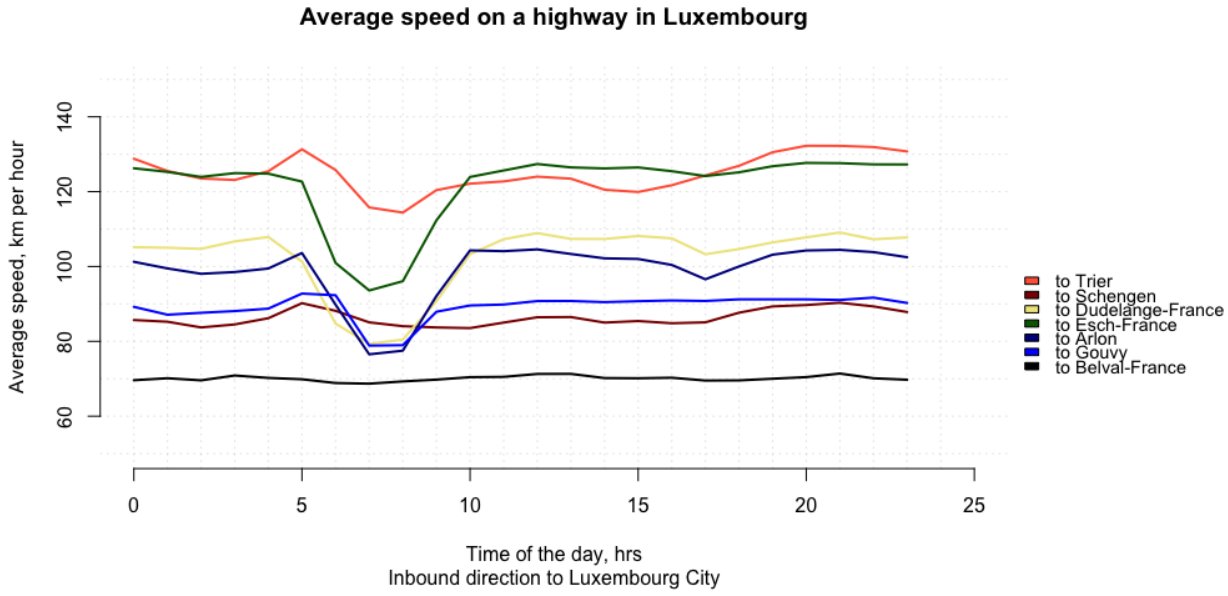

Figure 3.B.1: Average change in speed by highway and hour of the day, inbound direction.

We observe a pronounced drop in average speed on highways during the morning peak hour in the inbound direction. The off-peak hour average speed on all highways is close to the official speed limit. However, during peak hours, the average speed falls by roughly 20% for each highway in the set of observations. Therefore, we use the peak hour estimate of the average speed on motorways as 80% of the speed limit. The remaining weights are set as follows: for urban and rural tertiary roads, we set the speed to 20 kilometers per hour. For motorways, we set the speed to 80% of the maximum speed limit. For motorways without a speed limit, we set an average speed of 80 km/h.

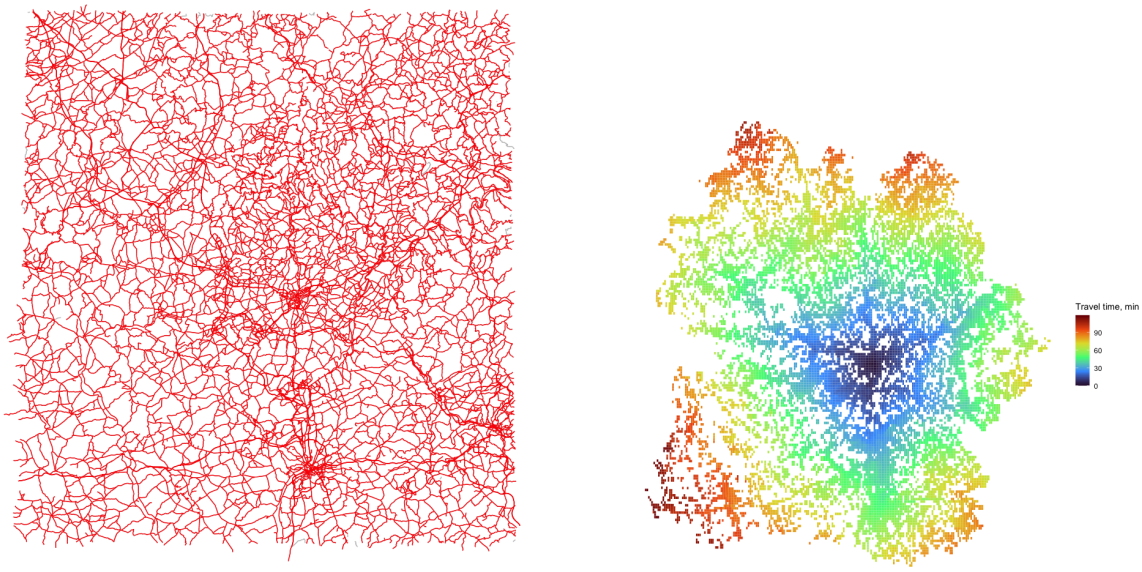

Note: The left panel displays the biggest connected component of the road network (red) and the whole road network (grey). The right panel visualizes travel time to the most populous pixel in the economy (Luxembourg City center) computed using the road network with estimated weights.

Figure 3.B.2: Road network (left) and average travel time to Luxembourg City (right).

Travel time across pixels is generated using road network data for the Greater Region, obtained from the Open Source Routing Machine (OSRM). We use the extract dating from July 2024. We observe data on the type of roads (motorway, primary, secondary, or tertiary), the speed limits associated with those roads, and their geographical coordinates. For each road segment, we compute the average travel time, which is equal to the length of the segment divided by the imputed speed obtained in the previous stage. We then convert the shapefile of the road network into a graph using the `sfnetworks` package in R. This package allows us to compute the travel time matrix between centroids of pixels, using assigned travel times as weights of the network. `sfnetworks` computes the shortest distance along network paths using Dijkstra's algorithm. We use the largest connected component of the graph to ensure that every origin and destination pixel can be reached along the network paths. The largest connected component, covering 99.8% of the initial network nodes, is depicted in Figure 3.B.2.

3.C Simulation algorithm

The simulation algorithm works as follows: starting from the parameters $\{\alpha_o, \beta_o, \gamma, \eta, \rho, \sigma\}$, exogenous inputs $\{\mu_{jo}, A_j, \theta_{jo}, L_o, b_{io}, r\}$, and the counterfactual travel time matrix t'_{ij}, the model iterates to achieve spatial equilibrium in terms of the endogenous parameters $\{L_{Rio}, L_{Fjo}, \pi^o_{j|i}, v_{ijo}, w_{jo}, B_{io}, K_j, \bar{U}^o\}$.

The numerical solver consists of two loops: the inner loop, which solves for employment and wages using equation (3.2.18) given the population distribution, and the outer loop, which solves for population and density-dependent disamenity given employment and wages.

In the inner loop, the labor market equilibrium is determined based on the population distribution: for every occupation o, radiation-style probabilities (3.2.19) generate a matrix of flows which, upon summation over origins, yield updated employment counts L'_{Fjo}. These employment levels enter a zero-profit condition for labor (3.2.21) that updates wages w'_{jo} via a Cobb-Douglas rule in each cell. The inner loop iterates until the change in both employment and wages between iterations is smaller than the predefined threshold.

In the outer loop, the wage distribution obtained in the inner loop feeds into a utility calculation (3.2.24) for each occupation and cell, combining commuting disutility and density-dependent disamenity. The residences are then reallocated across the cells until utilities equalize across space while preserving the total population and employment for each occupation, as per (3.2.25). Those new residential counts, in turn, drive an update of the disamenity according to the density-amenity elasticity relationship.

The outer loop continues until the change in residential populations between two subsequent iterations is smaller than the predefined threshold. The final output includes equilibrium employment by occupation, wages by occupation, and resident distributions by occupation.

3.D Changes by Occupation

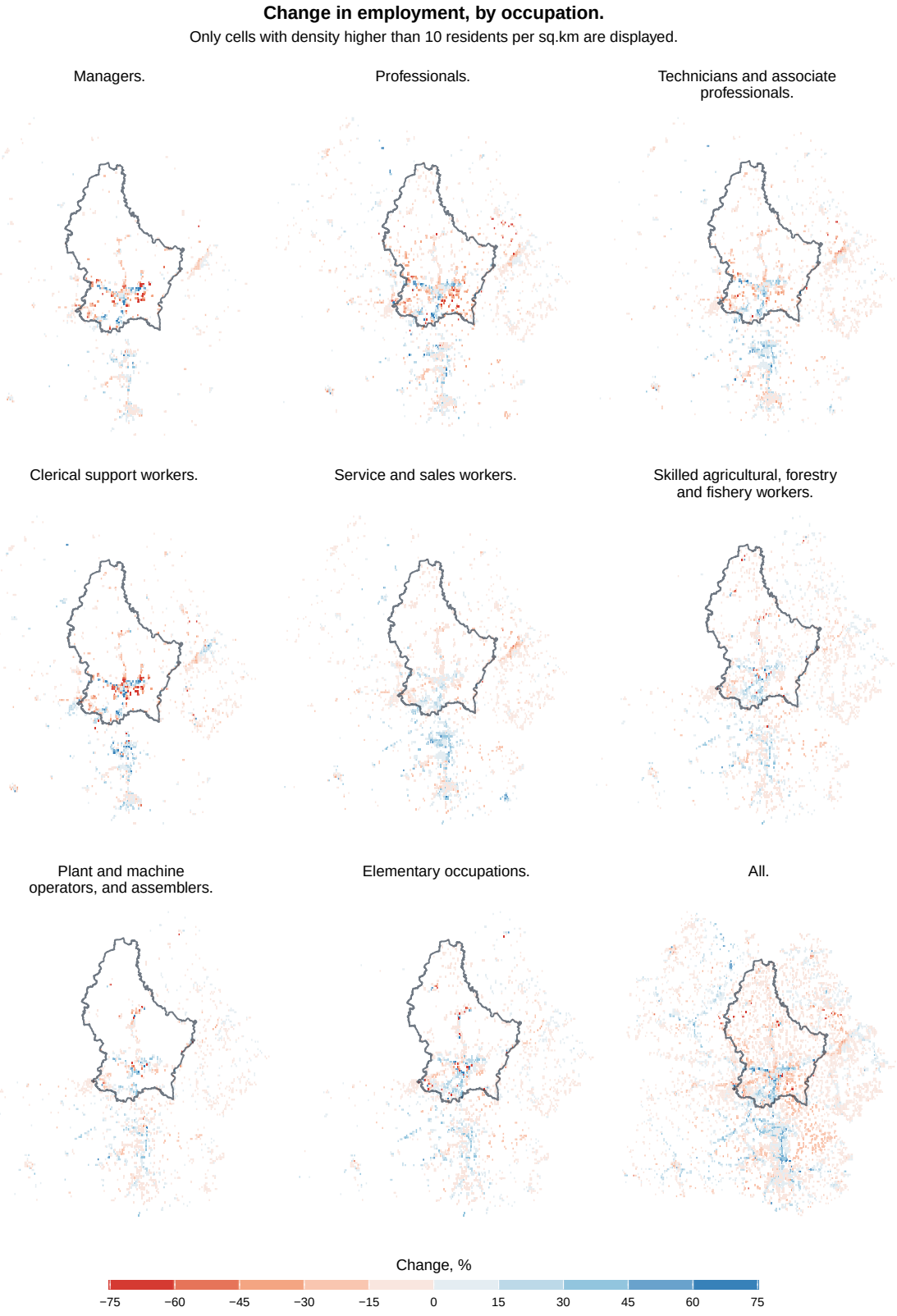

Note: The change in employment-weighted average wages at workplace is in the bottom left panel. Only pixels with density of more than 10 workers per km^2 are displayed. We use area-weighted interpolation of wages from communes onto pixels.

Figure 3.D.1: Percentage change in employment per pixel for 8 ISCO occupations.

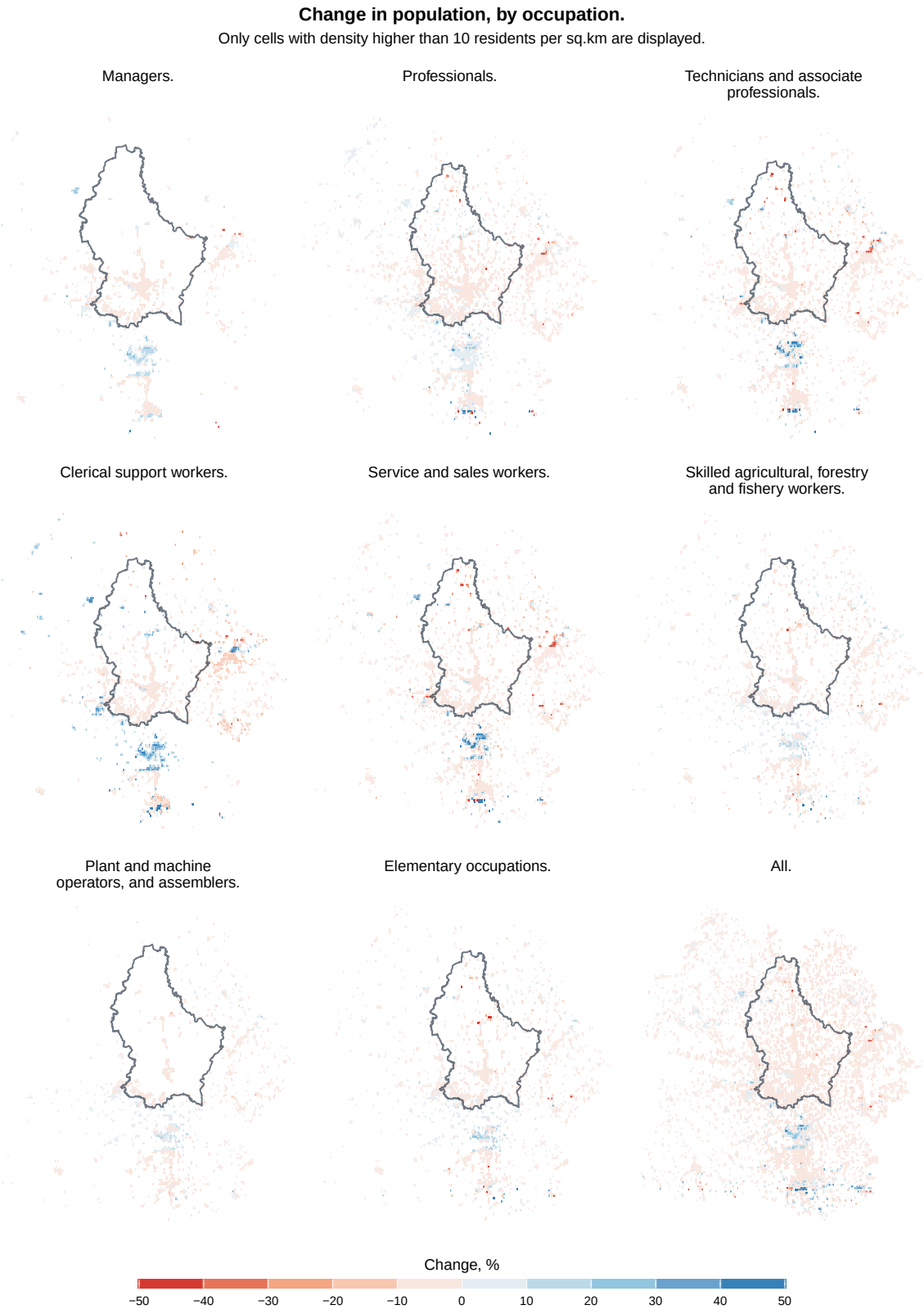

Note: The change in employment-weighted average wages at workplace is in the bottom left panel. Only pixels with density of more than 10 workers per km^2 are displayed. We use area-weighted interpolation of wages from communes onto pixels.

Figure 3.D.2: Percentage change in population per pixel for 8 ISCO occupations.

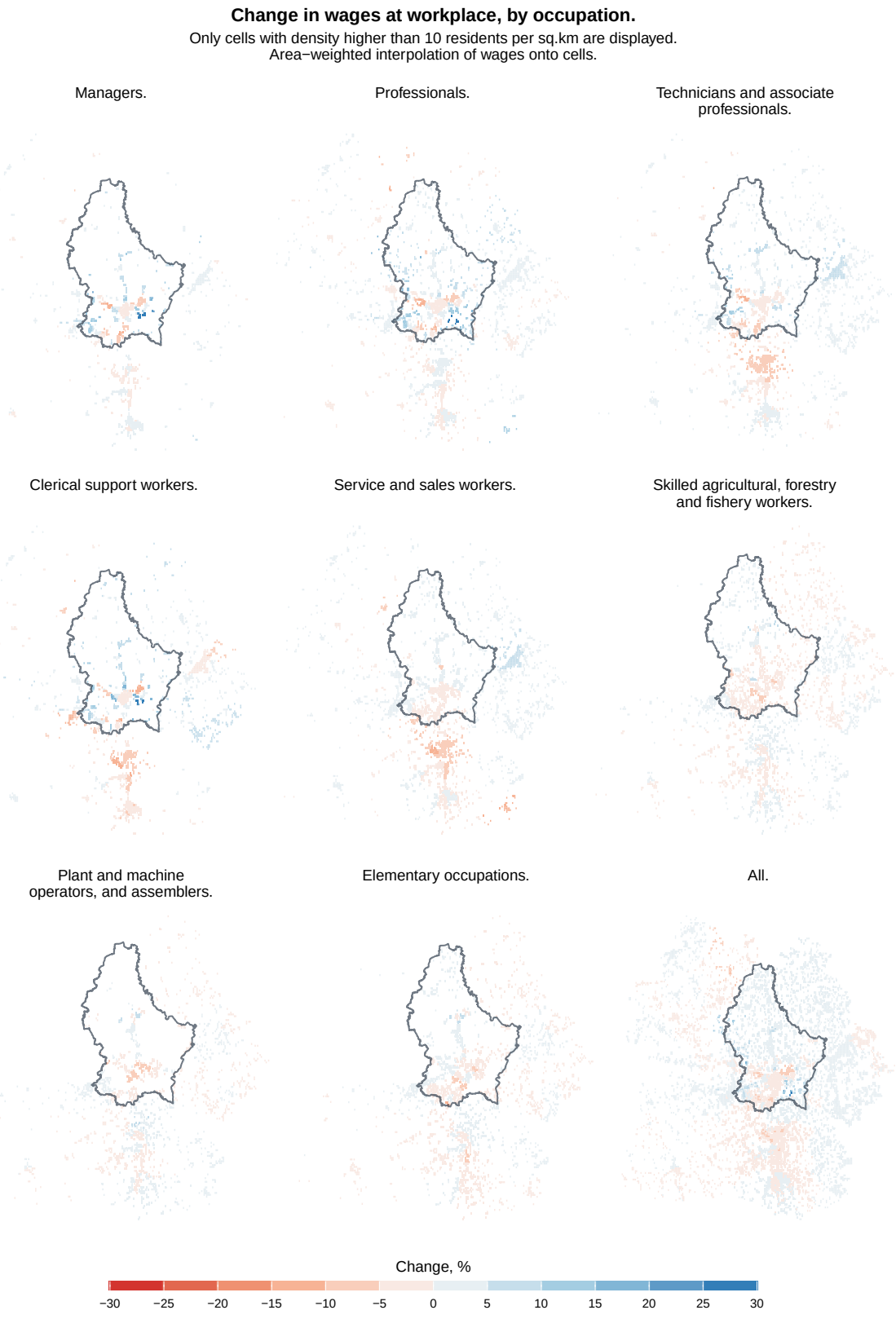

Note: The change in employment-weighted average wages at workplace is in the bottom left panel. Only pixels with density of more than 10 workers per km^2 are displayed. We use area-weighted interpolation of wages from communes onto pixels.

Figure 3.D.3: Percentage change in wages at workplace per pixel for 8 ISCO occupations.

Conclusion

This thesis has examined three structural frictions that shape economic activity in the Greater Region of Luxembourg: cross-border tax importation, congestion, and job search frictions. Together, these chapters provide new evidence on how fiscal and spatial mechanisms interact in one of Europe's most integrated, yet asymmetric, labor markets.

The first chapter quantified the contribution of taxation to cross-border differences in housing and commercial real estate markets. By combining a quantitative spatial model with regression discontinuity techniques, it showed that international differences in labor taxation play a secondary role compared to tax importation and productivity differentials. The analysis highlighted how tax importation generates substantial redistribution in favor of Luxembourg residents, and how it affects the housing market.

The second chapter measured the scale and distributional impact of congestion in cross-border commuting. Using empirical evidence and counterfactual simulations, it documented that congestion relief would increase aggregate output and fiscal revenues in Luxembourg, while redistributing welfare toward foreign commuter towns. The analysis underscored that congestion generates sharp spatial trade-offs: while most residents of the Greater Region gain from relief, residents of Luxembourg City may experience losses due to intensified labor market competition and housing pressures.

The third chapter introduces a new spatial equilibrium framework that incorporates sequential job search into quantitative urban models. This approach provides a tractable way to include realistic frictions in commuting decisions and explains how improved accessibility can raise both wages and employment by expanding the opportunity set of workers. When applied to Luxembourg, the model reveals that transport improvements generate uneven spatial and occupational effects, disproportionately benefiting service and sales workers, as well as border areas.

On the policy side, three main insights emerge. First, some reduction in tax importation appears desirable, and from the perspective of a social planner, it could improve aggregate welfare. Second, residents of the Greater Region and of Luxembourg – excluding Luxembourg City – are willing to pay for congestion relief, and the associated fiscal revenues could partly finance such measures. Third, labor market frictions and occupational heterogeneity play a central role in shaping the distribution of gains, implying that the benefits of these measures are likely to vary not only across space, but also across occupations.

On the methodological side, this thesis makes three contributions. First, it extends the quantitative spatial urban model framework by introducing a public good whose provision is endogenously linked to cross-border commuting flows. This establishes a connection between the tax

competition literature and quantitative models of urban economics and economic geography. Second, it incorporates asymmetric travel times into the modeling framework, demonstrating the importance of accounting for directional differences in congestion and accessibility. Third, it enriches the quantitative spatial literature by embedding a frictional, radiation-style job search process into the standard toolbox. The resulting model preserves the tractability of existing approaches while offering new insights into the spatial organization of economic activity.

At the same time, the analysis points to clear avenues for future research. A more comprehensive treatment of fiscal federalism is needed to assess how compensation mechanisms could address the imbalances created by tax importation. This thesis provides evidence that public goods in neighboring countries are undersupplied, that the degree of tax importation is large enough to cause a fiscal surplus in countries bordering Luxembourg in the counterfactual scenario of complete border closures, and that the total elimination of tax importation attracts more residents to the Greater Region, which serves as evidence of an increase in aggregate welfare. But is there a way to enforce this allocation? Moreover, some positive level of redistribution may not only increase aggregate welfare, but also be Pareto improving, and therefore beneficial for residents of Luxembourg themselves, especially when housing markets are explicitly considered as components of the welfare function. Endogenizing congestion dynamics and modal choice would improve the realism of policy counterfactuals and allow for the evaluation of transport investments. Finally, integrating an endogenous housing market with dynamic supply responses into the search-based framework would permit a more complete characterization of long-run equilibria. Extending the model to incorporate trade flows and cross-border institutional features would further enhance its relevance for evaluating joint transport, housing, and labor market policies.

Bibliography

Agrawal, D. R., & Hoyt, W. H. (2018). Commuting and taxes: Theory, empirics and welfare implications. *The Economic Journal*, *128*(616), 2969–3007.

Ahlfeldt, G. M. (2011). If alonso was right: Modeling accessibility and explaining the residential land gradient. *Journal of Regional Science*, *51*(2), 318–338.

Ahlfeldt, G. M., & Feddersen, A. (2018). From periphery to core: Measuring agglomeration effects using high-speed rail. *Journal of Economic Geography*, *18*(2), 355–390.

Ahlfeldt, G. M., Heblich, S., & Seidel, T. (2021). Micro-geographic property price and rent indices.

Ahlfeldt, G. M., Redding, S. J., Sturm, D. M., & Wolf, N. (2015). The economics of density: Evidence from the berlin wall. *Econometrica*, *83*(6), 2127–2189.

Akbar, P. A., Couture, V., Duranton, G., & Storeygard, A. (2023). *The fast, the slow, and the congested: Urban transportation in rich and poor countries* (tech. rep.). National Bureau of Economic Research.

Allen, T., & Arkolakis, C. (2014). Trade and the topography of the spatial economy. *The Quarterly Journal of Economics*, *129*(3), 1085–1140.

Allen, T., & Arkolakis, C. (2022). The welfare effects of transportation infrastructure improvements. *Review of Economic Studies*, *89*(6), 2911–2957.

Alonso, W. (1967). A reformulation of classical location theory and its relation to rent theory. *Papers of the Regional Science Association*, *19*(1), 22–44.

Anas, A. (2012). The optimal pricing, finance and supply of urban transportation in general equilibrium: A theoretical exposition. *Economics of transportation*, *1*(1-2), 64–76.

Ang, A., Christensen, P., & Vieira, R. (2020). Should congested cities reduce their speed limits? evidence from são paulo, brazil. *Journal of Public Economics*, *184*, 104155.

Baldwin, R. E., & Krugman, P. (2004). Agglomeration, integration and tax harmonisation. *European Economic Review*, *48*(1), 1–23.

Baselgia, E., & Martínez, I. Z. (2023). Behavioral responses to special tax regimes for the super–rich: Insights from swiss rich lists.

Bondarenko, M., Kerr, D., Sorichetta, A., & Tatem, A. (2020). Estimates of 2020 total number of people per grid square, adjusted to match the corresponding unpd 2020 estimates and broken down by gender and age groupings, produced using built-settlement growth model (bsgm) outputs. *WorldPop, University of Southampton, UK. doi:10.5258/SOTON/WP00698*.

Börjesson, M., Eliasson, J., Hugosson, M. B., & Brundell-Freij, K. (2012). The stockholm congestion charges—5 years on. effects on traffic, mobility and accessibility. *Transport Policy*, *20*, 1–12.

Choi, C.-Y., Quigley, D., & Wang, X. (2025). The impacts of local housing markets on us presidential elections: Via the collateral channel. *Oxford Bulletin of Economics and Statistics*.

Combes, P.-P., Duranton, G., & Gobillon, L. (2019). The costs of agglomeration: House and land prices in french cities. *The Review of Economic Studies*, *86*(4), 1556–1589.

Combes, P.-P., Duranton, G., & Gobillon, L. (2021). The production function for housing: Evidence from france. *Journal of Political Economy*, *129*(10), 2766–2816.

Combes, P.-P., Duranton, G., Gobillon, L., & Roux, S. (2010). Estimating agglomeration economies with history, geology, and worker effects. In *Agglomeration economics* (pp. 15–66). University of Chicago Press.

Combes, P.-P., & Gobillon, L. (2015). The empirics of agglomeration economies. In *Handbook of regional and urban economics* (pp. 247–348, Vol. 5). Elsevier.

Cook, C., Kreidieh, A., Vasserman, S., Allcott, H., Arora, N., van Sambeek, F., Tomkins, A., & Turkel, E. (2025). *The short-run effects of congestion pricing in new york city* (tech. rep.). National Bureau of Economic Research.

Couture, V., Duranton, G., & Turner, M. A. (2018). Speed. *Review of Economics and Statistics*, *100*(4), 725–739.

Cressie, N. (1988). Spatial prediction and ordinary kriging. *Mathematical geology*, *20*(4), 405–421.

Delventhal, M. J., Kwon, E., & Parkhomenko, A. (2022). Jue insight: How do cities change when we work from home? *Journal of Urban Economics*, *127*, 103331.

Desmet, K., Nagy, D. K., & Rossi-Hansberg, E. (2018). The geography of development. *Journal of Political Economy*, *126*(3), 903–983.

Duranton, G., & Puga, D. (2004). Micro-foundations of urban agglomeration economies. In *Handbook of regional and urban economics* (pp. 2063–2117, Vol. 4). Elsevier.

Duranton, G., & Turner, M. A. (2011). The fundamental law of road congestion: Evidence from us cities. *American Economic Review*, *101*(6), 2616–2652.

Duranton, G., & Turner, M. A. (2012). Urban growth and transportation. *Review of Economic Studies*, *79*(4), 1407–1440.

Eaton, J., & Kortum, S. (2002). Technology, geography, and trade. *Econometrica*, *70*(5), 1741–1779.

Eliasson, J. (2009). A cost–benefit analysis of the stockholm congestion charging system. *Transportation Research Part A: Policy and Practice*, *43*(4), 468–480.

Fajgelbaum, P. D., Morales, E., Suárez Serrato, J. C., & Zidar, O. (2019). State taxes and spatial misallocation. *The Review of Economic Studies*, *86*(1), 333–376.

Fajgelbaum, P. D., & Schaal, E. (2020). Optimal transport networks in spatial equilibrium. *Econometrica*, *88*(4), 1411–1452.

Fujita, M., & Ogawa, H. (1982). Multiple equilibria and structural transition of non-monocentric urban configurations. *Regional science and urban economics*, *12*(2), 161–196.

Giraud, T. (2022). Osrm: Interface between r and the openstreetmap-based routing service osrm. *Journal of Open Source Software*, *7*(78), 4574.

Gollin, D. (2002). Getting income shares right. *Journal of political Economy*, *110*(2), 458–474.

Graham, D. J., & Gibbons, S. (2019). Quantifying wider economic impacts of agglomeration for transport appraisal: Existing evidence and future directions. *Economics of Transportation*, *19*, 100121.

Heblich, S., Redding, S. J., & Sturm, D. M. (2020). The making of the modern metropolis: Evidence from london. *The Quarterly Journal of Economics*, *135*(4), 2059–2133.

Hörcher, D., & Graham, D. J. (2024). A quantitative urban model for transport appraisal. *Available at SSRN 5067099*.

Hymel, K. M., Small, K. A., & Van Dender, K. (2010). Induced demand and rebound effects in road transport. *Transportation Research Part B: Methodological*, *44*(10), 1220–1241.

Janeba, E., & Osterloh, S. (2013). Tax and the city - a theory of local tax competition. *Journal of Public Economics*, *106*, 89–100.

Jia, J. S., Lu, X., Yuan, Y., Xu, G., Jia, J., & Christakis, N. A. (2020). Population flow drives spatio-temporal distribution of covid-19 in china. *Nature*, *582*(7812), 389–394.

Kanbur, R., & Keen, M. (1993). Jeux sans frontieres: Tax competition and tax coordination when countries differ in size. *The American Economic Review*, 877–892.

Katz, L. F., & Murphy, K. M. (1992). Changes in relative wages, 1963–1987: Supply and demand factors. *The quarterly journal of economics*, *107*(1), 35–78.

Kleven, H., Landais, C., Munoz, M., & Stantcheva, S. (2020). Taxation and migration: Evidence and policy implications. *Journal of Economic Perspectives*, *34*(2), 119–142.

Knight, F. H. (1924). Some fallacies in the interpretation of social cost. *The Quarterly Journal of Economics*, *38*(4), 582–606.
Leape, J. (2006). The london congestion charge. *Journal of Economic Perspectives*, *20*(4), 157–176.
Lucas, R. E., & Rossi–Hansberg, E. (2002). On the internal structure of cities. *Econometrica*, *70*(4), 1445–1476.
Mathä, T. Y., Porpiglia, A., & Ziegelmeyer, M. (2018). Wealth differences across borders and the effect of real estate price dynamics: Evidence from two household surveys. *Journal of Income Distribution*, 1–35.
Matheron, G. (1963). Principles of geostatistics. *Economic geology*, *58*(8), 1246–1266.
McCall, J. J. (1970). Economics of information and job search. *The Quarterly Journal of Economics*, *84*(1), 113–126.
Monte, F., Redding, S. J., & Rossi-Hansberg, E. (2015). Commuting, migration and local employment elasticities. *The American Economic Review*, *105*(3), 678–714.
Monte, F., Redding, S. J., & Rossi-Hansberg, E. (2018a). Commuting, migration, and local employment elasticities. *American Economic Review*, *108*(12), 3855–3890.
Monte, F., Redding, S. J., & Rossi-Hansberg, E. (2018b). Commuting, migration, and local employment elasticities. *American Economic Review*, *108*(12).
Mortensen, D. T., & Pissarides, C. A. (1994). Job creation and job destruction in the theory of unemployment. *The review of economic studies*, *61*(3), 397–415.
Nilforoshan, H., Looi, W., Pierson, E., Villanueva, B., Fishman, N., Chen, Y., Sholar, J., Redbird, B., Grusky, D., & Leskovec, J. (2023). Human mobility networks reveal increased segregation in large cities. *Nature*, *624*(7992), 586–592.
Pesaresi, M., & Panagiotis, P. (2023). Ghs-built-s r2023a - ghs built-up surface grid, derived from sentinel2 composite and landsat, multitemporal (1975-2030). *European Commission, Joint Research Centre (JRC)*, 1–88.
Pieretti, P., & Zanaj, S. (2011). On tax competition, public goods provision and jurisdictions' size. *Journal of international economics*, *84*(1), 124–130.
Pigou, A. C. (1920). *The economics of welfare*. Macmillan.
Piketty, T. (2014). *Capital in the twenty-first century*. Harvard University Press.
Redding, S. J. (2016). Goods trade, factor mobility and welfare. *Journal of International Economics*, *101*, 148–167.
Redding, S. J., & Rossi-Hansberg, E. (2017). Quantitative spatial economics. *Annual Review of Economics*, *9*, 21–58.
Roback, J. (1982). Wages, rents, and the quality of life. *Journal of political Economy*, *90*(6), 1257–1278.
Rogerson, R., Shimer, R., & Wright, R. (2005). Search-theoretic models of the labor market: A survey. *Journal of economic literature*, *43*(4), 959–988.
Rosen, S. (1979). Wage-based indexes of urban quality of life. *Current issues in urban economics*, 74–104.
Rotemberg, J. J. (1985). The efficiency of equilibrium traffic flows. *Journal of Public Economics*, *26*(2), 191–205.
Schläpfer, M., Dong, L., O'Keeffe, K., Santi, P., Szell, M., Salat, H., Anklesaria, S., Vazifeh, M., Ratti, C., & West, G. B. (2021). The universal visitation law of human mobility. *Nature*, *593*(7860), 522–527.
Schmidheiny, K., & Slotwinski, M. (2015). Behavioral responses to local tax rates: Quasi-experimental evidence from a foreigners' tax scheme in switzerland.
Seidel, T., & Wickerath, J. (2020). Rush hours and urbanization. *Regional Science and Urban Economics*, *85*, 103580.
Sielker, F., Longobardi, B., Larrea, E., Gibert, E., & Ulied, A. (2022). Cross-border housing markets in europe: Measuring and understanding the dynamics in 11 countries through web-scraping processes.
Simini, F., Barlacchi, G., Luca, M., & Pappalardo, L. (2021). A deep gravity model for mobility flows generation. *Nature communications*, *12*(1), 6576.
Simini, F., González, M. C., Maritan, A., & Barabási, A.-L. (2012). A universal model for mobility and migration patterns. *Nature*, *484*(7392), 96–100.

Small, K. A. (1992). *Urban transportation economics*. Harwood Academic Publishers.
Small, K. A., & Verhoef, E. T. (2007). *The economics of urban transportation*. Routledge.
Stigler, G. J. (1961). The economics of information. *Journal of political economy*, *69*(3), 213–225.
Thisse, J.-F., Turner, M. A., & Ushchev, P. (2024). Foundations of cities. *Journal of Urban Economics*, *143*, 103684.
Tsivanidis, N. (2019). Evaluating the impact of urban transit infrastructure: Evidence from bogotas transmilenio. *Unpublished manuscript*.
Valentinyi, A., & Herrendorf, B. (2008). Measuring factor income shares at the sectoral level. *Review of Economic Dynamics*, *11*(4), 820–835.
Vickrey, W. S. (1963). Pricing in urban and suburban transport. *The American Economic Review*, *53*(2), 452–465.
Wackernagel, H. (2003). Ordinary kriging. In *Multivariate geostatistics* (pp. 79–88). Springer.
Walters, A. A. (1961). The theory and measurement of private and social cost of highway congestion. *Econometrica*, *29*(4), 676–699.